NONLINEAR DYNAMICS AND SYSTEMS THEORY
An International Journal of Research and Surveys

Volume 6 Number 2 2006

CONTENTS

 ISSN 1562-8353 Printed in Ukraine
To receive contents and abstracts by e-mail, visit our Website at: **http://www.e-ndst.kiev.ua**

NONLINEAR DYNAMICS & SYSTEMS THEORY Volume 6, No. 2, 2006

Volume 6, Number 2, 2006 **ISSN 1562-8353**

Nonlinear Dynamics and Systems Theory

An International Journal of Research and Surveys

Academic Periodical Press

Nonlinear Dynamics and Systems Theory
An International Journal of Research and Surveys

NONLINEAR DYNAMICS AND SYSTEMS THEORY
An International Journal of Research and Surveys

INSTRUCTIONS FOR CONTRIBUTORS

(1) General. The Journal will publish original carefully refereed papers, brief notes and reviews on a wide range of nonlinear dynamics and systems theory problems. Contributions will be considered for publication in ND&ST if they have not been published previously. Before preparing your submission, it is essential that you consult our style guide; please visit our website: http://www.e-ndst.kiev.ua

(2) Manuscript and Correspondence. Contributions are welcome from all countries and should be written in English. Two copies of the manuscript, double spaced one column format, and the electronic version by AMSTEX, TEX or LATEX program (on diskette) should be sent directly to

Professor A.A. Martynyuk
Institute of Mechanics,
Nesterov str.3, 03057, MSP 680
Kiev-57, Ukraine
(e-mail: anmart@stability.kiev.ua).

or to one of the Editors or to a member of the Editorial Board.

The title of the article must include: author(s) name, name of institution, department, address, FAX, and e-mail; an Abstract of 50-100 words should not include any formulas and citations; key words, and AMS subject classifications number(s). The size for regular paper should be 10-14 pages, survey (up to 24 pages), short papers, letter to the editor and book reviews (2-3 pages).

(3) Tables, Graphs and Illustrations. All figures must be suitable for reproduction without being retouched or redrawn and must include a title. Line drawings should include all relevant details and should be drawn in black ink on plain white drawing paper. In addition to a hard copy of the artwork, it is necessary to attach a PC diskette with files of the artwork (preferably in PCX format).

(4) References. Each entry must be cited in the text by author(s) and number or by number alone. All references should be listed in their alphabetic order. Use please the following style:

Journal: [1] Poincaré, H. Title of the article. *Title of the Journal* **Vol.1**(No.1) (year) pages. [Language].
Book: [2] Liapunov, A.M. *Title of the book.* Name of the Publishers, Town, year.
Proceeding: [3] Bellman, R. Title of the article. In: *Title of the book.* (Eds.). Name of the Publishers, Town, year, pages. [Language].

(5) Proofs and Reprints. Proofs sent to authors should be returned to the Editor with corrections within three days after receipt. Acceptance of the paper entitles the author to 10 free reprints.

(6) Editorial Policy. Every paper is reviewed by the regional editor, and/or a referee, and it may be returned for revision or rejected if considered unsuitable for publication.

(7) Copyright Assignment. When a paper is accepted for publication, author(s) will be requested to sign a form assigning copyright to Informath Publishing Group. Failure to do it promptly may delay the publication.

NONLINEAR DYNAMICS AND SYSTEMS THEORY

An International Journal of Research and Surveys

Published since 2001

Volume 6 Number 2 2006

CONTENTS

Founded by A.A.Martynyuk in 2001.
Registered in Ukraine Number: KB №5267 / 04.07.2001.

NONLINEAR DYNAMICS AND SYSTEMS THEORY

An International Journal of Research and Surveys

Nonlinear Dynamics and Systems Theory (ISSN 1562-8353 (Print), ISSN 1813-7385 (Online)) is an international journal published under the auspices of the S.P.Timoshenko Institute of Mechanics of National Academy of Sciences of Ukraine and the Laboratory for Industrial and Applied Mathematics (LIAM) at York University (Toronto, Canada). It is aimed at publishing high quality original scientific papers and surveys in area of nonlinear dynamics and systems theory and technical reports on solving practical problems. The scope of the journal is very broad covering:

SCOPE OF THE JOURNAL

Analysis of uncertain systems • Bifurcations and instability in dynamical behaviors • Celestial mechanics, variable mass processes, rockets • Control of chaotic systems • Controllability, observability, and structural properties • Deterministic and random vibrations • Differential games • Dynamical systems on manifolds • Dynamics of systems of particles • Hamilton and Lagrange equations • Hysteresis • Identification and adaptive control of stochastic systems • Modeling of real phenomena by ODE, FDE and PDE • Nonlinear boundary problems • Nonlinear control systems, guided systems • Nonlinear dynamics in biological systems • Nonlinear fluid dynamics • Nonlinear oscillations and waves • Nonlinear stability in continuum mechanics • Non-smooth dynamical systems with impacts or discontinuities • Numerical methods and simulation • Optimal control and applications • Qualitative analysis of systems with aftereffect • Robustness, sensitivity and disturbance rejection • Soft computing: artificial intelligence, neural networks, fuzzy logic, genetic algorithms, etc. • Stability of discrete systems • Stability of impulsive systems • Stability of large-scale power systems • Stability of linear and nonlinear control systems • Stochastic approximation and optimization • Symmetries and conservation laws

PUBLICATION AND SUBSCRIPTION INFORMATION

The **Nonlinear Dynamics and Systems Theory** is published four times per year in 2006. Base list subscription price per volume: US$149.00. This price is available only to individuals whose library subscribes to the journal OR who warrant that the Journal is for their own use and provide a home address for mailing. Separate rates apply to academic and corporate/government institutions. Our charge includes postage, packing, handling and airmail delivery of all issues. Mail order and inquires to: Department of Processes Stability, S.P.Timoshenko Institute of Mechanics NAS of Ukraine, Nesterov str.,3, 03057, Kiev-57, MSP 680, Ukraine, Tel: ++38-044-456-6140, Fax: ++38-044-456-0319, E-mail: anchern@stability.kiev.ua, http://www.sciencearea.com.ua; http://www.e-ndst.kiev.ua

ABSTRACTING AND INDEXING SERVICES

EBSCO Databases, Swets Information Services, Mathematical Reviews/MathSciNet, Zentralblatt MATH/Mathematics Abstracts.

Nonlinear Dynamics and Systems Theory, **6**(2) (2006) 111–127

Minimal Representations, Controllability and Free Energies in a Heat Conductor with Memory

A.M. Caucci*

Department of Mathematics, University of Bologna,
Piazza di Porta San Donato 5, 40126 Bologna, Italy

Received: July 8, 2005; Revised: June 7, 2006

Abstract: A rigid linear heat conductor with memory effects is considered. Some results about state-space representation, minimality and controllability of heat conductors with memory kernel of exponential type are presented. In such a context, the asymptotic behavior and the existence of a bounded absorbing set for solutions of the energy equation are studied by means of a suitable class of quadratic free energies.

Keywords: *Heat conduction; free energy; absorbing set.*

Mathematics Subject Classification (2000): 80A20, 74D05, 35K05.

1 Introduction

In this paper we consider a rigid linear heat conductor with memory effects — within the framework proposed by Gurtin and Pipkin [10] — when the memory kernel is finite sum of exponentials, namely

$$\dot{K}(s) = \sum_{i=1}^{n} b_i \, e^{-a_i \, s},$$

where n is a positive integer, $a_i, b_i \in R,\ a_i > 0,\ i = 1, 2, \ldots, n$.

On the basis of Coleman's results concerning materials with memory [3], a non-linear model for a rigid heat conductor was developed by Gurtin and Pipkin in [10]. Moreover, they considered the linearization of their theory appropriate to infinitesimal temperature gradients, which for isotropic materials yields a constitutive equation for the heat flux $\boldsymbol{q}$ expressed in terms of the history of the temperature gradient $\boldsymbol{g}$; this linear theory is important because the obtained constitutive equation for $\boldsymbol{q}$ is a generalization of the

*Corresponding author: caucci@dm.unibo.it

so-called Cattaneo–Maxwell equation [2], which follows from it as a special case. Subsequently, many authors considered this linearized equation to study problems connected with heat propagation. Among all the results so obtained, we remember, in particular, those derived in [6], where an approximate theory of thermodynamics is developed for Gurtin and Pipkin's model and maximal free energy and maximal free enthalpy functions are explicitly constructed and used to prove stability and domain of dependence results. We recall that in [6], following [11], the thermodynamic states and processes are connected with the integrated history of the temperature gradient and the temperature gradient, respectively.

In this work, the linear theory introduced in [10] is taken into account in Section 2.

In Section 3, following the lines of [4] and [5], where analogous problems are studied for viscoelastic solids of exponential type, we prove that the minimal representation of the state space is a finite dimensional vector space and each minimal state element represents an equivalence class of integrated histories; the full controllability of the minimal state space is also verified.

In the following Section 4, an explicit representation of a class of quadratic free energies is taken into consideration with respect to some minimal, finite-dimensional state space. Finally, the last part of the paper is devoted to study, by means of uniform energy estimate, the asymptotic behavior of solutions of the evolutive (semilinear) equation, obtained by substituting the constitutive equations for the internal energy e and for the heat flux $\boldsymbol{q}$ into the energy equation for rigid heat conductors.

2 Preliminary Notions and Setting of the Problem

Within the linear theory of thermodynamics developed in [10], the *internal energy* e is assumed of the form

$$e(\boldsymbol{x}, t) = \alpha_0\, \theta(\boldsymbol{x}, t), \tag{2.1}$$

where α_0 is here assumed to be constant, $\boldsymbol{x} \in R^3$ denotes the position within the conductor[1], $t \in R^+$ denotes the time variable[2] and $\theta = (\Theta - \Theta_0)$ is the temperature difference with respect to a fixed reference absolute temperature $\Theta_0 > 0$, uniform in R^3. The *heat flux* $\boldsymbol{q} \in R^3$ is assumed to satisfy the constitutive equation

$$\boldsymbol{q}(\boldsymbol{x}, t) = -\int_0^\infty K(\tau) \nabla\theta(\boldsymbol{x},\, t - \tau)\, d\tau, \tag{2.2}$$

where $K(\tau)$ is the *heat flux relaxation function*, given by

$$K(t) = K_0 + \int_0^t \dot{K}(s)\, ds; \tag{2.3}$$

[1] More precisely, it should be require that $\boldsymbol{x} \in \mathcal{B} \subset R^3$, where $\mathcal{B}$ denotes the bounded closed set in R^3 which represents the configuration domain of the conductor, here not specified since of no interest in the present study.

[2] Throughout the whole paper, $R^+ = [0, \infty)$ and $R^{++} = (0, \infty)$.

K_0 represents the initial (positive) value of the flux relaxation function, thus termed *initial heat flux relaxation coefficient*. It is further required that

$$\dot{K} \in L^1(R^+) \cap L^2(R^+) \quad \text{and} \quad K \in L^1(R^+), \tag{2.4}$$

which implies

$$K_\infty = \lim_{t\to\infty} K(t) = 0.$$

The latter can be physically interpreted recalling that there is no heat flux when, at infinity, the thermal equilibrium is reached.

In the sequel, we will focus our attention on a material element of the conductor; thus we will omit to show explicit dependence on the position $\boldsymbol{x}$ in the conductor and all the quantities introduced will be represented by functions of the time variable alone.

When the integral kernel satisfies both the requirements (2.3) and (2.4), (2.2) is equivalent to the following

$$\boldsymbol{q}(t) = \int_0^\infty \dot{K}(t)\, \overline{\boldsymbol{g}}^t(\tau)\, d\tau, \tag{2.5}$$

where $\boldsymbol{g} = \nabla\theta$ denotes the temperature-gradient and

$$\overline{\boldsymbol{g}}^t(\tau) = \int_{t-\tau}^t \boldsymbol{g}(s)\, ds$$

represents the *integrated history of the temperature-gradient*.

To specify those thermodynamical phenomena to study, the following vectorial space can be introduced

$$\Gamma = \left\{ \overline{\boldsymbol{g}}^t \colon\ R^+ \to R^3 \colon\ \left| \int_0^\infty \dot{K}(s+\tau) \overline{\boldsymbol{g}}^t(s)\, ds \right| < \infty, \quad \forall \tau \geq 0 \right\}. \tag{2.6}$$

Following the theory proposed by Noll, Coleman and Owen in the seventies, we introduce some basic definitions.

The *thermodynamic state* of the conductor is chosen to be

$$\sigma(t) = (\theta(t), \overline{\boldsymbol{g}}^t), \quad \forall\, t \geq 0,$$

where $\theta(t) > 0$ and $\overline{\boldsymbol{g}}^t$ belongs to Γ. Such a definition implies that, the thermodynamic state function is known as soon as the temperature and the integrated history of the temperature-gradient are given. The (metric) space, Σ, of all admissible states (*state space*) is the set comprising all those states σ which correspond to a finite heat flux; Σ may be written as

$$\Sigma = R^{++} \times \Gamma$$

where Γ is given by (2.6).

We define *thermal process of duration* $T > 0$ as a map

$$P \colon\ [0, T) \to R \times R^3,$$

piecewise continuous on the time interval $[0,T)$ and such that

$$P(\tau) = (\dot{\theta}_P(\tau),\, \boldsymbol{g}_P(\tau)), \quad \forall \tau \in [0,T).$$

Let Π be the set of all admissible thermal processes P, that is the set of piecewise continuous functions $P\colon\ [0,T) \to R\times R^3,\ T>0,$ which satisfies the following properties:

(1) if $P \in \Pi,$ then its restriction $P_{[t_1,t_2)}$ to the interval $[t_1,t_2) \subseteq [0,T)$ belongs to Π;
(2) if $P_1, P_2 \in \Pi,$ then the composition $P_1 * P_2,$ defined as

$$(P_1 * P_2)(t) = \begin{cases} P_1(t) & \text{if} \quad t \in [0,T_1), \\ P_2(t-T_1) & \text{if} \quad t \in [T_1,\, T_1+T_2), \end{cases}$$

belongs to Π.

To any given rigid heat conductor are associated two maps:

(i) $\rho\colon\ \Sigma \times \Pi \to \Sigma$ called *evolution* (or *state-transition*) *function*, which transforms the state σ_1 under the process P into $\sigma_2 = \rho(\sigma_1, P)$. The map ρ obeys the semi-group property. If $(\sigma_0, P) \in \Sigma\times\Pi,$ where $\sigma_0 = \sigma(0) = (\theta_\star(0), \overline{\boldsymbol{g}}^0_\star)$ ($\theta_\star(0)$ denotes the temperature and $\overline{\boldsymbol{g}}^0_\star$ the integrated history of the temperature-gradient at time $t=0$) and $P = (\dot{\theta}_P, \boldsymbol{g}_P),$ then, through the map ρ, it is possible to define the state function

$$\sigma(t) = \left(\theta(t), \overline{\boldsymbol{g}}^t\right) = \rho\left(\sigma_0, P_{[0,t)}\right), \quad t \in [0,T)$$

in the following manner

$$\theta(t) = \theta_\star(0) + \int_0^t \dot{\theta}_P(\zeta)\, d\zeta,$$

$$\overline{\boldsymbol{g}}^t(s) = \begin{cases} \displaystyle\int_{t-s}^{t} \boldsymbol{g}_P(\zeta)\, d\zeta, & 0 \le s < t, \\ \displaystyle\int_0^t \boldsymbol{g}_P(\zeta)\, d\zeta + \overline{\boldsymbol{g}}^0_\star(s-t), & s \ge t. \end{cases}$$

The particular nature of the state space Σ and the properties of the state-transition function ρ provide all the thermal properties of the system and enable it to model physical phenomena. We say that a state $\sigma^f \in \Sigma$ is *attainable* from a state $\sigma^i \in \Sigma$ if there exists a process $P \in \Pi$ such that

$$\rho(\sigma^i, P) = \sigma^f.$$

The state space Σ is

* *attainable* from a state σ_0 if, for every final state $\bar{\sigma} \in \Sigma,$ there exists a process $P \in \Pi$ such that

$$\rho(\sigma_0, P) = \bar{\sigma};$$

* *controllable* in a state σ_0 if σ_0 is attainable from any state of Σ;
* *completely controllable*, if, for any pair $\sigma_1,\ \sigma_2 \in \Sigma,$ there exists *at least* a process $P \in \Pi$ such that

$$\rho(\sigma_1, P) = \sigma_2.$$

(ii) $\mathcal{Q}$ called *response function* which maps the pair $(\sigma(t), P(t))$ into the pair $(e(t), \boldsymbol{q}(t))$ at time t, namely

$$(e(t), \boldsymbol{q}(t)) = \mathcal{Q}(\sigma(t), P(t)), \quad t \in [0, T).$$

The notion of *equivalence between material states* is introduced to associate together all those different thermal histories which correspond to the same heat flux.

Definition 2.1 Two states $\sigma_1, \sigma_2 \in \Sigma$ are said to be *equivalent* $(\sigma_1 \sim \sigma_2)$ if

$$\mathcal{Q}(\sigma_1, P) = \mathcal{Q}(\sigma_2, P), \quad \forall\, P \in \Pi.$$

For rigid heat conductors described by constitutive equations (2.1), (2.2), the thermodynamic states

$$\sigma_1(t) = (\theta_1(t), \overline{\boldsymbol{g}}_1^t), \quad \sigma_2(t) = (\theta_2(t), \overline{\boldsymbol{g}}_2^t)$$

are equivalent in the sense of Definition 2.1 if and only if $\theta_1(t) = \theta_2(t),\ \forall\, t \geq 0$ and

$$\int_0^\infty \dot{K}(s+\tau)\overline{\boldsymbol{g}}_1(s)\, ds = \int_0^\infty \dot{K}(s+\tau)\overline{\boldsymbol{g}}_2(s)\, ds, \quad \forall\, \tau \geq 0. \tag{2.7}$$

An equivalent way to rephrase relationship (2.7) can be found in [1].

Remark 2.1 Definition 2.1 introduces an *equivalence relation* between states; the quotient space

$$\Sigma_R = \Sigma/_\sim$$

is the *minimal representation* of the state space.

3 Minimal Representation and Controllability: The Exponential Case

For linear heat conductors with relaxation function of exponential type $(n \geq 1)$, the explicit form of the relaxation function $K(s)$ is given by

$$K(s) = \sum_{i=1}^{n} k_i\, e^{-a_i\, s},$$

$$K_0 = \sum_{i=1}^{n} k_i, \quad K_\infty = \lim_{s\to\infty} K(s) = 0,$$

where a_i and $k_i,\ i = 1, \ldots, n,$ are assumed to be strictly positive; moreover, it is reasonable to assume $a_i \neq a_j,\ \forall\, i \neq j,$ and $a_i < a_j,\ i < j.$ Then

$$\dot{K}(s) = \sum_{i=1}^{n} b_i e^{-a_i s}, \quad b_i = -a_i k_i < 0, \tag{3.1}$$

and, substituting (3.1) into (2.5), the heat flux $\boldsymbol{q}(t)$ becomes

$$\boldsymbol{q}(t) = \sum_{i=1}^{n} b_i \int_0^{\infty} e^{-a_i s} \overline{\boldsymbol{g}}^t(s)\, ds. \tag{3.2}$$

Recalling (2.7), two different integrated histories of the temperature-gradient, $\overline{\boldsymbol{g}}_1^t$, $\overline{\boldsymbol{g}}_2^t$, are equivalent if

$$\sum_{i=1}^{n} b_i e^{-a_i \tau} \int_0^{\infty} e^{-a_i s} (\overline{\boldsymbol{g}}_1^t(s) - \overline{\boldsymbol{g}}_2^t(s))\, ds = 0, \quad \tau \geq 0,$$

which in turn implies

$$\int_0^{\infty} e^{-a_i s} (\overline{\boldsymbol{g}}_1^t(s) - \overline{\boldsymbol{g}}_2^t(s))\, ds = 0, \quad i = 1, \ldots, n.$$

This means that two thermodynamic states

$$\sigma_1(t) = (\theta_1(t), \overline{\boldsymbol{g}}_1^t), \quad \sigma_2(t) = (\theta_2(t), \overline{\boldsymbol{g}}_2^t)$$

are equivalent if and only if $\theta_1(t) = \theta_2(t)$, $\forall\, t \geq 0$ and

$$\boldsymbol{g}_{1,a_i} = \boldsymbol{g}_{2,a_i}, \quad i = 1, \ldots, n, \tag{3.3}$$

where

$$\boldsymbol{g}_{a_i}(t) = \int_0^{\infty} e^{-a_i s} \overline{\boldsymbol{g}}^t(s)\, ds, \quad i = 1, \ldots, n, \tag{3.4}$$

are called *internal variables*. If this is the case, the *minimal representation* of the state space, $\Sigma_R = \Sigma/_{\sim}$, is a *finite* dimensional vector space and we can choose

$$\sigma_R = [\, \theta, \quad \boldsymbol{g}_{a_1}, \quad \boldsymbol{g}_{a_2}, \quad \ldots, \quad \boldsymbol{g}_{a_n}\,] \in R^{3n+1}.$$

Moreover, if $P = (\dot{\theta}_P, \boldsymbol{g}_P) \in \Pi$, the evolution function ρ is described through the following system of ordinary differential equations

$$\begin{aligned} \dot{\theta}(t) &= \dot{\theta}_P(t), \\ \dot{\boldsymbol{g}}_{a_i}(t) &= \frac{1}{a_i}\, \boldsymbol{g}_P(t) - a_i \boldsymbol{g}_{a_i}(t), \quad i = 1, \ldots, n, \quad t \geq 0, \end{aligned} \tag{3.5}$$

with the initial condition

$$\sigma_0 = \sigma(0) = (\theta_\star(0), \boldsymbol{g}_{a_1\star}(0), \boldsymbol{g}_{a_2\star}(0), \ldots, \boldsymbol{g}_{a_n\star}(0)), \tag{3.6}$$

where

$$\boldsymbol{g}_{a_i\star}(0) = \int_0^{\infty} e^{-a_i s} \overline{\boldsymbol{g}}_\star^0(s)\, ds, \quad i = 1, \ldots, n.$$

Now, our aim is to verify the complete controllability of system (3.5) – (3.6). System (3.5) – (3.6) is linear of dimension $(n+1)$; the control is the function P.

Let $\mathcal{M}(n, m)$ be the space of all real matrices $n \times m$; we recall the following Theorem (see for instance [12]).

Theorem 3.1 *A linear system*

$$\dot{\boldsymbol{x}} = A\boldsymbol{x} + B\boldsymbol{u},$$
$$\boldsymbol{x}(0) = \boldsymbol{x}_0$$

with $A \in \mathcal{M}(n,n)$, $B \in \mathcal{M}(n,m)$, $\boldsymbol{u} \in R^m$, $\boldsymbol{x}, \boldsymbol{x}_0 \in R^n$, $m < n$, *is completely controllable if and only if*

$$\operatorname{rank}[A|B] = n$$

("Kalman rank condition") where $[A|B]$ *denotes the matrix*

$$[\,B, \quad AB, \quad A^2B, \quad \ldots, \quad A^{n-1}B\,] \in \mathcal{M}(n, nm)$$

which consists of consecutively written columns of matrices B, AB, A^2B, $\ldots$, $A^{n-1}B$.

By Theorem 3.1, the controllability of system (3.5) – (3.6) depends on the rank of the square $(n+1)$ matrix

$$[A|B] = \begin{bmatrix} 1 & 0 & 0 & 0 & 0 & \ldots & 0 \\ 0 & \dfrac{1}{a_1} & -1 & a_1 & -{a_1}^2 & \ldots & (-1)^{n-1}\,{a_1}^{n-2} \\ 0 & \dfrac{1}{a_2} & -1 & a_2 & -{a_2}^2 & \ldots & (-1)^{n-1}\,{a_2}^{n-2} \\ \ldots & \ldots & \ldots & \ldots & \ldots & \ldots & \ldots \\ 0 & \dfrac{1}{a_n} & -1 & a_n & -{a_n}^2 & \ldots & (-1)^{n-1}\,{a_n}^{n-2} \end{bmatrix}.$$

Since

$$\det([A|B]) = \prod_{l=1}^{n} a_l \prod_{1 \le j < i \le n} (a_j - a_i),$$

where $a_l \neq 0$ for any $l = 1, \ldots, n$ and $a_i \neq a_j$ for any $i \neq j$, the matrix $[A|B]$ is non singular; therefore the state space Σ_R is completely controllable.

Finally, introduced the following differential operators

$$\mathcal{V} = \sum_{h=0}^{n} v_h \frac{d^h}{dt^h}, \qquad \mathcal{T} = \sum_{h=0}^{n-1} l_h \frac{d^h}{dt^h}, \tag{3.7}$$

we prove the equivalence between (3.2) and the *implicit constitutive equation* (see [9])

$$\mathcal{V}\boldsymbol{q} = \mathcal{T}\boldsymbol{g}. \tag{3.8}$$

Theorem 3.2 *Let* $\mathcal{V}$ *and* $\mathcal{T}$, *as in (3.7), be differential operators of order* n *and* $(n-1)$ *respectively, with constant coefficients. For the sake of simplicity, we assume* $v_0 = 1$*; moreover, for physical reasons, we assume* $v_n \neq 0$. *Implicit constitutive equation (3.8) and integral constitutive equation (3.2) are equivalent, namely every solution of (3.8) is also solution of (3.2), and vice versa.*

Proof We put

$$\mathcal{I}(\tau, \overline{\boldsymbol{g}}^t) = \sum_{i=1}^{n} b_i e^{-a_i \tau} \boldsymbol{g}_{a_i}(t), \quad \tau \geq 0,$$

where, for all $i = 1, \dots, n$, $\boldsymbol{g}_{a_i}$ is given by (3.4). From (3.2), we have

$$\boldsymbol{q}(t) = \mathcal{I}(0, \overline{\boldsymbol{g}}^t) = \sum_{i=1}^{n} b_i \boldsymbol{g}_{a_i}(t) \tag{3.9}$$

and, deriving n times with respect to t, we obtain

$$\frac{d^m}{dt^m}\,\boldsymbol{q}(t) = \frac{d^m}{dt^m}\,\mathcal{I}(0, \overline{\boldsymbol{g}}^t) = \sum_{i=1}^{n} b_i\,\frac{d^m}{dt^m}\,\boldsymbol{g}_{a_i}(t), \quad m = 1, \dots, n, \tag{3.10}$$

with

$$\frac{d^m}{dt^m}\,\boldsymbol{g}_{a_i}(t) = (-1)^m {a_i}^m \boldsymbol{g}_{a_i}(t) + \sum_{j=0}^{m-1} (-1)^{m-j+1} {a_i}^{m-j-2} \frac{d^j}{dt^j}\,\boldsymbol{g}(t), \quad i = 1, \dots, n, \tag{3.11}$$

due to $(3.5)_2$. Because of relation (3.11), system (3.10) can be finally rewritten as

$$\frac{d^m}{dt^m}\,\boldsymbol{q}(t) = (-1)^{m+1} \sum_{i=1}^{n} k_i a_i^{m+1} \boldsymbol{g}_{a_i}(t) + \sum_{i=1}^{n} k_i \sum_{j=0}^{m-1} (-1)^{m-j+2} {a_i}^{m-j-1} \frac{d^j}{dt^j}\,\boldsymbol{g}(t), \quad m = 1, \dots, n. \tag{3.12}$$

The matrix M, given by the coefficients of $\boldsymbol{g}_{a_i}(t)$, $i = 1, \dots, n$, is equal to

$$M = \begin{bmatrix} k_1 (-a_1)^2 & k_2 (-a_2)^2 & \dots & k_n (-a_n)^2 \\ k_1 (-a_1)^3 & k_2 (-a_2)^3 & \dots & k_n (-a_n)^3 \\ \dots & \dots & \dots & \dots \\ k_1 (-a_1)^{n+1} & k_2 (-a_2)^{n+1} & \dots & k_n (-a_n)^{n+1} \end{bmatrix} = [\mathrm{diag}\,(k_1, k_2, \dots, k_n)\,\Lambda]^\top,$$

where

$$\Lambda = \begin{bmatrix} (-a_1)^2 & (-a_1)^3 & \dots & (-a_1)^{n+1} \\ (-a_2)^2 & (-a_2)^3 & \dots & (-a_2)^{n+1} \\ \dots & \dots & \dots & \dots \\ (-a_n)^2 & (-a_n)^3 & \dots & (-a_n)^{n+1} \end{bmatrix}.$$

Since

$$\det(\Lambda) = \prod_{j=1}^{n} {a_j}^2 \prod_{1 \le l < i \le n} (a_l - a_i),$$

we have

$$\det(M) = \prod_{j=1}^{n} k_j {a_j}^2 \prod_{1 \le l < i \le n} (a_l - a_i);$$

then, being k_j, $a_j > 0$ for all $j = 1, \dots, n$ and $a_l < a_i$ for all $l < i$, the matrix M has non-zero determinant. Hence, eliminating the n terms $g_{a_i}(t)$ from equations (3.12) and

substituting into (3.9), we obtain equation (3.8). On the other hand, the substitution of (3.9) into (3.8) leads (3.12).

4 Asymptotic Behavior for Rigid Linear Heat Conductors with Memory via Free Energies

This section is devoted to scrutinize the asymptotic behavior in time of rigid linear heat conductors with memory, *when the memory kernel is finite sum of exponentials*, by means of energy type inequality coming from free energy functionals.

Definition 4.1 A function $\psi\colon \Sigma \to R$ is called a *free energy* if the following conditions are satisfied:

(i) for any $t \geq 0$, the function ψ is differentiable and satisfies the inequality

$$\dot{\psi}(t) \leq -\mathbf{g}(t) \cdot \boldsymbol{q}(t);$$

(ii) the function ψ is minimal only at zero integrated histories of the temperature gradient, namely for every $(\theta(t), \bar{\mathbf{g}}^t) \in \Sigma$

$$\psi(\theta(t), \bar{\mathbf{g}}^t) \geq \psi(\theta(t), \mathbf{0}^\dagger(t)),$$

where $\mathbf{0}^\dagger(s) = \mathbf{0}$, for any $s \geq 0$, is the zero integrated history of the temperature gradient.

Since the systems involved are linear, it is natural to assume that the free energy is a quadratic function of the minimal representation of the state, which is of finite dimension.

We consider the following family of free energies that can be written as functions of $\widetilde{\sigma_R} = [\,\mathbf{g}_{a_1}, \quad \mathbf{g}_{a_2}, \quad \ldots, \quad \mathbf{g}_{a_n}\,]$, namely

$$\psi(t) = \frac{1}{2} \sum_{i,j=1}^{n} C_{ij} a_i a_j \mathbf{g}_{a_i}(t) \cdot \mathbf{g}_{a_j}(t). \tag{4.1}$$

Now, we are looking for suitable algebraic conditions on the symmetric matrix $C = [C_{ij}] \in \mathcal{M}(n,n)$, such that $\psi(t)$ is a free energy, according to Definition 4.1. The following Theorem holds.

Theorem 4.1 *Let $C = [C_{ij}]$, $\Gamma = [\Gamma_{ij}] \in \mathcal{M}(n,n)$. If*

$$\sum_{i=1}^{n} C_{ij} = \sum_{j=1}^{n} C_{ij} = k_j, \quad j = 1, \ldots, n; \tag{4.2}$$

$$\Gamma_{ij} = C_{ij} a_i a_j \, \frac{a_i + a_j}{2}, \quad i, j = 1, \ldots, n; \tag{4.3}$$

C is symmetric and positive semi-definite, Γ is positive semi-definite,

then (4.1) is a free energy in the sense of Definition 4.1.

Proof By virtue of $(3.5)_2$, condition (i) is equivalent to require that

$$\dot{\psi}(t) = \mathbf{g}(t) \cdot \Big(\sum_{i,j=1}^{n} C_{ij} a_j \, \mathbf{g}_{a_j}(t) \Big) - \sum_{i,j=1}^{n} C_{ij} {a_i}^2 a_j \, \mathbf{g}_{a_i}(t) \cdot \mathbf{g}_{a_j}(t) \leq \mathbf{g}(t) \cdot \Big(\sum_{j=1}^{n} a_j k_j \, \mathbf{g}_{a_j}(t) \Big);$$

this inequality is satisfied if and only if

$$\begin{aligned} \sum_{i,j=1}^{n} C_{ij} a_j \, \mathbf{g}_{a_j}(t) &= \sum_{j=1}^{n} a_j k_j \mathbf{g}_{a_j}(t) \\ \sum_{i,j=1}^{n} C_{ij} {a_i}^2 a_j \mathbf{g}_{a_i}(t) \cdot \mathbf{g}_{a_j}(t) &\geq 0. \end{aligned} \tag{4.4}$$

From $(4.4)_1$, we find

$$k_j = \sum_{i=1}^{n} C_{ij} = \sum_{j=1}^{n} C_{ij}, \quad j = 1, \ldots, n.$$

Moreover, observing that

$$\Gamma_{ij} = C_{ij} a_i a_j \, \frac{a_i + a_j}{2}$$

is the symmetric part of the matrix $\Gamma^*_{ij} = C_{ij} {a_i}^2 a_j$, it follows that inequality $(4.4)_2$ is satisfied if and only if the symmetric matrix Γ is positive semi-definite.

With regard to condition (ii), it is easily seen that this holds if and only if the matrix C is positive semi-definite.

Remark 4.1 It is worth noting that in the sequel the matrices C and Γ will be assumed positive definite.

Let $\Omega \subset R^3$ be a bounded domain with Lipschitz boundary $\partial\Omega$. The energy equation for a linear rigid heat conductor is

$$\rho_0 \, e_t = -\nabla \cdot \boldsymbol{q} + \rho_0 \, r \quad \text{in} \;\; \Omega \times R^+, \tag{4.5}$$

where $\cdot_t = d\cdot/dt$, ρ_0 is the constant mass density, the internal energy e and the heat flux $\boldsymbol{q}$ are given by (2.1) and (2.2) respectively.

We take for simplicity $\rho_0 \alpha_0 = 1$ and we denote the source $\rho_0 r$ by f; substituting equations (2.1) and (2.2) into (4.5) and assuming the memory kernel as finite sum of exponentials

$$K(s) = \sum_{i=1}^{n} k_i e^{-a_i \, s},$$

the corresponding initial boundary value problem becomes

$$\begin{aligned} \theta_t(\boldsymbol{x}, t) - \sum_{i=1}^{n} k_i \int_0^{\infty} e^{-a_i \, s} \, \Delta\theta(\boldsymbol{x}\,, t - s) \, ds + f(\theta(\boldsymbol{x}, t)) = 0 \quad &\text{in} \;\; \Omega \times R^+, \\ \theta(\boldsymbol{x}, 0) = \theta_0(\boldsymbol{x}) \quad &\text{in} \;\; \Omega, \\ \theta(\boldsymbol{x}, t) = 0 \quad &\text{in} \;\; \partial\Omega \times R^+. \end{aligned} \tag{4.6}$$

We introduce the vector

$$\boldsymbol{\eta}(t) = (\eta_1(t), \ldots, \eta_n(t)) \,,$$

where

$$\eta_i(t) = \int_0^{\infty} e^{-a_i s} \theta(t - s) \, ds, \quad i = 1, \ldots, n. \tag{4.7}$$

As a consequence, by differentiation with respect to t, we get

$$\eta_{it}(t) = \theta(t) - a_i\,\eta_i(t), \quad i = 1, \dots, n.$$

In view of (4.7), the energy equation in (4.6) transforms into the following system

$$\begin{aligned} \theta_t &= \sum_{i=1}^{n} k_i\,\Delta\eta_i - f(\theta) \qquad\qquad \text{in } \ \Omega \times R^+, \\ \eta_{it} &= \theta - a_i\eta_i, \quad i = 1, \dots, n, \quad \text{in } \ \Omega \times R^+. \end{aligned} \tag{4.8}$$

Initial-boundary conditions are then given by

$$\begin{aligned} \theta(x,0) &= \theta_0(x), \qquad\qquad x \in \Omega, \\ \eta_i(x,0) &= \eta_{i0}(x), \quad i = 1, \dots, n, \quad x \in \Omega, \\ \theta(x,t) &= 0 \qquad\qquad (x,t) \in \partial\Omega \times R^+, \\ \eta_i(x,t) &= 0, \quad i = 1, \dots, n, \quad (x,t) \in \partial\Omega \times R^+. \end{aligned} \tag{4.9}$$

With usual notation, we introduce the spaces $L^2(\Omega)$ and $H_0^1(\Omega)$, acting on Ω. Hereafter, $\langle \cdot, \cdot \rangle$ denotes the L^2-inner product and $\| \cdot \|$ denotes the L^2-norm. If $C = [C_{ij}] \in \mathcal{M}(n,n)$ is positive definite, we put

$$\mathcal{H} = L^2(\Omega) \times \mathcal{W},$$

where

$$\mathcal{W} = \left\{ \boldsymbol{\eta} = (\eta_1, \eta_2, \dots, \eta_n) \in \left[H_0^1(\Omega)\right]^n : \quad \sum_{i,j=1}^{n} \langle \nabla\eta_i,\, C_{ij}\nabla\eta_j \rangle < +\infty \right\}.$$

The corresponding inner product is given by

$$\langle z_1, z_2 \rangle_{\mathcal{H}} = \langle v_1, v_2 \rangle + \sum_{i,j=1}^{n} \langle \nabla w_i, C_{ij}\nabla w_j \rangle,$$

where $z_i = (v_i, w_i) \in \mathcal{H},\ i = 1, 2.$

Definition 4.2 Let $T > 0$ and $f \in L^1\left([0,T]; L^2(\Omega)\right)$. We say that a function $\boldsymbol{z}(t) = (\theta(t), \boldsymbol{\eta}(t)) \in C\left([0,T]; \mathcal{H}\right)$ is a solution of system (4.8)–(4.9) in the time interval $[0,T]$, with initial data $\boldsymbol{z}_0 = \boldsymbol{z}(0) = (\theta_0, \boldsymbol{\eta}_0) \in \mathcal{H}$, if the following identities are satisfied

$$\begin{gathered} \langle \theta_t, \tilde{\theta} \rangle + \sum_{i=1}^{n} k_i \langle \nabla\eta_i, \nabla\tilde{\theta} \rangle + \langle f(\theta), \tilde{\theta} \rangle = 0, \\ \sum_{i,j=1}^{n} \langle \eta_{it}, C_{ij}\Delta\tilde{\eta}_j \rangle - \sum_{i,j=1}^{n} \langle \theta, C_{ij}\Delta\tilde{\eta}_j \rangle + \sum_{i,j=1}^{n} \langle a_i\eta_i, C_{ij}\Delta\tilde{\eta}_j \rangle = 0 \end{gathered}$$

for all $\tilde{\theta} \in H_0^1(\Omega),\ \tilde{\boldsymbol{\eta}} \in \left([H^2(\Omega)]^n \cap \mathcal{W}\right)$ and a.e. $t \in [0,T]$.

We denote by $\mathcal{S}(t)\boldsymbol{z}_0$ the solution of (4.8)–(4.9) with initial data $\boldsymbol{z}_0$. Because the system is autonomous, $\mathcal{S}(t)$ is a strongly continuous semigroup of the continuous operator on $\mathcal{H}$, related to the system (4.8)–(4.9). The total energy associated to (4.8)–(4.9) at time t is

$$\begin{aligned}\mathcal{E}(t) &= \frac{1}{2}\left[\|\theta(t)\|^2 + \sum_{i,j=1}^{n} \langle \nabla\eta_i(t), C_{ij}\nabla\eta_j(t)\rangle\right] \\ &= \frac{1}{2}\left[\int_\Omega |\theta(t)|^2\, d\boldsymbol{x} + \int_\Omega \left|C^{\frac{1}{2}}\nabla\boldsymbol{\eta}(t)\right|_2^2 d\boldsymbol{x}\right].\end{aligned} \tag{4.10}$$

Then, we obtain the following result.

Theorem 4.2 *Let us suppose that $\boldsymbol{z} = (\theta, \boldsymbol{\eta})$ is a solution of system (4.8)–(4.9) in the sense of Definition 4.2. Let $f \in C^1(R)$ satisfying the following hypotheses*

(h1) $\liminf_{|y|\to\infty} \frac{f(y)}{y} \geq 0$;

(h2) *there exists a positive constant β such that $|f'(y)| \leq \beta$, $\forall\, y \in R$.*

If the matrices $C = [C_{ij}]$, $\Gamma = [\Gamma_{ij}] \in \mathcal{M}(n,n)$, defined by (4.2), (4.3) respectively, are positive definite, then there exist positive constants A, Λ, ε such that the relation

$$\mathcal{E}(t) \leq A\, e^{-\varepsilon t}\mathcal{E}(0) + \Lambda \tag{4.11}$$

holds for every $t \geq 0$. In particular, if $f \equiv 0$ then $\Lambda = 0$.

To prove Theorem 4.2 we make use of some preparatory lemmas.

Lemma 4.1 *If $f \in C^1(R)$ satisfies hypotheses (h1) and (h2), then*

(1) *for $\gamma > 0$ there exists a positive constant $\mathcal{C}_\gamma$ such that, $\forall\, y \in H_0^1(R)$*

$$\int_\Omega y\, f(y)\, d\boldsymbol{x} \geq -\gamma \int_\Omega |y|^2\, d\boldsymbol{x} - \mathcal{C}_\gamma; \tag{4.12}$$

(2) $\forall\, y \in R$

$$|f(y)| \leq \beta|y| + |f(0)|. \tag{4.13}$$

Proof Inequality (4.12) follows directly from hypothesis (h1) (cf. [7]); (4.13) is an easy consequence of hypothesis (h2).

Lemma 4.2 *Let $f \in C^1(R)$ satisfying hypothesis (h1); let assume $C, \Gamma \in \mathcal{M}(n,n)$ as in Theorem 4.2. If $\boldsymbol{z} = (\theta, \boldsymbol{\eta})$ is a solution of system (4.8)–(4.9) in the sense of Definition 4.2, then the energy norm (4.10) verifies*

$$\frac{d}{dt}\,\mathcal{E}(t) \leq \gamma \int_\Omega |\theta(t)|^2\, d\boldsymbol{x} + \mathcal{C}_\gamma - \alpha_1 \int_\Omega \left|C^{\frac{1}{2}}\nabla\boldsymbol{\eta}(t)\right|_2^2 d\boldsymbol{x}, \tag{4.14}$$

where γ, $\mathcal{C}_\gamma$, α_1 are positive constants.

Proof If $\boldsymbol{z} = (\theta, \boldsymbol{\eta})$ is a solution of system (4.8)–(4.9), then, recalling (4.2), we have

$$\frac{d}{dt}\,\mathcal{E}(t) = -\langle f, \theta(t)\rangle - \sum_{i,j=1}^{n} \langle \nabla\eta_i(t),\, a_i C_{ij}\nabla\eta_j(t)\rangle.$$

Now, by means of inequality (4.12), we find

$$-\langle f, \theta(t)\rangle \leq \int_\Omega |\theta(t)|^2\, d\boldsymbol{x} + \mathcal{C}_\gamma, \qquad \gamma, \mathcal{C}_\gamma > 0 \tag{4.15}$$

and, thanks to our hypotheses on the matrices $C = [C_{ij}]$ and $\Gamma = [\Gamma_{ij}]$, there exist positive constants $\overline{\alpha_1}$, $\overline{\overline{\alpha_1}}$ such that

$$\begin{aligned} -\sum_{i,j=1}^{n} \langle \nabla\eta_i(t),\, a_i C_{ij} \nabla\eta_j(t)\rangle &= -\sum_{i,j=1}^{n} \left\langle \frac{\nabla\eta_i(t)}{a_i},\, \Gamma_{ij} \frac{\nabla\eta_j(t)}{a_j} \right\rangle \\ &\le -\overline{\alpha_1}\, \|\nabla\boldsymbol{\eta}(t)\|^2 \le -\overline{\alpha_1}\,\overline{\overline{\alpha_1}} \sum_{i,j=1}^{n} \langle \nabla\eta_i(t),\, C_{ij}\nabla\eta_j(t)\rangle. \end{aligned} \tag{4.16}$$

From (4.15) and (4.16), putting $\alpha_1 = \overline{\alpha_1}\,\overline{\overline{\alpha_1}}$, estimate (4.14) follows.

Lemma 4.3 *Suppose that $\boldsymbol{z} = (\theta, \boldsymbol{\eta})$ is a solution of system (4.8) – (4.9) in the sense of Definition 4.2 and assume hypotheses of Theorem 4.2 on f, C and Γ. Introduce the following functional*

$$\mathcal{K}(t) = -\left\langle |\theta(t)|, \sum_{i=1}^{n} k_i\, \eta_i(t) \right\rangle, \quad \forall\, t \ge 0;$$

then we have

$$\begin{aligned} \frac{d}{dt}\mathcal{K}(t) \le{}& \frac{1}{2}(\nu - M_1) \int_{\Omega} |\theta(t)|^2 d\boldsymbol{x} + \mathcal{C}_0 \\ &+ \left[\alpha_2 + \frac{M_1\alpha_3}{2}\left(1 + \frac{\beta^2}{\nu}\right) + \frac{M_2\alpha_4}{2M_1}\right] \int_{\Omega} \left|C^{\frac{1}{2}} \nabla\boldsymbol{\eta}(t)\right|_2^2 dx\,, \end{aligned} \tag{4.17}$$

for some positive constants α_2, α_3, α_4, ν, M_1, M_2, $\mathcal{C}_0$.

Proof The derivative of $\mathcal{K}(t)$ with respect to t entails

$$\frac{d}{dt}\mathcal{K}(t) = \underbrace{-\mathrm{sgn}(\theta)\left\langle \theta_t, \sum_{i=1}^{n} k_i\eta_i \right\rangle}_{=I_1} \underbrace{-\left\langle |\theta|, \sum_{i=1}^{n} k_i\eta_{it} \right\rangle}_{=I_2}. \tag{4.18}$$

Substituting $(4.8)_1$ in the first term at the right-hand side of (4.18) and using Young inequality, we obtain

$$\begin{aligned} I_1 &= -\mathrm{sgn}(\theta)\left\langle \sum_{j=1}^{n} k_j\Delta\eta_j - f, \sum_{i=1}^{n} k_i\eta_i \right\rangle \le \left\| \sum_{i=1}^{n} k_i\, \nabla\eta_i \right\|^2 + \left\langle f, \sum_{i=1}^{n} k_i\, \eta_i \right\rangle \\ &\le n \int_{\Omega} \left(\sum_{i,h=1}^{n} \nabla\eta_i \delta_{ih} {k_i}^2 \nabla\eta_h \right) d\boldsymbol{x} + \left\langle f, \sum_{i=1}^{n} k_i\eta_i \right\rangle \\ &\le n \left| K_\star^{\frac{1}{4}} \left(K_\star^{-\frac{1}{4}} C K_\star^{-\frac{1}{4}} \right)^{-\frac{1}{2}} \right|_2^2 \int_{\Omega} \left| C^{\frac{1}{2}} \nabla\boldsymbol{\eta} \right|_2^2 d\boldsymbol{x} + \underbrace{\left\langle f, \sum_{i=1}^{n} k_i\eta_i \right\rangle}_{=I_3}, \end{aligned}$$

where $K_\star = [\delta_{ih} {k_i}^2] = \mathrm{diag}(k_i^2)$. From (4.13), applying Young and Poincaré inequalities, we find

$$
\begin{aligned}
I_3 &\leq \left\langle \beta|\theta| + |f(0)|, \sum_{i=1}^n k_i \eta_i \right\rangle \\
&\leq \int_\Omega \left[|\theta| \left(\beta \sum_{i=1}^n \left| (k_i)^{\frac{1}{2}} \, (k_i^{\frac{1}{2}} \, \eta_i) \right| \right) \right] d\boldsymbol{x} + \int_\Omega \left(|f(0)| \sum_{i=1}^n \left| (k_i)^{\frac{1}{2}} (k_i^{\frac{1}{2}} \eta_i) \right| \right) d\boldsymbol{x} \\
&\leq \frac{\nu}{2} \|\theta\|^2 + \frac{1}{2} \left(1 + \frac{\beta^2}{\nu} \right) \left(\sum_{i=1}^n k_i \right) \left(\sum_{i=1}^n \frac{k_i}{\lambda_0^i} \|\nabla \eta_i\|^2 \right) + \frac{1}{2} |f(0)|^2 \, \mathrm{vol}(\Omega) \\
&\leq \frac{\nu}{2} \|\theta\|^2 + \frac{1}{2} \left(1 + \frac{\beta^2}{\nu} \right) \left(\sum_{i=1}^n k_i \right) \left(\sum_{i,h=1}^n \langle \nabla \eta_i, \, \delta_{ih} \frac{k_i}{\lambda_0^i} \nabla \eta_h \rangle \right) + \frac{1}{2} |f(0)|^2 \mathrm{vol}(\Omega) \\
&\leq \frac{\nu}{2} \|\theta\|^2 + \frac{1}{2} \left(1 + \frac{\beta^2}{\nu} \right) \left(\sum_{i=1}^n k_i \right) \left| K_\lambda^{\frac{1}{4}} \left(K_\lambda^{-\frac{1}{4}} C K_\lambda^{-\frac{1}{4}} \right)^{-\frac{1}{2}} \right|_2^2 \int_\Omega \left| C^{\frac{1}{2}} \nabla \boldsymbol{\eta} \right|_2^2 d\boldsymbol{x} \\
&\quad + \frac{1}{2} |f(0)|^2 \, \mathrm{vol}(\Omega),
\end{aligned}
$$

where ν and λ_0^i, $i = 1, \ldots, n$, are positive constants and $K_\lambda = \left[\delta_{ih} \, \dfrac{k_i}{\lambda_0^i} \right] = \mathrm{diag} \left(\dfrac{k_i}{\lambda_0^i} \right)$.

By means of $(4.8)_2$, the second term in (4.18) can be written as

$$
I_2 = -\left\langle |\theta|, \sum_{i=1}^n k_i \, (\theta - a_i \, \eta_i) \right\rangle = -\left(\sum_{i=1}^n k_i \right) \|\theta\|^2 + \underbrace{\left\langle |\theta|, \sum_{i=1}^n k_i a_i \eta_i \right\rangle}_{= I_4}.
$$

By virtue of Young and Poincaré inequalities, we have

$$
\begin{aligned}
I_4 &\leq \int_\Omega |\theta| \sum_{i=1}^n \left| (k_i a_i)^{\frac{1}{2}} (k_i \, a_i)^{\frac{1}{2}} \eta_i \right| d\boldsymbol{x} \\
&\leq \frac{\delta}{2} \|\theta\|^2 + \frac{1}{2\delta} \left(\sum_{i=1}^n k_i a_i \right) \left(\sum_{i=1}^n \frac{k_i a_i}{\lambda_0^i} \, \|\nabla \eta_i\|^2 \right) \\
&\leq \frac{\delta}{2} \|\theta\|^2 + \frac{1}{2\delta} \left(\sum_{i=1}^n k_i \, a_i \right) \left(\sum_{i,h=1}^n \left\langle \nabla \eta_i, \, \delta_{ih} \frac{k_i a_i}{\lambda_0^i} \nabla \eta_h \right\rangle \right) \\
&\leq \frac{\delta}{2} \|\theta\|^2 + \frac{1}{2\delta} \left(\sum_{i=1}^n k_i a_i \right) \left| K_a^{\frac{1}{4}} \left(K_a^{-\frac{1}{4}} C K_a^{-\frac{1}{4}} \right)^{-\frac{1}{2}} \right|_2^2 \int_\Omega \left| C^{\frac{1}{2}} \nabla \boldsymbol{\eta} \right|_2^2 d\boldsymbol{x},
\end{aligned}
$$

where δ is a positive constant and $K_a = \left[\delta_{ih} \, \dfrac{k_i a_i}{\lambda_0^i} \right] = \mathrm{diag} \left(\dfrac{k_i \, a_i}{\lambda_0^i} \right)$. Choosing $\delta = \sum\limits_{i=1}^n k_i$, we find

$$
\begin{aligned}
I_2 \leq & -\frac{1}{2} \left(\sum_{i=1}^n k_i \right) \|\theta\|^2 \\
& + \frac{1}{2} \left(\sum_{i=1}^n k_i \right)^{-1} \left(\sum_{i=1}^n k_i a_i \right) \left| K_a^{\frac{1}{4}} \left(K_a^{-\frac{1}{4}} C K_a^{-\frac{1}{4}} \right)^{-\frac{1}{2}} \right|_2^2 \int_\Omega \left| C^{\frac{1}{2}} \nabla \boldsymbol{\eta} \right|_2^2 d\boldsymbol{x}.
\end{aligned}
$$

Finally, collecting the previous inequalities and putting

$$\alpha_2 = n\left|K_\star^{\frac{1}{4}}\left(K_\star^{-\frac{1}{4}}CK_\star^{-\frac{1}{4}}\right)^{-\frac{1}{2}}\right|_2^2, \qquad \alpha_3 = \left|K_\lambda^{\frac{1}{4}}\left(K_\lambda^{-\frac{1}{4}}CK_\lambda^{-\frac{1}{4}}\right)^{-\frac{1}{2}}\right|_2^2,$$
$$\alpha_4 = \left|K_a^{\frac{1}{4}}\left(K_a^{-\frac{1}{4}}CK_a^{-\frac{1}{4}}\right)^{-\frac{1}{2}}\right|_2^2, \qquad M_1 = \sum_{i=1}^n k_i,$$
$$M_2 = \sum_{i=1}^n k_i a_i, \qquad \mathcal{C}_0 = \frac{1}{2}\left|f(0)\right|^2 \mathrm{vol}(\Omega),$$

we obtain (4.17).

At this point, we can prove Theorem 4.2.

Proof For $N > 0$ we introduce the following functional

$$\mathcal{L}(t) = N\mathcal{E}(t) + \mathcal{K}(t), \quad \forall\, t \geq 0;$$

it is easily seen that, if we choose

$$N > \max\left\{1,\, M_1\alpha_3\right\},$$

there exist positive constants

$$\gamma_1 = \min\left\{N-1,\, N - M_1\alpha_3\right\}, \quad \gamma_2 = \max\left\{N+1,\, N + M_1\alpha_3\right\}$$

such that

$$\gamma_1\mathcal{E}(t) \leq \mathcal{L}(t) \leq \gamma_2\mathcal{E}(t), \quad \forall\, t \geq 0. \tag{4.19}$$

Moreover, collecting inequalities (4.14) and (4.17), we have

$$\frac{d}{dt}\mathcal{L}(t) \leq -\left(\frac{M_1}{2} - \frac{\nu}{2} - N\gamma\right)\|\theta\|^2 + \tilde{\Lambda}(N,\gamma,\Omega)$$
$$- \left[N\alpha_1 - \alpha_2 - \frac{M_1\alpha_3}{2}\left(1 + \frac{\beta^2}{\nu}\right) - \frac{M_2\alpha_4}{2M_1}\right]\int\limits_\Omega \left|C^{\frac{1}{2}}\,\nabla\boldsymbol{\eta}\right|_2^2 d\boldsymbol{x},$$

where $\tilde{\Lambda}(N,\gamma,\Omega) = N\mathcal{C}_\gamma + \mathcal{C}_0$. Taking now

$$\nu = \frac{M_1}{2},$$

choosing N large enough such that

$$N \geq N^* = \frac{1}{\alpha_1}\left(\alpha_2 + \frac{M_1\alpha_3}{2} + \alpha_3\beta^2 + \frac{M_2\alpha_4}{2M_1} + \frac{M_1}{8}\right)$$

and letting

$$\gamma = \frac{M_1}{8N},$$

we have

$$\frac{d}{dt}\mathcal{L}(t) \leq -\frac{M_1}{8}\|\theta\|^2 - \frac{M_1}{8}\int\limits_{\Omega}\left|C^{\frac{1}{2}}\,\nabla\boldsymbol{\eta}\right|_2^2 d\boldsymbol{x} + \tilde{\Lambda}\left(N, \frac{M_1}{8N}, \Omega\right). \tag{4.20}$$

By means of (4.19), inequality (4.20) yields

$$\frac{d}{dt}\,\mathcal{L}(t) \leq -\frac{M_1}{4}\,\mathcal{E}(t) + \tilde{\Lambda} \leq -\varepsilon\mathcal{L}(t) + \tilde{\Lambda}\,,$$

where

$$\varepsilon = \frac{M_1}{4\gamma_2}\,.$$

By virtue of the Gronwall Lemma, we obtain

$$\mathcal{L}(t) \leq \mathcal{L}(0)\,\mathrm{e}^{-\varepsilon t} + \frac{\tilde{\Lambda}}{\varepsilon}\left(1 - \mathrm{e}^{-\varepsilon t}\right)\,, \quad \forall\, t \geq 0. \tag{4.21}$$

Finally, from (4.19) and (4.21), it follows that

$$\mathcal{E}(t) \leq \frac{1}{\gamma_1}\,\mathcal{L}(t) \leq \frac{\gamma_2}{\gamma_1}\,\mathcal{E}(0)\,\mathrm{e}^{-\varepsilon t} + \frac{\tilde{\Lambda}}{\varepsilon\gamma_1}$$

holds for every $t \geq 0$, so that taking

$$A = \frac{\gamma_2}{\gamma_1}, \qquad \Lambda = \frac{\tilde{\Lambda}}{\varepsilon\gamma_1}$$

our conclusion follows.

Now, we state the main result of this section.

Theorem 4.3 *Assume $C = [C_{ij}] \in \mathcal{M}(n,n)$ and $f \in C^1(R)$ as in Theorem 4.2. The uniform energy estimate (4.11) implies the existence of a bounded absorbing set $\mathcal{B}^* \subset \mathcal{H}$ for the semigroup $\mathcal{S}(t)$. That is, if $\mathcal{B}^*$ is any ball of $\mathcal{H}$ of radius less than $\sqrt{2\Lambda}$, for any bounded set $\mathcal{B} \subset \mathcal{H}$ there exists $t(\mathcal{B}) \geq 0$ such that*

$$\mathcal{S}(t)\mathcal{B} \subset \mathcal{B}^*, \quad \forall\, t \geq t(\mathcal{B}).$$

Proof The existence of an absorbing set for $\mathcal{S}(t)$ follows directly by (4.11) (see for example [8]).

References

[1] Amendola, G. and Carillo, S. Thermal work and minimum free energy in a heat conductor with memory. *Quarterly J. Mech. Appl. Math.* **57** (2004) 429–446.

[2] Cattaneo, C. Sulla conduzione del calore. *Atti Sem. Mat. Fis. Univ. Modena* **3** (1948) 83–101.

[3] Coleman, B.D. Thermodynamics of materials with memory. *Arch. Rational Mech. Anal.* **17** (1964) 1–46.

[4] Fabrizio, M., Giorgi, C. and Naso, M.G. Viscoelastic solids of exponential type. I. Minimal representations and controllability of the state space. *Meccanica* **39**(6) (2004) 531–546.
[5] Fabrizio, M., Giorgi, C. and Naso, M.G. Viscoelastic solids of exponential type. II. Free energies, stability and attractors. *Meccanica* **39**(6) (2004) 547–561.
[6] Fabrizio, M., Gentili, G. and Reynolds, D.W. On rigid heat conductors with memory. *Int. J. Eng. Sci.* **36** (1998) 765–782.
[7] Ghidaglia, J.M. and Temam, R. Attractors for damped nonlinear hyperbolic equations. *J. Math. Pures Appl.* **66**(3) (1987) 273–319.
[8] Giorgi, C., Muñoz Rivera, J.E. and Pata, V. Global attractors for a semilinear hyperbolic equation in viscoelasticity. *J. Math. Anal. Appl.* **260**(1) (2001) 83–99.
[9] Graffi, D. and Fabrizio, M. On the notion of state for viscoelastic materials of "rate" type. *Atti Accad. Naz. Lincei Rend. Cl. Sci. Fis. Mat. Natur.* **83** (1990) 201–208.
[10] Gurtin, M.E. and Pipkin, A.C. A general theory of heat conduction with finite wave speeds. *Arch. Rational Mech. Anal.* **31** (1968) 113–126.
[11] McCarthy, M. Constitutive equations for thermomechanical materials with memory. *Int. J. Eng. Sci.* **8** (1970) 467–474.
[12] Zabczyk, J. *Mathematical control theory: an introduction*. Birkhäuser Boston Inc., Boston, MA, 1992.

Nonlinear Dynamics and Systems Theory, **6**(2) (2006) 129–142

Dynamics of a Spinning Rocket with Internal Mass Flow

F.O. Eke[1*], T. Tran[2] and J. Sookgaew[3]

[1] *Department of Mechanical and Aeronautical Engineering, University of California, Davis, CA 95616, USA*
[2] *Lockheed-Martin Space Systems Co., Sunnyvale, CA 94089*
[3] *Department of Mechanical Engineering, Prince of Songkla University, Hatyai, Thailand*

Received: September 27, 2005; Revised: June 30, 2006

Abstract: One of the main simplifying assumptions made in the study of the attitude motions of a rocket-type variable mass system is that the motion of the fluid products of combustion relative to the rocket body, as these fluid particles exit the rocket's combustion chamber, remains symmetric with respect to the rocket axis, and the fluid particles have no transverse motion relative to the rocket body. This assumption brings about a tremendous simplification of the equations that govern the attitude motion of a rocket, and is thus very attractive. Yet, one recognizes that such an assumption becomes questionable if the rocket body is allowed to spin. This paper examines the validity of this common assumption. The paper attempts to reconstruct what is lost when this assumption is made, and quantifies the effects on attitude dynamics predictions. Results obtained show that this assumption is in fact reasonable. Although internal fluid whirling motion can cause deviations in spin rate predictions, the actual effects are not dramatic. There is a noticeable impact on the frequencies of the transverse angular velocity components, but the amplitude of the transverse angular velocity vector is largely unaffected.

Keywords: *Rockets; variable mass processes; attitude dynamics.*

Mathematics Subject Classification (2000): 70P05, 70M20, 34C60.

*Corresponding author: foeke@ucdavis.edu

1 Introduction

It has now become quite common to derive the equations of motion of general variable mass systems using the so-called control volume approach [1–4]. This method can capture the overall rigid-body-type motion of the system as well as the details of internal mass flow. Simplifying assumptions are introduced after the equations of motion are derived in order to bring these equations into forms that make further analyses manageable.

Rocket systems constitute one class of variable mass systems that is of interest in the aerospace field. In studying the effects of mass variation on the behavior of rocket systems, the system of interest is often assumed to comprise two phases at any given instant: a solid phase and a fluid phase. The assumptions that are traditionally made in the study of these systems include one concerning the motion of the fluid phase relative to the solid phase. Several studies [1, 3, 5] assume, explicitly or implicitly, that the motion of the fluid products of combustion relative to the solid part of the system is such that each fluid particle has constant velocity that is parallel to the rocket axis. Other studies [3, 6–8] consider that the velocity field of the fluid particles has axial symmetry, and that no "whirling motion" of the fluid phase relative to the solid phase exists. These two assumptions have to do with internal fluid flow within a rocket's combustion chamber. They stipulate that the internal motion of fluid particles relative to the rocket body is symmetric with respect to the rocket axis. In addition, the relative velocity vectors for these particles are assumed not to have a transverse component. In other words, these particles, in their motion relative to the rocket body, are assumed to be incapable of helical motion for example. This is quite reasonable for a rocket that is not spinning, but seems unreasonable for a spinning rocket. It turns out that this assumption can bring tremendous simplifications to the equations that govern rocket motion [3], and this makes the assumption quite attractive.

The goal of this work is to check the validity of this assumption; that is, to evaluate what is lost, if any, by assuming that the velocity vectors of fluid particles within a rocket's combustion chamber have no roll component relative to the rocket body. Wang and Eke [6] took a cursory look at this problem and concluded that the neglect of whirling motion does not affect transverse angular velocity magnitudes, but does affect the frequencies of these quantities. This paper builds on Wang and Eke's work, and presents the results of a more general investigation of how internal fluid whirling motion affects rocket attitude dynamics.

2 Equations of Motion

The type of system that is of interest in this study can be represented by the simple model shown in Figure 2.1. This model considers that the rocket system under study is made up of two main parts — a solid portion B, whose mass is expected to diminish with time as propellant is expended, and the fluid products of combustion F. B is taken to be rigid and symmetric about the z-axis, and is assumed to remain so as parts of it are depleted by combustion. S^* is the instantaneous mass center of the system, and always lies on the z-axis, and C is an imaginary shell that delimits the system.

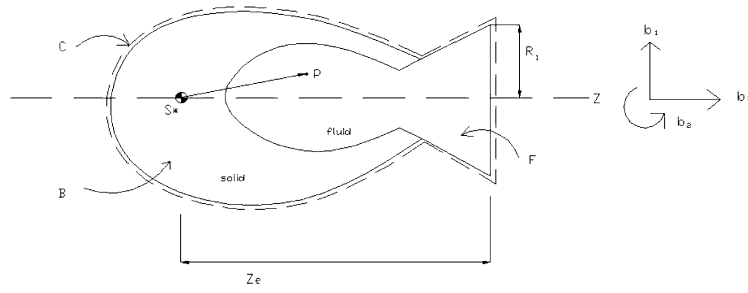

Figure 2.1. Model of a Rocket.

One version of the equation of rotational motion for this type of system has the form [3]

$$\begin{aligned}\mathbf{I}\cdot\boldsymbol{\alpha}+\boldsymbol{\omega}\times\mathbf{I}\cdot\boldsymbol{\omega}+\left(\frac{{}^{B}d\mathbf{I}}{dt}\right)\cdot\boldsymbol{\omega}+\int\limits_{C}\rho[\mathbf{p}\times(\boldsymbol{\omega}\times\mathbf{p})](\mathbf{v}\cdot\mathbf{n})\,dS\\ +\frac{{}^{B}d}{dt}\int\limits_{C}\rho(\mathbf{p}\times\mathbf{v})\,dV+\int\limits_{C}\rho(\mathbf{p}\times\mathbf{v})(\mathbf{v}\cdot\mathbf{n})\,dS+\int\limits_{C}\rho\boldsymbol{\omega}\times(\mathbf{p}\times\mathbf{v})\,dV=\mathbf{M}.\end{aligned}\tag{1}$$

In this equation, $\mathbf{I}$ represents the inertia dyadic of the system, $\boldsymbol{\omega}$ and $\boldsymbol{\alpha}$ are the inertial angular velocity and angular acceleration respectively of B, ρ is the mass density, $\mathbf{p}$ is the position vector from the system's mass center S^* to a generic particle P of the system, $\mathbf{v}$ is the velocity of P relative to the main body B, $\mathbf{n}$ is a unit outward normal to the surface C, and $\mathbf{M}$ is the resultant moment about S^* of all the external forces on the system. The left superscript on the time derivative simply indicates that the derivative is to be taken while the reference frame B is kept fixed.

If we assume that $\boldsymbol{\omega}$ has the form,

$$\boldsymbol{\omega}=\omega_1\mathbf{b}_1+\omega_2\mathbf{b}_2+\omega_3\mathbf{b}_3\tag{2}$$

and that

$$\mathbf{I}=I(\mathbf{b}_1\mathbf{b}_1+\mathbf{b}_2\mathbf{b}_2)+J\mathbf{b}_3\mathbf{b}_3\tag{3}$$

where the unit vector basis $\mathbf{b}_1$, $\mathbf{b}_2$, $\mathbf{b}_3$ is fixed in B and oriented as in Figure 2.1, then, the first three terms of equation (1) can be written as

$$\mathbf{I}\cdot\boldsymbol{\alpha}=I(\dot{\omega}_1\mathbf{b}_1+\dot{\omega}_2\mathbf{b}_2)+J\dot{\omega}_3\mathbf{b}_3,\tag{4}$$

$$\boldsymbol{\omega}\times\mathbf{I}\cdot\boldsymbol{\omega}=(J-I)\omega_3(\omega_2\mathbf{b}_1-\omega_1\mathbf{b}_2)\tag{5}$$

and

$$\left(\frac{{}^{B}d\mathbf{I}}{dt}\right)\cdot\boldsymbol{\omega}=\dot{I}(\omega_1\mathbf{b}_1+\omega_2\mathbf{b}_2)+\dot{J}\omega_3\mathbf{b}_3.\tag{6}$$

The fourth term of equation (1) has been evaluated by several authors and shown to depend on the velocity field of exhaust gas particles as they cross the nozzle exit plane. For uniform velocity profile with constant exhaust gas velocity u, the rate at which mass is lost from the system is

$$\dot{m}=-\pi\rho uR_1^2\tag{7}$$

and the fourth term can be expressed as (see for example Wang [6])

$$\int_C \rho[\mathbf{p} \times (\boldsymbol{\omega} \times \mathbf{p})](\mathbf{v} \cdot \mathbf{n})\, dS = -\dot{m}\left[\left(z_e^2 + \frac{R_1^2}{4}\right)(\omega_1 \mathbf{b}_1 + \omega_2 \mathbf{b}_2) + \frac{R_1^2}{2}\,\omega_3 \mathbf{b}_3\right] \tag{8}$$

where the distances z_e and R_1 are as shown in Figure 2.1. None of these first four terms is affected by the introduction of fluid whirling motion. This is so because the first three terms do not contain the fluid velocity vector at all, and the fourth term only involves the axial component of this velocity. We recall that whirling motion comes from the existence of a transverse component of the fluid relative velocity.

The fifth term of equation (1) vanishes if one makes the assumption that fluid flow within the system's combustion chamber has reached steady state — a generally reasonable approximation, which will be assumed to hold here. We are then left with the last two terms on the left hand side of equation (1):

$$\mathbf{M}_6 = \int_C \rho(\mathbf{p} \times \mathbf{v})(\mathbf{v} \cdot \mathbf{n})\, dS \tag{9}$$

and

$$\mathbf{M}_7 = \int_C \rho\boldsymbol{\omega} \times (\mathbf{p} \times \mathbf{v})\, dV. \tag{10}$$

Each of these contains the vector $\mathbf{v}$, which represents the velocity vector of a generic fluid particle relative to the rocket's main body. Spin motion of the rocket body introduces helical or whirling motion of the fluid particles, and this in turn influences $\mathbf{v}$, and hence both $\mathbf{M}_6$ and $\mathbf{M}_7$. We note that if whirling motion is ignored, then (see [3])

$$\mathbf{M}_6 = \mathbf{M}_7 = 0 \tag{11}$$

and equation (1) is simplified tremendously. This is one reason the "no whirling motion" assumption has remained very attractive in the study of rocket dynamics. To assess the impact of fluid whirling motion on rocket dynamics, we will start by determining expressions for the quantities $\mathbf{M}_6$ and $\mathbf{M}_7$ when whirling motion is present.

3 The Surface Integral Term

Consider a generic fluid particle within the combustion chamber of a rocket as this fluid particle crosses the nozzle exit plane. Such a particle is shown as point P in Figure 3.1. The position vector of P from the system mass center can be written as

$$\mathbf{p} = x\mathbf{e}_x + z_e\mathbf{e}_z \tag{12}$$

and its velocity relative to the rocket body B has the general form

$$\mathbf{v} = v_x\mathbf{e}_x + v_\theta\mathbf{e}_\theta + v_z\mathbf{e}_z \tag{13}$$

where $\mathbf{e}_x$, $\mathbf{e}_\theta$, and $\mathbf{e}_z$ are the unit vectors normally associated with the use of cylindrical coordinates, and are as shown in Figure 3.1. For the particle P,

$$(\mathbf{p} \times \mathbf{v})_p = -z_e v_\theta \mathbf{e}_x + (z_e v_x - x v_z)\mathbf{e}_\theta + x v_\theta \mathbf{e}_z. \tag{14}$$

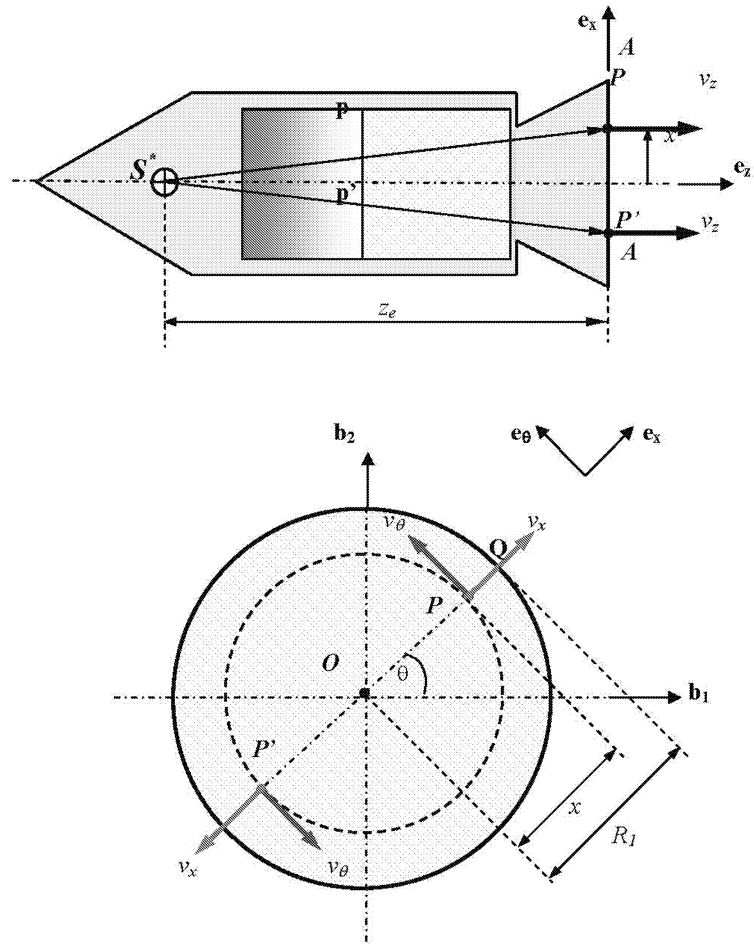

Figure 3.1. A generic fluid particle P at the nozzle exit plane.

If motion of the fluid particles relative to the rocket body is assumed to be axisymmetric with respect to the z-axis, then, for each particle such as P, there always exists another particle P' on the nozzle exit plane, located at the same radial distance x from the rocket axis, and 180 degrees away from P, and for which

$$(\mathbf{p} \times \mathbf{v})_{P'} = z_e v_\theta \mathbf{e}_x - (z_e v_x - x v_z)\mathbf{e}_\theta + x v_\theta \mathbf{e}_z. \tag{15}$$

Hence, the combined contributions of P and P' to $\mathbf{M}_6$ in equation (9) has neither a radial nor a transverse component, so that one need only evaluate the axial component of the surface integral $\mathbf{M}_6$. In other words,

$$\mathbf{M}_6 = (\mathbf{M}_6 \cdot \mathbf{e}_z)\mathbf{e}_z = \mathbf{e}_z \int_C \rho \mathbf{p} \cdot (\mathbf{v} \times \mathbf{e}_z)(v_z)\, dS = \mathbf{e}_z \int_C \rho x v_\theta v_z \, dS. \tag{16}$$

The axisymmetry assumption stated above also leads to the conclusion that neither v_z nor v_θ depends on the angle θ. However, both can depend on the distance x from the rocket axis. We can re-write equation (16) as

$$\mathbf{M}_6 = \left[2\pi\rho \int_0^{R_1} x^2 v_\theta u \, dx\right] \mathbf{b}_3. \tag{17}$$

This expression assumes a constant axial velocity u for fluid particles as well as a constant fluid density over the nozzle exit plane.

To make further progress with equation (17), the manner in which v_θ varies with x must be determined. To this end, we will assume that at steady state, the motion of a typical fluid particle relative to the rocket body, as the particle moves towards the nozzle exit plane, is such that the path of the particle has the approximate shape of a helix centered on the rocket axis. We immediately recognize that the transverse component of the velocity of such a particle is influenced mainly by the spin motion of the rocket body. This leads us to start the process of determining an expression for v_θ by making the additional simplifying assumption that the axial motion of the fluid particles is decoupled from their transverse motion. This means that the transverse motion of the fluid particles can be understood by considering only the spin motion of the rocket body. Thus, we consider in Figure 3.2, that initially, the rocket body B, including the nozzle and the fluid it contains, is stationary. Next, B is given a spin rate ω_3 as shown. Friction causes the fluid particle Q in contact with the nozzle wall to acquire an inertial velocity $\omega_3 R_1$ in the transverse direction, while the fluid particle O on the spin axis remains stationary. Those fluid particles between O and Q acquire speeds that vary between zero and $\omega_3 R_1$. For the range of spin rates normally encountered in rocket dynamics, the speed distribution between O and Q would be linear, and the relationship between the speed of the fluid particle P at a distance x from O and the fluid particle at Q would be

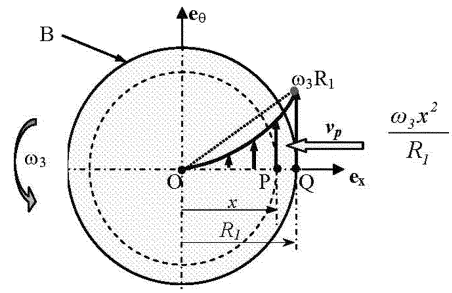

Figure 3.2. Fluid velocity distribution.

$$v^P/v^Q = x/R_1 \tag{18}$$

so that

$$\mathbf{v}^P = (x/R_1)v^Q \mathbf{e}_\theta = \omega_3 x \mathbf{e}_\theta. \tag{19}$$

On the other hand, the fictitious particle P_O of B that is coincident with the fluid particle P at the instant under consideration also has velocity

$$\mathbf{v}^{P_O} = \omega_3 x \mathbf{e}_\theta. \tag{20}$$

P would then have zero velocity relative to the rocket body; a fact that seems at odds with what would be expected if such an experiment were actually performed.

The decoupling of the axial fluid velocities from the transverse velocities has one major flaw — it implies that one is dealing with linear phenomena. Furthermore, the assumption that the velocity distribution between points O and Q is linear requires that the flow be laminar (not turbulent). What is most likely in reality is that the combination of very high axial fluid velocities found inside rocket combustion chambers, together with the relatively slow transverse motion of the fluid particles, as well as the changing combustion chamber geometry will result in overall turbulent and complex flow of the fluid products of combustion. It is thus most unlikely that spinning of the rocket body will introduce a linear distribution of transverse fluid velocities between points O and Q; in other words, the relative transverse speeds for the fluid particles are not likely to be zero. The velocity function v_θ is likely to be quite complex, with no simple closed form expression.

One way to move this analysis forward is to make reasonable guesses for the function v_θ. We adopt this approach and assume that the velocity distribution between points O and Q of Figure 3.2 is not linear, but parabolic. One then finds that

$$\mathbf{v}^P = (\omega_3 x^2/R_1)\mathbf{e}_\theta \tag{21}$$

and hence, the transverse speed of the general fluid particle P relative to the spinning body B becomes

$$v_\theta = \omega_3 x\left(\frac{x}{R_1} - 1\right). \tag{22}$$

We now substitute equation (22) into (17) to obtain

$$\mathbf{M}_6 = \left[2\pi \int_0^{R_1} \rho\left(\frac{x}{R_1} - 1\right)\omega_3 u x^3 dx\right]\mathbf{b}_3 = -\frac{\pi\rho u\omega_3 R_1^4}{10}\,\mathbf{b}_3 = \frac{\dot{m}\omega_3 R_1^2}{10}\,\mathbf{b}_3. \tag{23}$$

Clearly, $\mathbf{M}_6$ will have some influence on the spin rate but will not affect the transverse components of the rocket's angular velocity.

4 The Volume Integral Term

In this section, we determine an explicit expression for the seventh term of equation (1). This term is also shown as equation (10) above, and is a volume integral to be taken over the entire region of the combustion chamber, where fluid flow occurs. We note that this region's volume varies with time as propellant burn progresses, a fact that complicates the evaluation of the integral.

For a general axisymmetric combustion chamber such as the one shown in Figure 4.1, the vector $\mathbf{M}_7$ can be written as

$$\mathbf{M}_7 = \boldsymbol{\omega} \times \int_C (\rho\mathbf{p} \times \mathbf{v})\, dV = \boldsymbol{\omega} \times \boldsymbol{\Gamma} \tag{24}$$

where

$$\boldsymbol{\Gamma} = \int_C (\rho\mathbf{p} \times \mathbf{v})\, dV. \tag{25}$$

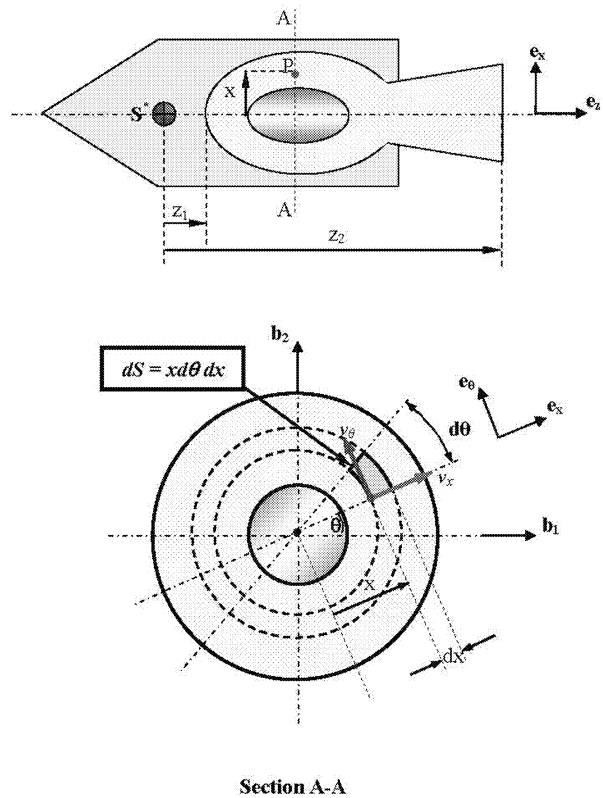

Figure 4.1. General axisymmetric combustion chamber.

We can let $\mathbf{p}$, which represents the position vector from the system mass center to a generic fluid particle P inside the combustion chamber, be

$$\mathbf{p} = x\mathbf{e}_x + z\mathbf{e}_z \tag{26}$$

while a general expression for the velocity of P remains as given in equation (13). The axisymmetric nature of both the combustion chamber and the fluid flow therein allows us to invoke the same arguments presented in the evaluation of $\mathbf{M}_6$, and these lead us to conclude that $\mathbf{\Gamma}$ is parallel to $\mathbf{e}_z$ or $\mathbf{b}_3$. Hence, equation (25) becomes

$$\mathbf{\Gamma} = \mathbf{e}_z \int_C (\rho\mathbf{p} \times \mathbf{v}) \cdot \mathbf{e}_z \, dV = \mathbf{b}_3 \int_C \rho x^2 v_\theta \, dx \, d\theta \, dz. \tag{27}$$

Equations (2) and (27) are now substituted into (24), and, assuming that the fluid density is constant at steady state, we obtain (see also Figure 4.1)

$$\mathbf{M}_7 = \left(2\pi\rho \int_{z_1}^{z_2} \int_x x^2 v_\theta \, dx \, dz \right) (\omega_2 \mathbf{b}_1 - \omega_1 \mathbf{b}_2). \tag{28}$$

Because $\mathbf{M}_7$ has no $\mathbf{b}_3$ component, it cannot have any influence on the spin rate.

The integral in equation (28) depends on the shape of the combustion chamber, and this in turn depends on the propellant burn type. We will thus need to stipulate a specific propellant burn scenario before the corresponding expression for $\mathbf{M}_7$ can be determined. The idealized propellant burn geometries that are closest to what obtains in real systems are those that have been described in the literature [7–9] as the end burn, the radial burn, and the uniform burn. Even for these idealized burn patterns, the true shape of the combustion chamber during the propellant burn remains quite complex. To simplify the task of evaluating the volume integral $\mathbf{M}_7$, we restrict this part of the analysis to a rocket model often referred to as the variable mass cylinder [7]. This is a very simple model that considers a rocket to be a solid right circular cylinder, made entirely of combustible material, and that burns while it flies around in space.

The end burn is the most useful propellant burn geometry for the variable mass cylinder. To see why this is so, we direct attention to Figure 4.2, which shows a typical rocket system that consists of the payload and several stages of the propulsion system. The rocket motor for each stage carries solid or liquid propellant that burns to generate propulsive force. Typically, solid fuel is burnt from inside out, somewhat similar to what we have referred to as radial burn. However, the fact that the fuel is generally located close to one end of the rocket system, means that the effect of this burn on the overall system geometry and mass/inertia properties, is reasonably well approximated by the end burn when the overall system is modeled as a cylinder. We will therefore only consider the end-burn whenever we model a rocket as a burning cylinder.

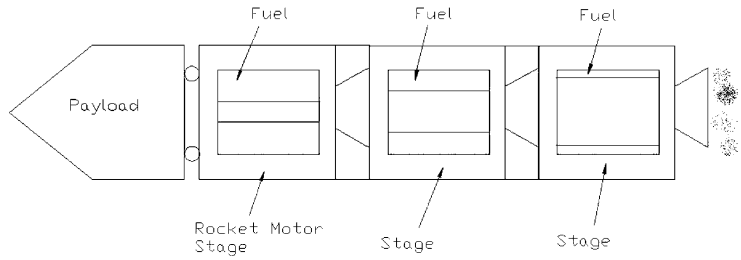

Figure 4.2. Typical rocket system.

For the end burning cylinder, the combustion chamber at any given instant has the shape of a cylinder of radius R, and whose length varies uniformly with the burn, as shown in Figure 4.3. In this case, $\mathbf{M}_7$ becomes

$$\begin{aligned}\mathbf{M}_7 &= \left(2\pi\rho \int_z^L \int_0^R x^2 v_\theta \, dx \, dz\right)(\omega_2 \mathbf{b}_1 - \omega_1 \mathbf{b}_2) \\ &= 2\pi\rho(L-z)\left(\int_0^R x^2 v_\theta \, dx\right)(\omega_2 \mathbf{b}_1 - \omega_1 \mathbf{b}_2).\end{aligned} \tag{29}$$

We assume that the expression obtained for v_θ in the previous section [see equation (22)] holds here, so that

$$\mathbf{M}_7 = -\frac{1}{10}\,\pi\rho R^4 (L-x)\omega_3(\omega_2 \mathbf{b}_1 - \omega_1 \mathbf{b}_2). \tag{30}$$

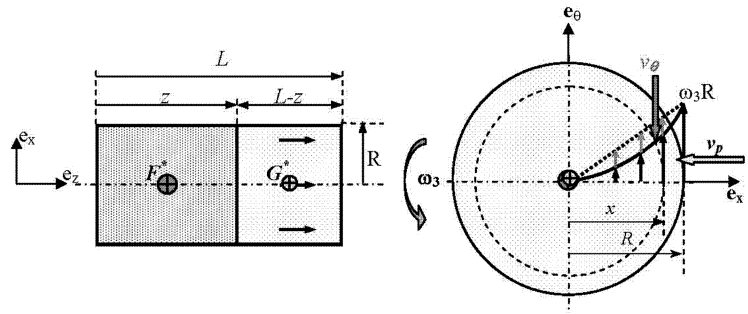

Figure 4.3. The end burning cylinder.

The mass flow rate can be introduced into equation (30), as was done earlier for the vector $\mathbf{M}_6$. For uniform exit velocity profile, $\mathbf{M}_7$ then becomes

$$\mathbf{M}_7 = \frac{\dot{m}R^2(L-z)}{10u}\,\omega_3(\omega_2\mathbf{b}_1 - \omega_1\mathbf{b}_2). \tag{31}$$

5 Scalar Equations of Attitude Motion

Now that the explicit expression for each term of equation (1) has been determined, including those contributed by fluid whirling motion, we are in a position to write the complete scalar equations of rotational motion. Using equations (4), (5), (6), (8), (23), and (31), and assuming the external moment $\mathbf{M}$ is zero, equation (1) can be broken into its scalar components along the $\mathbf{b}_1$, $\mathbf{b}_2$, and $\mathbf{b}_3$ directions respectively as follows:

$$I\dot{\omega}_1 + \left[\dot{I} - \dot{m}\left(z_e^2 + \frac{R^2}{4}\right)\right]\omega_1 + [(J-I)\omega_3 + \Delta\omega_3]\omega_2 = 0, \tag{32}$$

$$I\dot{\omega}_2 + \left[\dot{I} - \dot{m}\left(z_e^2 + \frac{R^2}{4}\right)\right]\omega_2 - [(J-I)\omega_3 + \Delta\omega_3]\omega_1 = 0, \tag{33}$$

and

$$J\dot{\omega}_3 + \left(\dot{J} - \dot{m}\,\frac{R_1^2}{2}\right)\omega_3 + \frac{1}{10}\,\dot{m}R_1^2\omega_3 = 0 \tag{34}$$

where

$$\Delta = \frac{\dot{m}(L-z)R^2}{10u}. \tag{35}$$

Equations (32) and (33) are only valid for the cylinder model, while equation (34) holds for a more general representation of a rocket because the term $\mathbf{M}_7$ that forced a return to the cylinder model contributes nothing to (34). The Δ term in equations (32) and (33), and the last term on the left hand side of (34) are contributed by fluid whirling motion.

6 Spin Motion

We now assess how the rocket's spin rate is affected by the inclusion of the extra term due to fluid whirling motion. The spin rate is obtainable from equation (34) and has the form

$$\frac{\omega_3(t)}{\omega_3(0)} = \exp\left[-\int_0^t \frac{\psi(t)}{J}\, dt \right] \tag{36}$$

where

$$\psi(t) = \psi_1(t) + \psi_2(t) + \psi_3(t) = \dot{J} - \frac{1}{2}\,\dot{m}R_1^2 + \frac{1}{10}\,\dot{m}R_1^2 \tag{37}$$

with

$$\psi_1(t) = \dot{J}, \quad \psi_2(t) = -\frac{1}{2}\,\dot{m}R_1^2, \quad \psi_3(t) = \frac{1}{10}\,\dot{m}R_1^2. \tag{38}$$

We know from equation (36) that the spin rate increases or decreases depending on the sign of $\psi(\tau)$: a positive sign indicates a decrease in spin rate, while a negative sign points to an increase in spin rate. The rate of change of the system's axial moment of inertia $\dot{J}$ and the mass flow rate $\dot{m}$ are negative quantities. Hence, $\psi_1(\tau)$ will tend to augment the spin rate, while $\psi_2(\tau)$ does the opposite. $\psi_3(\tau)$, which is contributed by internal fluid whirling motion, is a negative quantity. This means that fluid whirling motion tends to increase the spin rate value. In other words, an analysis that ignores fluid whirling motion will predict spin rate values that are less than those resulting from an analysis in which whirling motion is accounted for. In the remainder of this section, $\omega_3(t)$ will continue to represent the spin rate solution when fluid whirling motion is accounted for, while $\omega_{3nw}(t)$ will be used for the spin rate solution when whirling motion is neglected (i.e. when $\psi_3(\tau)$ is dropped).

For the specific case of a variable mass cylinder in end burn (see Figure 4.3),

$$\begin{aligned} \frac{\omega_3(t)}{\omega_3(0)} &= \exp\left[-\int_0^t \frac{\dot{J}}{J}\, dt + \frac{R^2}{2}\int_0^t \frac{\dot{m}}{J}\, dt - \frac{R^2}{10}\int_0^t \frac{\dot{m}}{J}\, dt \right] \\ &= \exp\left[-\ln\frac{J(t)}{J(0)} + \ln\frac{m(t)}{m(0)} - \frac{1}{5}\ln\frac{m(t)}{m(0)} \right] = \exp\left(-\frac{1}{5}\ln\frac{m(t)}{m(0)} \right). \end{aligned} \tag{39}$$

Observe that

$$\omega_{3nw}(t) = \omega_3(0). \tag{40}$$

Hence, if whirling motion is not accounted for, the spin rate for a spinning rocket is predicted to remain constant at its initial value. This is in fact quite close to what is observed in real flight. On the other hand, if whirling motion is accounted for, the predicted spin rate is somewhat higher. The percentage deviation of $\omega_3(t)$ from $\omega_{3nw}(t)$ is

$$D = \frac{\omega_3 - \omega_{3nw}}{\omega_{3nw}}\, 100 = 100\left[\left(\frac{m(0)}{m(t)} \right)^{1/5} - 1 \right] = 100\left[\left(\frac{L}{z} \right)^{1/5} - 1 \right]. \tag{41}$$

An equivalent z/L for a real rocket is very small, hence D is very small. We conclude then that accounting for whirling motion does not change the predicted spin rate by much.

7 Transverse Motion

We continue the investigation of the effects of internal whirling motion of fluid products of combustion on the attitude behavior of variable mass systems of the rocket type by examining the lateral or transverse attitude motion of such systems. The interest here is in the evolution with time, of the transverse angular velocity components ω_1 and ω_2 as the rocket's propellant burns. The variables ω_1 and ω_2 are governed by equations (32) and (33), which we combine and re-write in the form

$$\dot{\omega}_c = -\frac{1}{I}\left\{\left[\dot{I} - \dot{m}\left(z_e^2 + \frac{R^2}{4}\right)\right] - j[(J-I)+\Delta]\,\omega_3\right\}\omega_c \tag{42}$$

where

$$\omega_c = \omega_1 + j\omega_2 \tag{43}$$

with

$$j = \sqrt{-1} \tag{44}$$

and ω_3 is now a known function of time.

Equation (42) is integrated, leading to

$$\omega_c(t) = \omega_c(0)\Lambda(t)\exp[j\Theta(t)] \tag{45}$$

where

$$\Theta(t) = \int_0^t \frac{(J-I)+\Delta}{I}\,\omega_3\,dt \tag{46}$$

and

$$\Lambda(t) = \exp\left[-\int_0^t \frac{\dot{I} - \dot{m}(z_e^2 + R^2/4)}{I}\,dt\right]. \tag{47}$$

Equation (45) indicates that both components of the transverse angular velocity vector oscillate with varying amplitude and varying frequency. The function $\Lambda(t)$ controls the amplitude of these oscillations while Θ determines the frequency. We recall that in the differential equations governing ω_1 and ω_2 (see equations (32) and (33)), the terms containing Δ are the only terms contributed by fluid whirling motion. $\Lambda(t)$ contains no such terms, but Θ does. Hence, we can state that internal fluid whirling motion has no effect on the amplitude of the transverse angular velocity vector. However, the frequency predicted for the transverse angular velocity components when the no-whirling-motion assumption is made will generally differ from that obtained when whirling motion is accounted for.

From equation (46), we can write

$$\Theta(t) = \Theta_1(t) + \Theta_2(t) \tag{48}$$

where

$$\Theta_1(t) = \int_0^t \frac{J-I}{I}\,\omega_3\,dt \tag{49}$$

and

$$\Theta_2(t) = \int_0^t \frac{\Delta}{I}\,\omega_3\,dt = \int_0^t \frac{\dot{m}(L-z)R^2}{10uI}\,\omega_3\,dt. \tag{50}$$

If fluid whirling motion is ignored, $\Theta_2(t) = 0$. Otherwise, it is a negative quantity that increases in absolute value with time. On the other hand, the sign of $\Theta_1(t)$ depends on whether the overall rocket system is oblate or prolate in shape. For an oblate system, $J/I > 1$, and $\Theta_1(t)$ is positive and increases with time. For a prolate system — the most likely case — $J/I < 1$, and $\Theta_1(t)$ is negative and increases in absolute value with time. In summary, if fluid whirling motion is ignored, only $\Theta_1(t)$ determines the frequency. This means that the frequency of the transverse angular velocity will increase with time both for prolate and oblate systems. On the other hand, if whirling motion is accounted for in the modeling of the system under study, then the frequency will increase with time for prolate systems, and will be higher at all times than that predicted for no-whirling-motion. This is due to the fact that $\Theta_2(t)$ is then non-zero, and also the fact that the quantity $\omega_3(t)$ appearing in equation (50) is always greater for whirling motion than for no-whirling motion.

For oblate systems, $\Theta_1(t)$ will be positive and growing, while $\Theta_2(t)$ is negative and decreasing (growing in absolute value). So, the frequency could grow or decrease with time. What is clear though, is that the frequency in this case will always be less than the frequency for prolate systems. Finally, we observe that the frequency predicted when whirling motion is accounted for could, in this case, be less than that predicted when whirling motion is neglected.

8 Conclusion

This study evaluates the impact that helical motion of fluid products of combustion within the combustion chamber of a rocket can have on the attitude dynamics of rocket systems. Analysis performed using a variable mass cylinder as a model for rocket systems shows that spin rate predictions made with the no-whirling-motion assumption will be less than those which would have been predicted if whirling motion were properly accounted for. However, the deviation from the "correct" spin rate will be quite small.

The amplitude of a rocket's transverse angular velocity is unaffected by fluid whirling motion. The only impact that fluid whirling motion has on a rocket's transverse rotational motion shows up in the frequencies of the transverse angular velocity components of the rocket body. The degree to which these frequencies are affected also depends on the ratio of the system's spin inertia to its transverse inertia; in other words, on whether the system is prolate or oblate. If whirling motion is accounted for in the modeling of a prolate rocket system, the frequency of the transverse angular velocity components will be found to increase with time, and will be higher at all times than the frequency predicted with a no-whirling-motion assumption. For oblate systems, a model that takes whirling motion into account will show that the frequency of rocket transverse motion can increase or decrease with time, but will always be less than the frequency for a prolate system. Ignoring whirling motion can result in a higher or lower frequency.

References

[1] Meirovitch, L. General motion of a variable mass flexible rocket with internal flow. *Journal of Spacecraft and Rockets* **7**(2) (1970) 186–195.
[2] Belknap, S.B. A general transport rule for variable mass dynamics. *AIAA Journal* **10**(9) (1972) 1137–1138.
[3] Eke, F.O. and Wang, S.M. Equations of motion of two-phase variable mass systems with solid base. *Journal of Applied Mechanics* **61**(4) (1994) 855–860.
[4] Eke, F.O. and Mao, T.C. On the dynamics of variable mass systems. *The Int. J. of Mechanical Engineering Education* **30**(2) (2002) 123–137.
[5] Thomson, W.T. Equations of motion for the variable mass system. *AIAA Journal* **4**(4) (1966) 766–768.
[6] Wang, S.M., and Eke, F.O. Rotational dynamics of axisymmetric variable mass systems. *J. of Appl. Mechanics* **62**(4) (1995) 970–974.
[7] Mao, T.C. and Eke, F.O. Attitude dynamics of a torque-free variable mass cylindrical body. *The Journal of the Astronautical Sciences* **48**(4) (2000) 435–448.
[8] Sookgaew, J. and Eke, F.O. Effects of substantial mass loss on the attitude motions of a rocket-type variable mass system. *Nonlinear Dynamics and Systems Theory* **4**(1) (2004) 73–88.
[9] Eke, F.O. and Sookgaew, J. Influence of propellant burn pattern on the attitude dynamics of a spinning rocket. *Nonlinear Dynamics and Systems Theory* **5**(3) (2005) 251–264.

Nonlinear Dynamics and Systems Theory, **6**(2) (2006) 143–158

Robust Dynamic Parameter-Dependent Output Feedback Control of Uncertain Parameter-Dependent State-Delayed Systems

H.R. Karimi*

Control & Intelligent Processing Center of Excellence, ECE, Faculty of Engineering, University of Tehran, P. O. Box: 14395-515, Tehran, Iran

Received: June 29, 2005; Revised: April 27, 2006

Abstract: In this paper, we investigate the problem of robust dynamic parameter-dependent output feedback (RDP-DOF) stabilization under H_∞ performance index for a class of linear time invariant parameter-dependent (LTIPD) systems with multi-time delays in the state vector and in the presence of norm-bounded non-linear uncertainties. Using Hamiltonian–Jacobi–Isaac (HJI) method and the idea of polynomial parameter-dependent quadratic (PPDQ) Lyapunov–Krasovskii functions, a new sufficient condition is derived to ensure robust asymptotic stability and robust disturbance attenuation of the closed-loop system. Finally, an example is included that demonstrates the application of the results.

Keywords: *Parameter-dependent systems; multi-time delays; linear matrix inequality; robust dynamic parameter-dependent.*

Mathematics Subject Classification (2000): 34D20, 93A30, 93B36.

1 Introduction

The stability analysis and control design of linear time invariant parameter-dependent (LTIPD) systems where the state-space matrices depend affinely on parameter vector, whose values are not known *a priori*, but can be measured online for control process, have received considerable attention recently (see for instance [1, 2, 3, 5, 6, 18, 23, 25, 26, 28, 31] and the references therein). In many industrial applications, like flight control and process control, the operating point can indeed be determined from measurement, making the LTIPD approach viable, see for example [21, 24]. Establishing stability via the use of

*Corresponding author: hrkarimi@iat.uni-bremen.de, hrkarimi@ut.ac.ir

classical quadratic Lyapunov function is conservative for the LTIPD systems. To investigate the stability of LTIPD systems one needs to resort the use of parameter-dependent Lyapunov functions to achieve necessary and sufficient conditions of system stability, see [7, 10, 11, 14, 16, 30]. However, Bliman in [10] proposed robust stability analysis for LTIPD systems with polytopic uncertain parameters. He also developed some conditions for robust stability in terms of solvability of some linear matrix inequalities (LMIs) without conservatism. Moreover, the existence of a polynomial parameter-dependent quadratic (PPDQ) Lyapunov function for parameter-dependent systems, which are robustly stable, is stated in [11]. Recently, sufficient conditions for robust stability of the linear state-space models affected by polytopic uncertainty have been provided in [12] using homogeneous polynomial parameter-dependent quadratic Lyapunov functions, which are formulated in terms of LMI feasibility tests.

On the other hand, time delays are often present in engineering systems, which have been generally regarded as a main source on instability and poor performance. Therefore, the stabilization of LTIPD state-delayed systems is a field of intense research. Generally, a way to ensure stability robustness with respect to the uncertainty in the delays is to employ stability criteria valid for any nonnegative value of the delays that is *delay-independent results*. This assumption that no information on the value of the delay is known is often coarse in practice. Recently, a systematic way for the use of PPDQ Lyapunov functions in the *state feedback control* of the LTIPD systems with time-delay in the state vector was proposed in [19]. It was also shown that the PPDQ Lyapunov-Krasovskii functions make some *sufficient conditions* under the form of linear matrix inequalities (LMIs).

In this paper, we extend the robust parameter-dependent state-feedback stabilization problem of the LTIPD state-delayed systems in [9, 19] to *robust dynamic parameter-dependent output feedback* (RDP-DOF) control synthesis problem for the LTIPD systems with multi-time delays in the state vector and in the presence of norm-bounded non-linear uncertainties based on the Hamiltonian–Jacoby–Isaac (HJI) method. It is provided a systematic framework for the use of the PPDQ Lyapunov functions in the issue of RDP-DOF stabilization with preserving H_∞ performance criteria. Delay-independent stabilization problem of the system is stated in terms of some LMIs. It would be shown that the use of HJI method makes a *sufficient condition* to have a parameter-dependent bilinear matrix inequality (BMI) optimization problem; thereafter, parameter-independent BMI optimization problem is derived utilizing the PPDQ Lyapunov functions. Therefore, a complete synthesis technique is developed and solving a parameter-independent LMI and a set of linear algebraic equations can construct the RDP-DOF matrices. The simulation results show that the obtained RDP-DOF control can achieve the delay-independent stability and disturbance attenuation of the closed-loop system, simultaneously.

The notations used throughout the paper are fairly standard. The matrices I_n, 0_n and $0_{n\times p}$ are the identity matrix, the $n \times n$ and $n \times p$ zero matrices, respectively. The symbol $\otimes$ denotes Kronecker product, the power of Kronecker products being used with the natural meaning $M^{0\otimes} = 1$, $M^{p\otimes} = M^{(p-1)\otimes} \otimes M$. Let $\hat{J}_k, \tilde{J}_k \in R^{k\times(k+1)}$ and $u^{[k]}$ be defined by $\hat{J}_k = [I_k, 0_{k\times 1}]$, $\tilde{J}_k = [0_{k\times 1}, I_k]$ and $u^{[k]} = [1, u, \ldots, u^{k-1}]^{\mathrm{T}}$, respectively, which have essential roles for polynomial manipulations [10]. Finally given a signal $x(t)$, $\|x(t)\|_2$ denotes the L_2 norm of $x(t)$; i.e., $\|x(t)\|_2^2 = \int_0^\infty x(t)^{\mathrm{T}} x(t)\, dt$.

2 Problem Description

In this paper, we consider a class of LTIPD systems with multi-time delays in the state vector and in the presence of norm-bounded nonlinear uncertainties in which the state-space matrices depend affinely on the constant vector $\rho = [\rho_1, \rho_2, \ldots, \rho_m]^{\mathrm{T}} \in \zeta \subset R^m$ (with ζ being a compact set) as follows:

$$\begin{aligned} \dot{x}(t) &= A(\rho)x(t) + \sum_{i=1}^{r} A_d^{(i)}(\rho)x(t-h_i) + B_1 u(t) + E_1(\rho)w(t) + \Delta(x(t)), \\ x(t) &= \varphi(t), \qquad t \in [-h, 0], \\ z(t) &= C_1 x(t), \\ y(t) &= C_2 x(t) + E_2 w(t) \end{aligned} \tag{1}$$

where the constant parameter h_i is time-delay, $h = \max\limits_i\{h_i\}$ for $i = 1, 2, \ldots, r$, and $\varphi(t)$ is the continuous vector valued initial function, also $x(t) \in R^n$, $u(t) \in R^l$, $w(t) \in R^s$, $z(t) \in R^z$ and $y(t) \in R^p$ are the state vector, the control input, the disturbance vector, the controlled output and the output vector, respectively. Moreover, the parameter-dependent matrices $A(\rho)$, $A_d^{(i)}(\rho)$ and $E_1(\rho)$ are expressed as $A(\rho) = A_0 + \sum\limits_{i=1}^{m} \rho_i A_i$, $A_d^{(i)}(\rho) = A_{0d}^{(i)} + \sum\limits_{j=1}^{m} \rho_j A_{jd}^{(i)}$ and $E_1(\rho) = E_{01} + \sum\limits_{i=1}^{m} \rho_i E_{i1}$, respectively, and the vector function $\Delta(x(t))$ is non-linear term of uncertainty set. Furthermore, it is known that the vector ρ is contained in a priori given set whereas the actual curve of the vector ρ is unknown but can be measured online for control process.

Assumption 1 There exists a known real constant matrix $H \in R^{n\times n}$ for the nonlinear uncertainty vector $\Delta(\cdot) \in \Omega(\cdot)$ such that $\|\Delta(x(t))\|_2 \le \|Hx(t)\|_2$ for any $x(t) \in R^n$. Denote the corresponding uncertainty set by $\Omega(x(t)) = \{\Delta(x(t))\colon \|\Delta(x(t))\|_2 \le \|Hx(t)\|_2\}$.

The robust dynamic parameter-dependent output feedback (RDP-DOF) control problem that we address in this paper is of the form

$$\begin{aligned} \dot{x}_c(t) &= A_K(\rho)x_c(t) + B_K(\rho)y(t), \\ u(t) &= C_K(\rho)x_c(t), \end{aligned} \tag{2}$$

where $x_c(t) \in R^{n_c}$ and the parameter-dependent matrices of $A_K(\rho)$, $B_K(\rho)$ and $C_K(\rho)$ are defined as $A_K(\rho) = A_{0K} + \sum\limits_{i=1}^{m} \rho_i A_{iK} \in R^{n_c\times n_c}$, $B_K(\rho) = B_{0K} + \sum\limits_{i=1}^{m} \rho_i B_{iK} \in R^{n_c\times p}$ and $C_K(\rho) = C_{0K} + \sum\limits_{i=1}^{m} \rho_i C_{iK} \in R^{l\times n_c}$, respectively. In the sequel, the RDP-DOF control state-space matrices will be determined.

Applying the RDP-DOF control (2) into the system (1), we obtain the following augmented closed-loop system

$$\begin{aligned} \dot{X}(t) &= \bar{A}_\rho X(t) + \sum_{i=1}^{r} \bar{A}_{d\rho}^{(i)} X(t-h_i) + \overline{E}_\rho w(t) + \overline{\Delta}(SX(t)), \\ X(t) &= \overline{\varphi}(t), \quad t \in [-h,\, 0], \\ z(t) &= \overline{C}_1 X(t), \\ y(t) &= \overline{C}_2 X(t) + E_2 w(t), \end{aligned} \tag{3}$$

where $X(t) = [x^{\mathrm{T}}(t),\, x_c^{\mathrm{T}}(t)]^{\mathrm{T}}$, $S = [I_n,\, 0_{n\times n_c}]$, $\overline{C}_1 = [C_1,\, 0_{z\times n_c}]$, $\overline{C}_2 = [C_2,\, 0_{p\times n_c}]$,

$$\overline{\Delta}(\cdot) = \begin{bmatrix} \Delta(\cdot) \\ 0_{n_c\times 1} \end{bmatrix}, \quad \bar{A}_\rho = \tilde{A}_\rho + F_1\Gamma_\rho F_2, \quad \bar{A}_{d\rho}^{(i)} = \begin{bmatrix} A_{d\rho}^{(i)} & 0_{n\times n_c} \\ 0_{n_c\times n} & 0_{n_c} \end{bmatrix}, \quad \overline{E}_\rho = \widetilde{E}_\rho + \widehat{S}\Gamma_\rho\widehat{E}$$

and

$$\tilde{A}_\rho = \begin{bmatrix} A(\rho) & 0_{n\times n_c} \\ 0_{n_c\times n} & 0_{n_c} \end{bmatrix}, \quad F_1 = \begin{bmatrix} B_1 & 0_{n\times n_c} \\ 0_{n_c\times l} & I_{n_c} \end{bmatrix}, \quad F_2 = \begin{bmatrix} C_2 & 0_{p\times n_c} \\ 0_{n_c\times n} & I_{n_c} \end{bmatrix},$$
$$\Gamma_\rho = \begin{bmatrix} 0_{l\times p} & C_k(\rho) \\ B_k(\rho) & A_k(\rho) \end{bmatrix}, \quad \widetilde{E}_\rho = \begin{bmatrix} E_1(\rho) \\ 0_{n_c\times s} \end{bmatrix}, \quad \widehat{E} = \begin{bmatrix} E_2 \\ 0_{n_c\times s} \end{bmatrix},$$
$$\widehat{S} = \begin{cases} I_{n+n_c} & \text{for} \quad n = l, \\ \begin{bmatrix} 0_{(n-l)\times(l+n_c)} \\ I_{l+n_c} \end{bmatrix} & \text{for} \quad n > l. \end{cases}$$

The main objective of the paper is to seek the state-space matrices of the RDP-DOF control (2) that asymptotically stabilizes the closed-loop system (3) with multi-time delays and norm-bounded nonlinear uncertainties as well as guarantees a prescribed H_∞ performance, i.e.,

$$\|z(t)\|_2^2 < \gamma^2\|w(t)\|_2^2 \tag{4}$$

for all nonzero $w(t) \in L_2(0,\infty)$ under zero initial conditions and a positive scalar γ.

Definition 1 We call a polynomial parameter-dependent quadratic (PPDQ) Lyapunov function any quadratic function $x^{\mathrm{T}}(t)S(\rho)x(t)$ such that

$$S(\rho) = (\rho_m^{[k]} \otimes \cdots \otimes \rho_1^{[k]} \otimes I_n)^{\mathrm{T}} S_k (\rho_m^{[k]} \otimes \cdots \otimes \rho_1^{[k]} \otimes I_n)$$

for every $x(t) \in R^n$ and a certain $S_k \in R^{k^m n}$. The integer $k-1$ is called the degree of the PPDQ function $S(\rho)$.

3 Delay-Independent Stability Analysis

In this section, assuming that the structure of the RDP-DOF control (2) is known and we will investigate the conditions under which the closed-loop system (3) is asymptotically stable for all admissible vectors $\rho \in \zeta$ and any nonlinear function $\Delta(\cdot) \in \Omega(\cdot)$ independent of time delay parameters h_i for $i = 1, 2, \ldots, r$.

The approach employed here is to investigate the delay-independent stability analysis of the closed-loop system (3) in the presence of the disturbance (exogenous input) and norm-bounded nonlinear uncertainties based on the standard HJI method. In the literature, extensions of the Lyapunov method to the Lyapunov–Krasovskii method have been proposed for time-delayed systems [8, 20]. Hence, we define a class of PPDQ Lyapunov–Krasovskii functions of the degree $k-1$ for this purpose in the following form

$$V(X(t)) = X(t)^{\mathrm{T}}P_\rho X(t) + \sum_{i=1}^{r} \int_{t-h_i}^{t} X(\sigma)^{\mathrm{T}} Q_\rho^{(i)} X(\sigma)\, d\sigma \tag{5}$$

where the positive definite matrices $P_\rho = P(\rho) \in R^{n+n_c}$ and $Q_\rho^{(i)} = Q^{(i)}(\rho) \in R^{n+n_c}$ for $i = 1, 2, \ldots, r$ are expressed as

$$P_\rho = (\rho_m^{[k]} \otimes \cdots \otimes \rho_1^{[k]} \otimes I_{n+n_c})^{\mathrm{T}} P_k (\rho_m^{[k]} \otimes \cdots \otimes \rho_1^{[k]} \otimes I_{n+n_c}), \tag{6}$$

$$Q_\rho^{(i)} = (\rho_m^{[k]} \otimes \cdots \otimes \rho_1^{[k]} \otimes I_{n+n_c})^{\mathrm{T}} Q_k^{(i)} (\rho_m^{[k]} \otimes \cdots \otimes \rho_1^{[k]} \otimes I_{n+n_c}) \tag{7}$$

with $P_k, Q_k^{(i)} \in R^{k^m(n+n_c)}$ for $i = 1, 2, \ldots, r$. Therefore, the following HJI function is considered as

$$J[w(t),\, \Delta(\cdot)] = \frac{dV\,(X(t))}{dt} + z^{\mathrm{T}}(t) z(t) - \gamma^2 w^{\mathrm{T}}(t) w(t) \tag{8}$$

where derivative of $V(X(t))$ is evaluated along the trajectory of the closed-loop system (3). It is well known that a *sufficient condition* for achieving robust disturbance attenuation is that the inequality $J[w(t),\, \Delta(\cdot)] < 0$ for every $w \in L^2$, $\rho \in \zeta$ and $\Delta(\cdot) \in \Omega(\cdot)$ results in a function $V(X(t))$, which is strictly radially unbounded (see, for example, [27, 29]). Therefore, we will establish conditions under which

$$\sup_{\Delta \in \Omega} \sup_{w \in L^2} J[w(t),\, \Delta(\cdot)] < 0, \tag{9}$$

then for every T, taking the definite integral from 0 to T of both sides of (8) gives

$$\int_0^{\mathrm{T}} z^{\mathrm{T}}(t)\, z(t)\, dt - \gamma^2 \int_0^{\mathrm{T}} w^{\mathrm{T}}(t)\, w(t)\, dt < V(X(0)) - V(X(T)) \le V(X(0)) = 0$$

i.e., constraint of disturbance attenuation (4).

From (5) – (8), we find

$$\begin{aligned} J[w(t), \Delta(\cdot)] = {} & X(t)^{\mathrm{T}} (\bar{A}_\rho^{\mathrm{T}} P_\rho + P_\rho \bar{A}_\rho + \sum_{i=1}^{r} Q_\rho^{(i)} + \overline{C}_1^{\mathrm{T}} \overline{C}_1) X(t) \\ & + X(t)^{\mathrm{T}} P_\rho \sum_{i=1}^{r} \bar{A}_{d\rho}^{(i)} X(t - h_i) + \Big(\sum_{i=1}^{r} \bar{A}_{d\rho}^{(i)} X(t - h_i) \Big)^{\mathrm{T}} P_\rho X(t) \\ & - \sum_{i=1}^{r} X(t - h_i)^{\mathrm{T}} Q_\rho^{(i)} X(t - h_i) + \overline{\Delta}(SX(t))^{\mathrm{T}} P_\rho X(t) + X(t)^{\mathrm{T}} P_\rho \overline{\Delta}(S\, X(t)) \\ & + w(t)^{\mathrm{T}} \overline{E}_\rho^{\mathrm{T}} P_\rho X(t) + X(t)^{\mathrm{T}} P_\rho \overline{E}_\rho w(t) - \gamma^2 w(t)^{\mathrm{T}} w(t). \end{aligned} \tag{10}$$

It is easy to show that the worst-case disturbance in (10) occurs when

$$w^*(t) = \gamma^{-2} \overline{E}_\rho^{\mathrm{T}} P_\rho X(t). \tag{11}$$

By substituting (11) into (10), we obtain

$$\begin{aligned}\sup_{w\in L^2} J(w(t),\Delta) &= J(w^*,\Delta)\\ &= X(t)^{\mathrm{T}}\Big(\bar{A}_\rho^{\mathrm{T}}P_\rho + P_\rho\bar{A}_\rho + \gamma^{-2}P_\rho\overline{E}_\rho\overline{E}_\rho^{\mathrm{T}}P_\rho + \sum_{i=1}^{r} Q_\rho^{(i)} + \overline{C}_1^{\mathrm{T}}\overline{C}_1\Big)X(t)\\ &+ X(t)^{\mathrm{T}}P_\rho\sum_{i=1}^{r}\bar{A}_{d\rho}^{(i)}X(t-h_i) + \Big(\sum_{i=1}^{r}\bar{A}_{d\rho}^{(i)}X(t-h_i)\Big)^{\mathrm{T}}P_\rho X(t)\\ &- \sum_{i=1}^{r} X(t-h_i)^{\mathrm{T}}Q_\rho^{(i)}X(t-h_i) + \overline{\Delta}(SX(t))^{\mathrm{T}}P_\rho X(t) + X(t)^{\mathrm{T}}P_\rho\overline{\Delta}(S\,X(t)).\end{aligned} \tag{12}$$

Now, by utilizing Lemma 2 and Assumption 1, it is trivial to show that for any positive scalar ε the following matrix inequality holds

$$\begin{aligned}\overline{\Delta}(SX(t))^{\mathrm{T}}P_\rho X(t) + X(t)^{\mathrm{T}}P_\rho\overline{\Delta}(S\,X(t)) &\le \varepsilon X(t)^{\mathrm{T}}P_\rho^2X(t) + \varepsilon^{-1}\overline{\Delta}(S\,X(t))^{\mathrm{T}}\overline{\Delta}(SX(t))\\ &\le X(t)^{\mathrm{T}}(\varepsilon P_\rho^2 + \varepsilon^{-1}(HS)^{\mathrm{T}}(HS))X(t),\end{aligned} \tag{13}$$

then from (12)–(13), the following inequality is obtained

$$\sup_{\Delta\in\Omega}\sup_{w\in L^2} J[w(t),\,\Delta(\cdot)] = \sup_{\Delta\in\Omega} J(w^*,\Delta) \le \bar{X}(t)^{\mathrm{T}}M_\rho\bar{X}(t) \tag{14}$$

where the vector $\bar{X}(t) = [X(t)^{\mathrm{T}},\, X(t-h_1)^{\mathrm{T}},\, \ldots,\, X(t-h_r)^{\mathrm{T}}]^{\mathrm{T}}$ is an augmented state and the parameter-dependent matrix M_ρ is defined in the form

$$\begin{bmatrix} \bar{A}_\rho^{\mathrm{T}}P_\rho + P_\rho\bar{A}_\rho + \gamma^{-2}P_\rho\overline{E}_\rho\overline{E}_\rho^{\mathrm{T}}P_\rho + \varepsilon P_\rho^2 + & & & & \\ \sum_{i=1}^{r} Q_\rho^{(i)} + \varepsilon^{-1}(HS)^{\mathrm{T}}(HS) + \overline{C}_1^{\mathrm{T}}\overline{C}_1 & P_\rho\bar{A}_{d\rho}^{(1)} & \ldots & P_\rho\bar{A}_{d\rho}^{(r)} \\ (P_\rho\bar{A}_{d\rho}^{(1)})^{\mathrm{T}} & -Q_\rho^{(1)} & \ldots & 0 \\ \ldots & \ldots & \ldots & \ldots \\ (P_\rho\bar{A}_{d\rho}^{(r)})^{\mathrm{T}} & 0 & \ldots & -Q_\rho^{(r)} \end{bmatrix}. \tag{15}$$

Consequently, if there exist the positive scalar ε and the positive definite solutions P_ρ and $Q_\rho^{(i)}$ for $i = 1, 2, \ldots, r$ to the parameter-dependent matrix inequality $M_\rho < 0$, then we have

$$J[w(t),\,\Delta(\cdot)] < 0, \quad \forall\, w(t) \in L^2, \quad \rho \in \zeta, \quad \Delta(\cdot) \in \Omega(\cdot). \tag{16}$$

Using Schur Complement Lemma, the parameter-dependent inequality $M_\rho < 0$ can be represented as

$$\begin{bmatrix} \bar{A}_\rho^{\mathrm{T}}P_\rho + P_\rho\bar{A}_\rho + \sum_{i=1}^{r} Q_\rho^{(i)} + & & & & & & \\ \varepsilon^{-1}(HS)^{\mathrm{T}}(HS) + \overline{C}_1^{\mathrm{T}}\overline{C}_1 & P_\rho & P_\rho\overline{E}_\rho & P_\rho\bar{A}_{d\rho}^{(1)} & \ldots & P_\rho\bar{A}_{d\rho}^{(r)} \\ P_\rho & -\varepsilon^{-1}I_{n+n_c} & 0 & 0 & \ldots & 0 \\ (P_\rho\overline{E}_\rho)^{\mathrm{T}} & 0 & -\gamma^2 I_s & 0 & \ldots & 0 \\ (P_\rho\bar{A}_{d\rho}^{(1)})^{\mathrm{T}} & 0 & 0 & -Q_\rho^{(1)} & \ldots & 0 \\ \ldots & \ldots & \ldots & \ldots & \ldots & \ldots \\ (P_\rho\bar{A}_{d\rho}^{(r)})^{\mathrm{T}} & 0 & 0 & 0 & \ldots & -Q_\rho^{(r)} \end{bmatrix} < 0. \tag{17}$$

The following result is now concluded for the delay-independent stability analysis of the uncertain parameter-dependent state-delayed system (1).

Theorem 1 *Let the parameters $\gamma > 0$, $k > 1$ (degree of the PPDQ Lyapunov–Krasovskii functions) and the RDP-DOF control matrices $A_K(\rho)$, $B_K(\rho)$ and $C_K(\rho)$ are given. If there exist positive parameter ε and positive definite matrices P_ρ and $Q_\rho^{(i)}$ for $i = 1, 2, \ldots, r$ to the parameter-dependent matrix inequality (17), then the augmented closed-loop system (3) is asymptotically stable and preserves the H_∞ performance for all admissible vectors $\rho \in \zeta$ and any $\Delta(\cdot) \in \Omega(\cdot)$, independent of the time delay parameters h_i for $i = 1, 2, \ldots, r$.*

Remark 1 A general framework for relaxing parameter-dependent matrix inequality problems into parameter-independent matrix inequalities (conventional form) has been investigated in [4]. However, application of the PPDQ Lyapunov functions as a new tool for relaxing parameter dependency of the matrix inequalities will be stated in the next section.

4 RDP-DOF Control Design

This section is devoted to design of the state-space matrices $A_K(\rho)$, $B_K(\rho)$ and $C_K(\rho)$ for the RDP-DOF control (2) by using the result of Theorem 1 in the previous section.

In Theorem 1, the parameter-dependent inequality (17) can be written in the following from

$$\begin{bmatrix} \tilde{A}_\rho^{\mathrm{T}} P_\rho + P_\rho \tilde{A}_\rho + (F_1 \Gamma_\rho F_2)^{\mathrm{T}} P_\rho + & & & & & \\ P_\rho (F_1 \Gamma_\rho F_2) + \sum_{i=1}^{r} Q_\rho^{(i)} + & P_\rho & P_\rho \widetilde{E}_\rho + P_\rho \widehat{S} \Gamma_\rho \widehat{E} & P_\rho \bar{A}_{d\rho}^{(1)} & \ldots & P_\rho \bar{A}_{d\rho}^{(r)} \\ \varepsilon^{-1} (HS)^{\mathrm{T}} (HS) + \overline{C}_1^{\mathrm{T}} \overline{C}_1 & & & & & \\ P_\rho & -\varepsilon^{-1} I_{n+n_c} & 0 & 0 & \ldots & 0 \\ (P_\rho \widetilde{E}_\rho + P_\rho \widehat{S} \Gamma_\rho \widehat{E})^{\mathrm{T}} & 0 & -\gamma^2 I_s & 0 & \ldots & 0 \\ (P_\rho \bar{A}_{d\rho}^{(1)})^{\mathrm{T}} & 0 & 0 & -Q_\rho^{(1)} & \ldots & 0 \\ \cdots\cdots & \cdots & \cdots & \cdots & \cdots & \cdots \\ (P_\rho \bar{A}_{d\rho}^{(r)})^{\mathrm{T}} & 0 & 0 & 0 & \ldots & -Q_\rho^{(r)} \end{bmatrix} < 0 \tag{18}$$

and it is clear that the above constraint is however not simultaneously *convex* in the parameter P_ρ and the controller parameters Γ_ρ. In the literature, more attention has been paid to the problems having this nature, which called bilinear matrix inequality (BMI) problems [22].

In the sequel, we state application of the PPDQ Lyapunov functions to relax dependency of the BMI (18) into the parameter vector ρ. At first, for *parameter-dependent* matrix $R_\rho = \tilde{A}_\rho^{\mathrm{T}} P_\rho + P_\rho \tilde{A}_\rho$, the PPDQ Lyapunov function of degree k is expressed in the form

$$R_\rho = (\rho_m^{[k+1]} \otimes \cdots \otimes \rho_1^{[k+1]} \otimes I_{n+n_c})^{\mathrm{T}} R_k (\rho_m^{[k+1]} \otimes \cdots \otimes \rho_1^{[k+1]} \otimes I_{n+n_c}) \tag{19}$$

and by some matrix manipulations, in (19) the parameter-independent matrix $R_k \in R^{(k+1)^m (n+n_c)}$ which depends on matrix P_k linearly is obtained as follows

$$\begin{aligned} R_k = & \left((\hat{J}_k^{m\otimes} \otimes \tilde{A}_0) + \sum_{i=1}^{m} (\hat{J}_k^{(m-i)\otimes} \otimes \tilde{J}_k \otimes \hat{J}_k^{(i-1)\otimes} \otimes \tilde{A}_i) \right)^{\mathrm{T}} P_k (\hat{J}_k^{m\otimes} \otimes I_{n+n_c}) \\ & + (\hat{J}_k^{m\otimes} \otimes I_{n+n_c})^{\mathrm{T}} P_k \left((\hat{J}_k^{m\otimes} \otimes \tilde{A}_0) + \sum_{i=1}^{m} (\hat{J}_k^{(m-i)\otimes} \otimes \tilde{J}_k \otimes \hat{J}_k^{(i-1)\otimes} \otimes \tilde{A}_i) \right) \end{aligned} \tag{20}$$

where

$$\tilde{A}_\rho = \tilde{A}_0 + \sum_{i=1}^{m} \rho_i \tilde{A}_i \quad \text{and} \quad \tilde{A}_i = \begin{bmatrix} A_i & 0_{n\times n_c} \\ 0_{n_c\times n} & 0_{n_c} \end{bmatrix} \quad \text{for} \quad i = 0, 1, \ldots, m.$$

Similarly, the PPDQ Lyapunov function of degree k for the parameter-dependent matrix $\Sigma_\rho = (F_1\Gamma_\rho F_2)^{\mathrm{T}} P_\rho + P_\rho(F_1\Gamma_\rho F_2)$ will be as

$$\Sigma_\rho = (\rho_m^{[k+1]} \otimes \cdots \otimes \rho_1^{[k+1]} \otimes I_{n+n_c})^{\mathrm{T}} \Sigma_k (\rho_m^{[k+1]} \otimes \cdots \otimes \rho_1^{[k+1]} \otimes I_{n+n_c}) \tag{21}$$

where the parameter-independent matrix $\Sigma_k \in R^{(k+1)^m(n+n_c)}$ is shown as follows

$$\begin{aligned} \Sigma_k = &\left((\hat{J}_k^{m\otimes} \otimes F_1\Gamma_0 F_2) + \sum_{i=1}^{m} (\hat{J}_k^{(m-i)\otimes} \otimes \tilde{J}_k \otimes \hat{J}_k^{(i-1)\otimes} \otimes F_1\Gamma_i F_2) \right)^{\mathrm{T}} P_k (\hat{J}_k^{m\otimes} \otimes I_{n+n_c}) \\ &+ (\hat{J}_k^{m\otimes} \otimes I_{n+n_c})^{\mathrm{T}} P_k \left((\hat{J}_k^{m\otimes} \otimes F_1\Gamma_0 F_2) + \sum_{i=1}^{m} (\hat{J}_k^{(m-i)\otimes} \otimes \tilde{J}_k \otimes \hat{J}_k^{(i-1)\otimes} \otimes F_1\Gamma_i F_2) \right) \end{aligned} \tag{22}$$

where

$$\Gamma_\rho = \Gamma_0 + \sum_{i=1}^{m} \rho_i \Gamma_i \quad \text{with} \quad \Gamma_j = \begin{bmatrix} 0_{l\times p} & C_{jk} \\ B_{jk} & A_{jk} \end{bmatrix} \quad \text{for} \quad j = 1, 2, \ldots, m.$$

Lemma 4 *Let the degree of the PPDQ Lyapunov function P_ρ be $k-1$. The parameter-dependent matrix $P_\rho \mathrm{T}_\rho$ satisfies the following representation form*

$$P_\rho \mathrm{T}_\rho = (\rho_m^{[k+1t]} \otimes \cdots \otimes \rho_1^{[k+1]} \otimes I_{n+n_c})^{\mathrm{T}} H_k (\rho_m^{[k+1]} \otimes \cdots \otimes \rho_1^{[k+1]} \otimes I_q), \tag{23}$$

where $\mathrm{T}_\rho = \mathrm{T}_0 + \sum_{i=1}^{m} \rho_i \mathrm{T}_i$ and $\mathrm{T}_i \in R^{(n+n_c)\times q}$, then the matrix

$$H_k \in R^{((k+1)^m(n+n_c))\times((k+1)^m q)}$$

which depends on the matrix P_k linearly is defined as

$$H_k = (\hat{J}_k^{m\otimes} \otimes I_{n+n_c})^{\mathrm{T}} P_k \left((\hat{J}_k^{m\otimes} \otimes \mathrm{T}_0) + \sum_{i=1}^{m} (\hat{J}_k^{(m-i)\otimes} \otimes \tilde{J}_k \otimes \hat{J}_k^{(i-1)\otimes} \otimes \mathrm{T}_i) \right). \tag{24}$$

According to Lemma 4 for the parameter-dependent matrices $\widetilde{E}_\rho = \widetilde{E}_0 + \sum_{j=1}^{m} \rho_j \widetilde{E}_j$, $\bar{A}_{d\rho}^{(i)} = \bar{A}_{0d}^{(i)} + \sum_{j=1}^{m} \rho_j \bar{A}_{jd}^{(i)}$ and $\widehat{S}\Gamma_\rho\widehat{E} = \widehat{E}_0 + \sum_{j=1}^{m} \rho_j \widehat{E}_j$, we obtain

$$\begin{aligned} P_\rho \widetilde{E}_\rho &= (\rho_m^{[k+1]} \otimes \cdots \otimes \rho_1^{[k+1]} \otimes I_{n+n_c})^{\mathrm{T}} \widetilde{\Xi}_k (\rho_m^{[k+1]} \otimes \cdots \otimes \rho_1^{[k+1]} \otimes I_s), \\ P_\rho \bar{A}_{d\rho}^{(i)} &= (\rho_m^{[k+1]} \otimes \cdots \otimes \rho_1^{[k+1]} \otimes I_{n+n_c})^{\mathrm{T}} \overline{\Xi}_k^{(i)} (\rho_m^{[k+1]} \otimes \cdots \otimes \rho_1^{[k+1]} \otimes I_{n+n_c}), \\ P_\rho \widehat{S}\Gamma_\rho\widehat{E} &= (\rho_m^{[k+1]} \otimes \cdots \otimes \rho_1^{[k+1]} \otimes I_{n+n_c})^{\mathrm{T}} \widehat{\Xi}_k (\rho_m^{[k+1]} \otimes \cdots \otimes \rho_1^{[k+1]} \otimes I_s), \end{aligned} \tag{25}$$

where the parameter-independent matrices $\widetilde{\Xi}_k$, $\overline{\Xi}_k^{(i)}$ and $\widehat{\Xi}_k$ are represented in the forms

$$\begin{aligned}
\widetilde{\Xi}_k &= (\hat{J}_k^{m\otimes} \otimes I_{n+n_c})^{\mathrm{T}} P_k \Big((\hat{J}_k^{m\otimes} \otimes \widetilde{E}_0) + \sum_{j=1}^{m} (\hat{J}_k^{(m-j)\otimes} \otimes \tilde{J}_k \otimes \hat{J}_k^{(j-1)\otimes} \otimes \widetilde{E}_j) \Big), \\
\overline{\Xi}_k^{(i)} &= (\hat{J}_k^{m\otimes} \otimes I_{n+n_c})^{\mathrm{T}} P_k \Big((\hat{J}_k^{m\otimes} \otimes \bar{A}_{0d}^{(i)}) + \sum_{j=1}^{m} (\hat{J}_k^{(m-j)\otimes} \otimes \tilde{J}_k \otimes \hat{J}_k^{(j-1)\otimes} \otimes \bar{A}_{jd}^{(i)}) \Big), \\
\widehat{\Xi}_k &= (\hat{J}_k^{m\otimes} \otimes I_{n+n_c})^{\mathrm{T}} P_k \Big((\hat{J}_k^{m\otimes} \otimes \widehat{E}_0) + \sum_{j=1}^{m} (\hat{J}_k^{(m-j)\otimes} \otimes \tilde{J}_k \otimes \hat{J}_k^{(j-1)\otimes} \otimes \widehat{E}_j) \Big)
\end{aligned} \tag{26}$$

with

$$\bar{A}_{jd}^{(i)} = \begin{bmatrix} A_{jd}^{(i)} & 0 \\ 0 & 0 \end{bmatrix}, \quad \widetilde{E}_j = \begin{bmatrix} E_{j1} \\ 0_{n_c \times s} \end{bmatrix} \quad \text{and} \quad \widehat{E}_j = \widehat{S}\Gamma_j \begin{bmatrix} E_2 \\ 0_{n_c \times s} \end{bmatrix}$$

for $j = 1, 2, \ldots, m$ and $i = 1, 2, \ldots, r$.

Similarly, the parameter-independent matrices $\overline{C}_1^{\mathrm{T}}\overline{C}_1$, $(HS)^{\mathrm{T}}(HS)$ and I_s can be also represented as

$$\begin{aligned}
\overline{C}_1^{\mathrm{T}}\overline{C}_1 &= (\rho_m^{[k]} \otimes \cdots \otimes \rho_1^{[k]} \otimes I_{n+n_c})^{\mathrm{T}} \overline{C}_k (\rho_m^{[k]} \otimes \cdots \otimes \rho_1^{[k]} \otimes I_{n+n_c}) \\
&= (\rho_m^{[k+1]} \otimes \cdots \otimes \rho_1^{[k+1]} \otimes I_{n+n_c})^{\mathrm{T}} (\hat{J}_k^{m\otimes} \otimes I_{n+n_c})^{\mathrm{T}} \overline{C}_k \\
&\quad \times (\hat{J}_k^{m\otimes} \otimes I_{n+n_c}) (\rho_m^{[k+1]} \otimes \cdots \otimes \rho_1^{[k+1]} \otimes I_{n+n_c}),
\end{aligned} \tag{27}$$

$$\begin{aligned}
(HS)^{\mathrm{T}}(HS) &= (\rho_m^{[k]} \otimes \cdots \otimes \rho_1^{[k]} \otimes I_{n+n_c})^{\mathrm{T}} \bar{H}_k (\rho_m^{[k]} \otimes \cdots \otimes \rho_1^{[k]} \otimes I_{n+n_c}) \\
&= (\rho_m^{[k+1]} \otimes \cdots \otimes \rho_1^{[k+1]} \otimes I_{n+n_c})^{\mathrm{T}} (\hat{J}_k^{m\otimes} \otimes I_{n+n_c})^{\mathrm{T}} \bar{H}_k \\
&\quad \times (\hat{J}_k^{m\otimes} \otimes I_{n+n_c}) (\rho_m^{[k+1]} \otimes \cdots \otimes \rho_1^{[k+1]} \otimes I_{n+n_c}),
\end{aligned} \tag{28}$$

and

$$\begin{aligned}
I_s &= (\rho_m^{[k]} \otimes \cdots \otimes \rho_1^{[k]} \otimes I_s)^{\mathrm{T}} \bar{I}_k^s (\rho_m^{[k]} \otimes \cdots \otimes \rho_1^{[k]} \otimes I_s) \\
&= (\rho_m^{[k+1]} \otimes \cdots \otimes \rho_1^{[k+1]} \otimes I_s)^{\mathrm{T}} (\hat{J}_k^{m\otimes} \otimes I_s)^{\mathrm{T}} \bar{I}_k^s \\
&\quad \times (\hat{J}_k^{m\otimes} \otimes I_s) (\rho_m^{[k+1]} \otimes \cdots \otimes \rho_1^{[k+1]} \otimes I_s)
\end{aligned} \tag{29}$$

where the certain matrices $\overline{C}_k$, $\bar{H}_k$ and $\bar{I}_k^s$ are defined, respectively, as

$$\overline{C}_k = \operatorname{diag}(\overline{C}_1^{\mathrm{T}}\overline{C}_1, \underbrace{0_{n+n_c}, \ldots, 0_{n+n_c}}_{(k^m-1)\ \text{elements}}), \quad \bar{H}_k = \operatorname{diag}((HS)^{\mathrm{T}}(HS), \underbrace{0_{n+n_c}, \ldots, 0_{n+n_c}}_{(k^m-1)\ \text{elements}}),$$

$$\text{and} \quad \bar{I}_k^s = \operatorname{diag}(I_s, \underbrace{0_s, \ldots, 0_s}_{(k^m-1)\ \text{elements}}).$$

Therefore using the defined notations as well as the definition

$$\bar{I}_k^{n+n_c} = \operatorname{diag}(I_{n+n_c}, \underbrace{0_{n+n_c}, \ldots, 0_{n+n_c}}_{(k^m-1)\ \text{elements}})$$

and some matrix manipulations, the following parameter-independent BMI form can be obtained from the parameter-dependent inequality (18),

$$\begin{bmatrix} R_k+\Sigma_k+(\hat{J}_k^{m\otimes}\otimes I_{n+n_c})^{\mathrm{T}}\left(\varepsilon^{-1}\bar{H}_k+\overline{C}_k+\sum_{i=1}^{r}Q_k^{(i)}\right)(\hat{J}_k^{m\otimes}\otimes I_{n+n_c}) & \widetilde{\Xi}_k+\widehat{\Xi}_k & \overline{\Xi}_k^{(1)} & \cdots & \overline{\Xi}_k^{(r)} \\ (\hat{J}_k^{m\otimes}\otimes I_{n+n_c})^{\mathrm{T}}P_k(\hat{J}_k^{m\otimes}\otimes I_{n+n_c}) & 0 & 0 & \cdots & 0 \\ -\varepsilon^{-1}(\hat{J}_k^{m\otimes}\otimes I_{n+n_c})^{\mathrm{T}}\bar{I}_k^{n+n_c}(\hat{J}_k^{m\otimes}\otimes I_{n+n_c}) & 0 & 0 & \cdots & 0 \\ 0 & -\gamma^2(\hat{J}_k^{m\otimes}\otimes I_s)^{\mathrm{T}}\bar{I}_k^{s}(\hat{J}_k^{m\otimes}\otimes I_s) & -(\hat{J}_k^{m\otimes}\otimes I_{n+n_c})^{\mathrm{T}}Q_k^{(1)}(\hat{J}_k^{m\otimes}\otimes I_{n+n_c}) & \cdots & 0 \\ \cdots & \cdots & \cdots & \cdots & \cdots \\ 0 & 0 & 0 & \cdots & -(\hat{J}_k^{m\otimes}\otimes I_{n+n_c})^{\mathrm{T}}Q_k^{(r)}(\hat{J}_k^{m\otimes}\otimes I_{n+n_c}) \end{bmatrix}<0. \tag{30}$$

Remark 2 Using the property of $AC\otimes BD=(A\otimes B)(C\otimes D)$, the defined matrices $\widehat{\Xi}_k$ and Σ_k can be shown in the following forms

$$\begin{aligned}\widehat{\Xi}_k=&(\hat{J}_k^{m\otimes}\otimes I_{n+n_c})^{\mathrm{T}}P_k(\hat{J}_k^{m\otimes}\otimes\widehat{S})(I_{(k+1)^m}\otimes\Gamma_i)\left(I_{(k+1)^m}\otimes\begin{bmatrix}E_2\\0_{n_c\times s}\end{bmatrix}\right)\\&+\sum_{i=1}^{m}(\hat{J}_k^{m\otimes}\otimes I_{n+n_c})^{\mathrm{T}}P_k(\hat{J}_k^{(m-i)\otimes}\otimes\tilde{J}_k\otimes\hat{J}_k^{(i-1)\otimes}\otimes\widehat{S})\\&\times(I_{(k+1)^m}\otimes\Gamma_i)\left(I_{(k+1)^m}\otimes\begin{bmatrix}E_2\\0_{n_c\times s}\end{bmatrix}\right)\end{aligned} \tag{31}$$

and

$$\begin{aligned}\Sigma_k=&\Bigg((\hat{J}_k^{m\otimes}\otimes F_1)(I_{(k+1t)^m}\otimes\Gamma_0)(I_{(k+1)^m}\otimes F_2)\\&+\sum_{i=1}^{m}(\hat{J}_k^{(m-i)\otimes}\otimes\tilde{J}_k\otimes\hat{J}_k^{(i-1)\otimes}\otimes F_1)(I_{(k+1)^m}\otimes\Gamma_i)(I_{(k+1)^m}\otimes F_2)\Bigg)^{\mathrm{T}}P_k(\hat{J}_k^{m\otimes}\otimes I_{n+n_c})\\&+(\hat{J}_k^{m\otimes}\otimes I_{n+n_c})^{\mathrm{T}}P_k\Bigg((\hat{J}_k^{m\otimes}\otimes F_1)(I_{(k+1)^m}\otimes\Gamma_0)(I_{(k+1)^m}\otimes F_2)\\&+\sum_{i=1}^{m}(\hat{J}_k^{(m-i)\otimes}\otimes\tilde{J}_k\otimes\hat{J}_k^{(i-1)\otimes}\otimes F_1)(I_{(k+1)^m}\otimes\Gamma_i)(I_{(k+1)^m}\otimes F_2)\Bigg).\end{aligned} \tag{32}$$

The constraint (30) is not convex in terms of the parameter P_k and the controller parameters $\Gamma_0, \Gamma_1, \ldots, \Gamma_m$. Consequently, it cannot be used directly for synthesis. It is clear that constraint (30) includes multiplication of control matrices and Lyapunov function matrix. In the sequel, we will simplify and restate the BMI (30) along with the robust performance satisfaction to derive tractable solvability conditions.

Define new matrices as

$$\begin{aligned}\Omega_0 &= P_k(\hat{J}_k^{m\otimes} \otimes F_1)(I_{(k+1)^m} \otimes \Gamma_0),\\ \Omega_i &= P_k(\hat{J}_k^{(m-i)\otimes} \otimes \tilde{J}_k \otimes \hat{J}_k^{(i-1)\otimes} \otimes F_1)(I_{(k+1)^m} \otimes \Gamma_i), \quad i = 1, 2, \ldots, m,\end{aligned} \tag{33}$$

and

$$\begin{aligned}\Pi_0 &= P_k(\hat{J}_k^{m\otimes} \otimes \widehat{S})(I_{(k+1)^m} \otimes \Gamma_0),\\ \Pi_i &= P_k(\hat{J}_k^{(m-i)\otimes} \otimes \tilde{J}_k \otimes \hat{J}_k^{(i-1)\otimes} \otimes \widehat{S})(I_{(k+1)^m} \otimes \Gamma_i), \quad i = 1, 2, \ldots, m.\end{aligned} \tag{34}$$

From the above definitions, the following algebraic equations can be concluded

$$\begin{bmatrix} \hat{J}_k^{m\otimes} \otimes F_1 \\ \hat{J}_k^{m\otimes} \otimes \widehat{S} \end{bmatrix} (I_{(k+1)^m} \otimes \Gamma_0) = P_k^{-1} \begin{bmatrix} \Omega_0 \\ \Pi_0 \end{bmatrix} \tag{35}$$

and

$$\begin{bmatrix} \hat{J}_k^{(m-i)\otimes} \otimes \tilde{J}_k \otimes \hat{J}_k^{(i-1)\otimes} \otimes F_1 \\ \hat{J}_k^{(m-i)\otimes} \otimes \tilde{J}_k \otimes \hat{J}_k^{(i-1)\otimes} \otimes \widehat{S} \end{bmatrix} (I_{(k+1)^m} \otimes \Gamma_i) = P_k^{-1} \begin{bmatrix} \Omega_i \\ \Pi_i \end{bmatrix}, \quad i = 1, 2, \ldots, m, \tag{36}$$

in the case of the matrix F_1 or equivalently the matrix B_1 has the *full column rank*, it can be concluded from the linear algebra theory that the set of algebraic equations (35) and (36) has *at most* one solution $\Gamma_0, \Gamma_1, \ldots, \Gamma_m$.

According to (33) and (34), the matrices Σ_k and $\widehat{\Xi}_k$ in the BMI (30) can be represented in the forms

$$\begin{aligned}\Sigma_k = &\left(\left(\Omega_0 + \sum_{i=1}^{m} \Omega_i\right)(I_{(k+1)^m} \otimes F_2)\right)^{\mathrm{T}} P_k(\hat{J}_k^{m\otimes} \otimes I_{n+n_c})\\ &+ (\hat{J}_k^{m\otimes} \otimes I_{n+n_c})^{\mathrm{T}}\left(\Omega_0 + \sum_{i=1}^{m} \Omega_i\right)(I_{(k+1)^m} \otimes F_2)\end{aligned} \tag{37}$$

and

$$\widehat{\Xi}_k = (\hat{J}_k^{m\otimes} \otimes I_{n+n_c})^{\mathrm{T}}\left(\Pi_0 + \sum_{i=1}^{m} \Pi_i\right)\left(I_{(k+1)^m} \otimes \begin{bmatrix} E_2 \\ 0_{n_c \times s} \end{bmatrix}\right). \tag{38}$$

Then, from (33)–(37) the solutions of the BMI (30) can be stated as the solutions of an LMI and a set of algebraic equations. Finally, we summarize our result as follows.

Theorem 2 (Delay-independent stabilization) *Let the positive scalar $k-1$ as the degree of the PPDQ Lyapunov–Krasovskii functions is given. Consider the uncertain parameter-dependent system (1) with the constant time delay parameters h_i for $i = 1, 2, \ldots, r$ and full column rank of the matrix B_1. For a given performance bound γ, if there exist positive parameter ε and the positive definite matrices P_k, $Q_k^{(i)} \in R^{k^m(n+n_c)}$ for $i = 1, 2, \ldots, r$ as well as the matrices Ω_i, $\Pi_i \in R^{k^m(n+n_c)\times(k+1)^m(p+n_c)}$ for $i =$*

$0, 1, \ldots, m$ *to the parameter-independent BMI (30), then the sub-optimal RDP-DOF control law (2) with the following state-space matrices*

$$\Gamma_\rho = \Gamma_0 + \sum_{i=1}^{m} \rho_i \Gamma_i \tag{39}$$

may be obtained from the linear algebraic equations (35) and (36) to achieve robust delay-independent asymptotic stability and disturbance attenuation for all admissible vector $\rho \in \zeta$ *and any* $\Delta(\cdot) \in \Omega(\cdot)$.

Theorem 2 gives a solution to the sub-optimal RDP-DOF control problem. Note that this result can be reformulated as an optimal controller synthesis procedure by solving the following optimization problem

$$\begin{gathered} \text{Min} \quad \gamma \\ \text{subject to (30), (35) and (36).} \end{gathered} \tag{40}$$

Remark 3 It is observed that the inequality (30) is linear in P_k, $Q_k^{(1)}$, $Q_k^{(2)}$, $\ldots$, $Q_k^{(r)}$, Ω_0, Ω_1, $\ldots$, Ω_m and Π_0, Π_1, $\ldots$, Π_m which are calculated independently from the vector ρ. It is also seen from the above results that there exists some freedoms contained in the design of control law, such as the choices of appropriate the positive scalar ε and the degree of PPDQ Lyapunov function. These degrees of freedoms can be exploited to achieve other desired closed-loop properties.

5 Example

In this section, we illustrate the proposed methodology on a simple system. The state-space form of the uncertain parameter-dependent state-delayed plant is considered as

$$\begin{aligned} &\dot{x}(t) = (-5 - 2\,\rho_1)x(t) + (2 + \rho_1)x(t - h_1) + u(t) + (1 + \rho_1)w(t) + \Delta(x(t)), \\ &x(t) = 2, \quad t \in [-h_1,\, 0], \\ &z(t) = x(t), \\ &y(t) = 2\,x(t) + w(t), \end{aligned} \tag{41}$$

with $h_1 = 10$ seconds and $\sigma^2 = 0.5$ as the constant time delay and noise variance, respectively. The compact set of the parameter ρ_1 is considered as $\rho_1 \in (-1,\, 1)$. The non-linear uncertain term $\Delta(x(t))$ is assumed to be norm-bounded with the matrix bound $H = 1$. Using the definitions (33) and (34), solving the LMI (30) and the set of algebraic equations (35) and (36) for the performance bound $\gamma = 1.5$ by the Lmitool toolbox of the Matlab software [17] gives the following positive definite matrices P_k, $Q_k^{(1)}$ for $k = 2$,

$$P_k = \begin{bmatrix} 0.2256 & 0.0103 & -0.0264 & 0.0009 \\ 0.0103 & 0.0771 & -0.0846 & 0.0020 \\ -0.0264 & -0.0846 & 0.2001 & 0.0096 \\ 0.0009 & 0.0020 & 0.0096 & 0.0542 \end{bmatrix},$$

$$Q_k^{(1)} = \begin{bmatrix} 0.4484 & -0.0111 & 0.2732 & 0.0022 \\ -0.0111 & 0.5251 & 0.0047 & -0.0230 \\ 0.2732 & 0.0047 & 1.2472 & -0.0070 \\ 0.0022 & -0.0230 & -0.0070 & 0.6286 \end{bmatrix}.$$

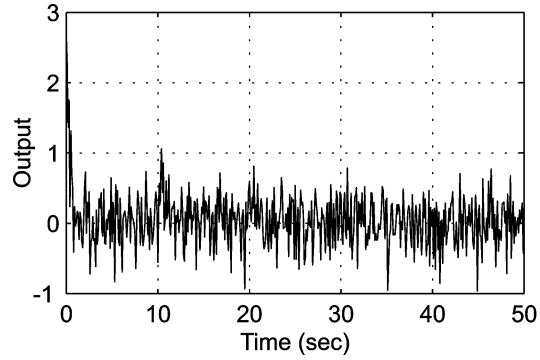

Figure 5.1. Time behavior of $y(t)$.

By considering the parameter $\rho_1 = 0.2225$, time behavior of the system dynamic (41) has been depicted in Figure 5.1.

The sub-optimal RDP-DOF control (2) with the following state-space matrices

$$\Gamma_0 = \begin{bmatrix} 0 & 0.0771 \\ -0.0264 & -0.0846 \end{bmatrix} \quad \text{and} \quad \Gamma_1 = \begin{bmatrix} 0 & 0.0020 \\ 0.0096 & 0.0542 \end{bmatrix}$$

ensures the asymptotic stability of the closed-loop system (3) which has been shown in Figure 5.2.

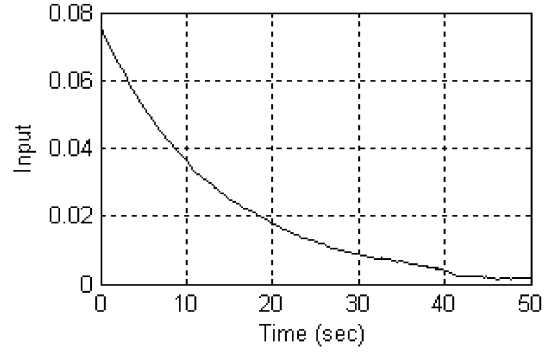

Figure 5.2. The sub-optimal RDP-DOF control.

Moreover, the correctness of disturbance attenuation on the controlled output, i.e. $\|z(t)\|_2^2 - \gamma^2\|w(t)\|_2^2 < 0$, has been depicted in Figure 5.3.

6 Conclusion

In this paper, we have presented a systematic framework for the RDP-DOF stabilization under H_∞ performance index for a class of LTIPD systems with multi-time delays in the state vector and in the presence of norm-bounded non-linear uncertainties. Our main contribution consists in providing a new sufficient condition as QMIs formulations for the existence of the RDP-DOF control using the PPDQ Lyapunov–Krasovskii functions

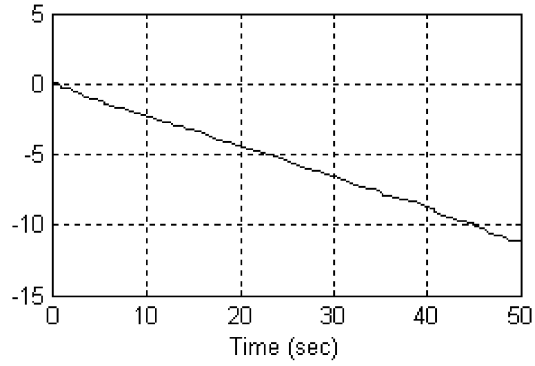

Figure 5.3. The plot of $\|z(t)\|_2^2 - \gamma^2\|w(t)\|_2^2$.

and HJI method. The applicability of the proposed method was illustrated on a simple example.

Acknowledgment

The author would like to thank the German Academic Exchange Service (DAAD) for providing the financial assistance to make this research possible.

References

[1] Apkarian, P. and Adams, R.J. Advanced gain-scheduling techniques for uncertain systems. *IEEE Trans. Control System Technology* **6** (1998) 2132.

[2] Apkarian, P. and Gahinet, P.A. A convex characterization of gain-scheduled H_∞ controllers. *IEEE Trans. Automatic Control* **40** (1995) 853–864.

[3] Apkarian, P., Gahinet, P.A. and Becker, G. Self-scheduled H_∞ control of linear parameter-varying systems: A design example. *Automatica* **31**(7) (1995) 1251–1261.

[4] Apkarian, P. and Tuan, H.D. Parameterized LMIs in control theory. *SIAM J. Control Optimization* **38**(4) (2000) 1241–1264.

[5] Bara, G.I. and Daafouz, J. Parameter-dependent control with γ performance for affine LPV systems. *Proc. of the 40-th Conference on Decision & Control*, Florida, USA, 2001, P.2378–2379.

[6] Becker, G. and Packard, A. Robust performance of linear parametrically-varying systems using parametrically-dependent linear feedback. *Syst. Control Lett.* **23**(3) (1994) 205–512.

[7] Bliman, P.A. LMI approach to spectral stabilizability of linear delay systems and stabilizability of linear systems with complex parameter. *Proc. 40-th IEEE CDC*, 2001, 1438–1443.

[8] Bliman, P.A. Lyapunov equation for the stability of linear delay systems of retarded and neutral type. *IEEE Trans. Automatic Contr.* **47** (2002) 327–335.

[9] Bliman, P.A. Stabilization of LPV systems. *Proc. 42-nd IEEE CDC*, 2003, 6103–6108.

[10] Bliman, P.A. A convex approach to robust stability for linear systems with uncertain scalar parameters. *SIAM J. Control Optim.* **42** (2004) 2016–2042.

[11] Bliman, P.A. An existence result for polynomial solutions of parameter-dependent LMIs. *Systems & Control Letters* **51** (2004) 165–169.

[12] Chesi, G., Garulli, A., Tesi, A. and Vicino, A. Polynomially parameter-dependent Lyapunov functions for robust stability of polytopic systems: An LMI approach. *IEEE Trans. Automatic Contr.* **59** (2005) 365–370.

[13] Doyle, J.C., Packard, A. and Zhou, K. Review of LFT's, LMI's and μ. In: *Proc. IEEE Conf. Decision Contr.*, Brighton, England, 1991, 1227–1232.

[14] Feron,E., Apkarian, P. and Gahinet, P. Analysis and synthesis of robust control systems via parameter-dependent Lyapunov functions. *IEEE Trans. Automatic Contr.* **41** (1996) 1041–1046.

[15] Gahinet, P. and Apkarian, P. A linear matrix inequality approach to H_∞ control. *Int. J. of Robust and Nonlinear Control* **4** (1994) 421–448.

[16] Gahinet, P., Apkarian, P. and Chilali, M. Affine parameter-dependent Lyapunov functions and real parametric uncertainty. *IEEE Trans. Automatic Control* **41** (1996) 436–442.

[17] Gahinet, P., Nemirovsky, A., Laub, A.J. and Chilali, M. *LMI control Toolbox: For use with Matlab.* Natik, MA, The MATH Works, Inc., 1995.

[18] Iwasaki, T. and Skelton, R.E. All controllers for the general H_∞ control design problem: LMI existence conditions and state-space formulas. *Automatica* **30** (1994) 1307–1317.

[19] Karimi, H.R., Jabedar Maralani, P., Lohmann, B. and Moshiri, B. H_∞ control of linear parameter-dependent state-delayed systems using polynomial parameter-dependent quadratic functions. *Int. J. of Control* **78** (2005) 254–263.

[20] Krasovskii, N.N. *Stability of motion.* Stanford, CA, Stanford University Press, 1963.

[21] Lu, B. and Wu, F. Control design of switched LPV systems using multiple parameter-dependent Lyapunov functions. *Proc. ACC* (2004) 3875–3880.

[22] Safonov, M.G., Goh, K.C. and Ly, J.H. Control system synthesis via bilinear matrix inequalities. In: *Proc. Amer. Contr. Conf.*, 1994, 45–49.

[23] Shamma, J.S. and Athans, M. Analysis of gain scheduled control for non-linear plants. *IEEE Trans. Automatic Control* **35** (1990) 898–907.

[24] Shamma, J.S. and Athans, M. Guaranteed properties of gain-scheduled control of linear parameter-varying plants. *Automatica* **27** (1991) 559–564.

[25] Tan, K., Grigoriadis, K.M. and Wu, F. H_∞ and L_2-to-L_∞ gain control of linear parameter-varying systems with parameter-varying delays. *IEE Proc. Control Theory Appl.* **150** (2003) 509–517.

[26] Wang, J., Wang, C. and Yuan, W. A novel H_∞ output feedback controller design for LPV systems with a state-delay. *J. of Nature and Science* **2** (2004) 53–60.

[27] Wang, L.Y. and Zhan, W. Robust disturbance attenuation with stability for linear systems with norm-bounded Nonlinear uncertainties. *IEEE Trans. Automatic Control* **41** (1996) 886–888.

[28] Wu, F. and Grigoriadis, K.M. LPV systems with parameter-varying time delays: analysis and control. *Automatica* **37** (2001) 221–229.

[29] Zhou, K. and Khargonekar, P.P. Robust stabilization of linear systems with norm-bounded time-varying uncertainty. *System Control Letters* **10** (1988) 17–20.

[30] Zhang, X., Tsiotras, P. and Iwasaki, T. Parameter-dependent Lyapunov functions for exact stability analysis of single-parameter dependent LTI systems. In: *42-nd IEEE Proc. CDC*, Vol. 5, 2003, P.5168–5173.

[31] Zhang, X.P., Tsiotras, P. and Knospe, C. Stability analysis of LPV time-delayed systems. *Int. J. of Control* **75** (2002) 538–558.

Appendix

Lemma 1 (Schur Complement Lemma) *Given constant matrices* Ψ_1, Ψ_2 *and* Ψ_3, *where* $\Psi_1 = \Psi_1^{\mathrm{T}}$ *and* $\Psi_2 = \Psi_2^{\mathrm{T}} > 0$, *then* $\Psi_1 + \Psi_3^{\mathrm{T}}\Psi_2^{-1}\Psi_3 < 0$ *if and only if*

$$\begin{bmatrix} \Psi_1 & \Psi_3^{\mathrm{T}} \\ \Psi_3 & -\Psi_2 \end{bmatrix} < 0 \quad \textit{or equivalently,} \quad \begin{bmatrix} -\Psi_2 & \Psi_3 \\ \Psi_3^{\mathrm{T}} & \Psi_1 \end{bmatrix} < 0.$$

Lemma 2 [28] *For any matrix X and Y with appropriate dimensions and for any constant $\eta > 0$, we have*

$$X^{\mathrm{T}}Y + Y^{\mathrm{T}}X \leq \eta X^{\mathrm{T}}X + \frac{1}{\eta}Y^{\mathrm{T}}Y.$$

Lemma 3 (Projection Lemma [13, 15]) *Given a symmetric matrix $H \in R^{h\times h}$ and two matrices $N \in R^{q\times h}$ and $M \in R^{p\times h}$, consider the problem of finding some matrices $X \in R^{p\times q}$ such that*

$$H + N^{\mathrm{T}}X^{\mathrm{T}}M + M^{\mathrm{T}}XN < 0$$

then, the inequality above is solvable for X if and only if

$$N^{\perp T}HN^{\perp} < 0 \quad \textit{and} \quad M^{T\perp T}HM^{T\perp} < 0.$$

Nonlinear Dynamics and Systems Theory, **6**(2) (2006) 159–169

INFORMATH Publishing Group

Stability of Delay Systems with Quadratic Nonlinearities

D. Khusainov[1], A. Ivanov[2] and I. Grytsay[1*]

[1] *Faculty of Cybernetics, Kyiv Taras Shevchenko National University, 64 Vladimirskaya Str., Kyiv, 01033, Ukraine*
[2] *Department of Mathematics, Pennsylvania State University, P.O.Box PSU, Lehman, PA 18708, USA*

Received: January 3, 2006; Revised: June 2, 2006

Abstract: In this paper differential systems with delay and quadratic nonlinear terms are considered. Sufficient stability conditions, estimations of the stability domain and estimations of the convergence rate are derived.

Keywords: *Systems of differential equations with delay; stability of zero solution; estimates on the stability domain; rate of convergence.*

Mathematics Subject Classification (2000): 34K20.

1 Introduction

Two modifications are typically used when differential delay systems are studied by using the second Liapunov method [9 – 11]. The first one is the Liapunov–Krasovsky method. In this case, a segment of the trajectory is identified with a point in Banach space. Also, the main ideas of the Liapunov functions method are carried over to this case of functionals, and the stability theorems usually contain the necessary and sufficient conditions [9, 11]. The second modification uses the finite-dimensional Liapunov functions. In this case the derivative of the solution is estimated under the assumption that the solution remains inside the level surface of the Liapunov function. This assumption is called the Razumikhin condition [10].

*Corresponding author: grytsay@mail.univ.kiev.ua

2 Preliminaries

In this paper we consider differential delay systems with a quadratic nonlinearity of the following form

$$\dot{x}(t) = Ax(t-\tau) + X^{\mathrm{T}}(t)Bx(t-\tau), \tag{1}$$

where $t \geq 0$, τ is a positive constant, $x(t) \in R^n$, A is a constant square matrix. The matrices $X^{\mathrm{T}}(t)$ and B are rectangular ones of the size $n \times n^2$ and $n^2 \times n$, respectively; $X^{\mathrm{T}}(t) = \left\{X_1^{\mathrm{T}}(t), X_2^{\mathrm{T}}(t), \ldots, X_n^{\mathrm{T}}(t)\right\}$, $B^{\mathrm{T}} = \{B_1, B_2, \ldots, B_n\}$. We suppose that square matrices B_i, $i = \overline{1,n}$, are constant and symmetric, and all elements of the square matrices $X_i^{\mathrm{T}}(t)$, $i = \overline{1,n}$, are zero except the i-th row, which equals to $x(t) = (x_1(t), x_2(t), \ldots, x_n(t))$ [2, 7].

Since the right hand side of system (1) does not contain the phase coordinate x at present time t the approach with the use of quadratic functionals encounters certain difficulties (see [10] for more details). Therefore, we shall study the stability of the zero solution $x(t) = 0$ and derive estimates on the stability region by using finite-dimensional Liapunov functions subject to the Razumikhin condition. For the Liapunov function we shall choose the following quadratic form

$$V(x,t) = e^{\gamma t} x^{\mathrm{T}} H x$$

with the positive definite matrix$H$ solving the Liapunov matrix equation [1, 10]

$$A^{\mathrm{T}}H + HA = -C. \tag{2}$$

The exponential factor $e^{\gamma t}$, $\gamma > 0$, does not guarantee the existence of an infinitesimal limit of higher order for the function $V(x,t)$ [8, 10, 12]. It allows us however to obtain an estimate on the upper bound of decrease rate of solutions starting in the stability domain of zero solution.

In the case when matrix A is asymptotically stable the matrix equation (2) has a unique solution, positive definite matrix H, for every positive definite matrix C. We shall use the standard vector and matrix norms [6] as follows

$$|A| = \{\lambda_{\max}(A^{\mathrm{T}}A)\}^{1/2}, \quad |x(t)| = \left\{\sum_{i=1}^{n} x_i^2(t)\right\}^{1/2}, \quad \|x(t)\|_\tau = \max_{-\tau \leq s \leq 0}\{|x(t+s)|\}.$$

Here and in the sequel $\lambda_{\min}(\cdot)$ and $\lambda_{\max}(\cdot)$ stand for the smallest and the largest eigenvalues respectively for the symmetric positive definite matrices.

Let ∂V_α^γ be a level surface of the Liapunov function V and V_α^γ be the corresponding domain in the space $R^n \times R$, that is

$$\partial V_\alpha^\gamma = \{(x,t)\colon\ V(x,t) = \alpha\}, \quad V_\alpha^\gamma = \{(x,t)\colon\ V(x,t) < \alpha\}.$$

3 Main Results

3.1 Linear case

Consider the following linear system with delay

$$\dot{x}(t) = Ax(t-\tau). \tag{3}$$

Lemma 1 *Suppose solution $x(t)$ of system (3) satisfies $(x(t),t) \in V_\alpha^\gamma$, for $t > -\tau$. Then*

$$|x(t)| < \sqrt{\alpha/\lambda_{\min}(H)}e^{-\frac{1}{2}\gamma t}, \quad t \geq \tau. \tag{4}$$

Proof The Liapunov functions of quadratic type $X(x,T) = e^{\gamma t}x^{\mathrm{T}}Hx$ are known to satisfy the following two-sided inequality [3]

$$e^{\gamma t}\lambda_{\min}(H)|x(t)|^2 \leq V(x(t),\, t) \leq e^{\gamma t}\lambda_{\max}(H)|x(t)|^2. \tag{5}$$

Therefore, the assumptions of Lemma imply

$$\lambda_{\min}(H)|x(t)|^2 < \alpha.$$

From the latter inequality the estimate (4) follows.

Lemma 2 *Suppose there exist constants $\alpha > 0$, $\gamma > 0$ such that the solution $x(t)$ of system (3) satisfies $(x(t),t) \in V_\alpha^\gamma$, for all $T - 2\tau \leq t < T$ and $(x(T),T) \in \partial V_\alpha^\gamma$. Then*

$$\begin{gathered} |x(T) - x(T-\tau)| < 2\,\frac{|A|}{\gamma}\, e^{\frac{1}{2}\gamma\tau}\sqrt{\varphi(H)}\big(e^{\frac{1}{2}\gamma\tau} - 1\big)|x(T)|, \\ \varphi(H) = \lambda_{\max}(H)/\lambda_{\min}(H)\lambda_{\min}(H). \end{gathered} \tag{6}$$

Proof Solutions of system (3) can be represented in the following integral form

$$x(t) = x(t-\tau) + \int\limits_{t-\tau}^{t} Ax(s-\tau)\, ds.$$

When $t = T$ the latter implies

$$|x(T) - x(T-\tau)| \leq \int\limits_{T-\tau}^{T} |A||x(s-\tau)|\, ds.$$

From the assumptions of Lemma 2 and inequality (5) the following holds

$$\begin{gathered} e^{\gamma(s-\tau)}\lambda_{\min}(H)|x(s-\tau)|^2 \leq V(x(s-\tau),\, s-\tau) \leq V(x(T),T) \\ < e^{\gamma T}\lambda_{\max}(H)|x(T)|^2 \quad \text{for all} \quad T-\tau \leq s \leq T. \end{gathered}$$

Therefore

$$|x(s-\tau)| < e^{\frac{1}{2}\gamma(T-s+\tau)}\sqrt{\varphi(H)}\,|x(T)|, \quad \varphi(H) = \lambda_{\max}(H)/\lambda_{\min}(H). \tag{7}$$

By using the last inequality in the integral representation we derive the required estimate

$$\begin{aligned} |x(T) - x(T-\tau)| &< \int\limits_{T-\tau}^{\mathrm{T}} |A|e^{\frac{1}{2}\gamma(T-s+\tau)}\sqrt{\varphi(H)}|x(T)|ds \\ &= 2\,\frac{|A|}{\gamma}\, e^{\frac{1}{2}\gamma\tau}\sqrt{\varphi(H)}\,\big[e^{\frac{1}{2}\gamma\tau} - 1\big]|x(T)|. \end{aligned}$$

Lemma 3 *Every solution $x(t)$ of system (3) satisfies the inequality*

$$|x(t)| \le (1 + |A|\tau)\|x(0)\|_\tau \tag{8}$$

on the time interval $0 \le t \le \tau$.

Proof Write system (3) in the integral form

$$x(t) = x(0) + \int_0^t Ax(s-\tau)\,ds.$$

Then

$$|x(t)| \le |x(0)| + \int_0^t |A||x(s-\tau)|\,ds \le |x(0)| + |A|\|x(0)\|_\tau \tau \le (1 + |A|\tau)\|x(0)\|_\tau.$$

By using the above Lemmas the following Theorem on asymptotic stability of the system with pure delay (3) is derived.

Theorem 1 *Assume that matrix A is asymptotically stable. Then the system with pure delay (3) is also asymptotically stable for all $\tau < \tau_0$, where*

$$\tau_0 = \frac{\lambda_{\min}(C)}{2|A||HA|\sqrt{\varphi(H)}}. \tag{9}$$

Moreover, the solutions of the system satisfy the following exponential estimate on their rate of decrease

$$|x(t)| < (1 + |A|\tau)\|x(0)\|_\tau \sqrt{\varphi(H)}\,\exp\left\{\frac{1}{2}\gamma t\right\}, \quad t \ge \tau, \tag{10}$$

where $0 < \gamma < \gamma^*$, γ^* is the positive solution of the equation

$$\gamma^*(\lambda_{\min}(C) - \gamma^*\lambda_{\max}(H)) = 4\sqrt{\varphi(H)}\,|HA||A|e^{\frac{1}{2}\gamma^*\tau}\left(e^{\frac{1}{2}\gamma^*\tau} - 1\right). \tag{11}$$

Proof Let $x(t)$ be any solution of system (3). Then, as it follows from Lemma 3, it satisfies the following inequality

$$|x(t)| \le (1 + |A|\tau)\|x(0)\|_\tau,$$

for all $0 \le t \le \tau$. Also on the same time interval $x(t)$ satisfies $(x(t), t) \in V_\alpha^\gamma$, where $\gamma > 0$ is a constant to be determined later, and $\alpha > \lambda_{\max}(H)(1 + |A|\tau)^2\|x(0)\|_\tau^2$.

We claim that also $(x(t), t) \in V_\alpha^\gamma$ for all $t > \tau$. Suppose not. Then there exists a time moment $T > \tau$, such that $(x(T), T) \in \partial V_\alpha^\gamma$. Evaluate now the total derivative of the Liapunov function V along the solutions of system (3):

$$\frac{d}{dt}V(x(t)) = e^{\gamma t}\gamma x^{\mathrm{T}}(t)Hx(t) + e^{\gamma t}\{x^{\mathrm{T}}(t)(A^{\mathrm{T}}H + HA)x(t) + 2x^{\mathrm{T}}(t)HA[x(t-\tau) - x(t)]\}.$$

If matrix A is asymptotically stable then, as it follows from the matrix Liapunov equation (2), for any positive define matrix C and matrix H solving the equation the total derivative of V satisfies

$$\frac{d}{dt}V(x(t)) \le e^{\gamma t}\{\gamma\lambda_{\max}(H) - \lambda_{\min}(C)\}|x(t)|^2 + 2e^{\gamma t}|HA||x(t)||x(t) - x(t-\tau)|.$$

As it follows from the assumptions of Theorem 1 and inequality (7) the last inequality at time $t = T$ reads

$$\frac{d}{dt}V(x(t)) \le -e^{\gamma T}\left\{\lambda_{\min}(C) - \gamma\lambda_{\max}(H) - 4|HA||A|\sqrt{\varphi(H)}\, e^{\frac{1}{2}\gamma\tau}\frac{e^{\frac{1}{2}\gamma\tau} - 1}{\gamma}\right\}|x(t)|^2.$$

If in addition the inequality

$$\lambda_{\min}(C) - \gamma\lambda_{\max}(H) - 4|HA||A|\sqrt{\varphi(H)}\, e^{\frac{1}{2}\gamma\tau}\,\frac{e^{\frac{1}{2}\gamma\tau} - 1}{\gamma} > 0 \tag{12}$$

holds, then the total derivative of the Liapunov function will be negative. This means that the velocity vector of the motion $x(t)$ is directed inside the domain at the moment $t = T$, and $(x(t), t) \in V_\alpha^\gamma$ for all $t > 0$. It follows from inequalities (4) and (8) that the following holds

$$|x(t)| < (1 + |A|\tau)\|x(0)\|_\tau\sqrt{\varphi(H)}\,\exp\left\{\frac{1}{2}\gamma t\right\}, \quad t \ge \tau,$$

that is, inequality (10) is true. Let us find the conditions for inequality (12) to be true. If $\gamma \to +0$ then inequality (11) has the form

$$\lambda_{\min}(C) - 2|HA||H|\sqrt{\varphi(H)}\,\tau > 0,$$

and if $\tau < \tau_0$, then

$$\tau_0 = \frac{\lambda_{\min}(C)}{2|HA||A|\sqrt{\varphi(H)}}.$$

That is, the maximum allowed delay τ_0 has the form given by (9). Let $\tau < \tau_0$. Then there is a threshold for the rate of exponential decrease of the solutions, which value is determined by the solution of equation (11).

Remark 1 In general it is not possible to represent the solution of equation (11) in an explicit analytic form. The value γ^* can be replaced by a smaller value $\tilde{\gamma}^*$, where

$$0 < \tilde{\gamma}^* = \gamma_0 - \frac{h(\gamma_0)}{\lambda_{\min}(C)}, \qquad \gamma_0 = \frac{\lambda_{\min}(C)}{\lambda_{\max}(H)},$$
$$h(\gamma_0) = 4|HA||A|\sqrt{\varphi(H)}\, e^{\frac{1}{2}\gamma_0\tau}\left(e^{\frac{1}{2}\gamma_0\tau} - 1\right).$$

Proof The left-hand side of system (11) is the parabola

$$g(\gamma) = \gamma[\lambda_{\min}(C) - \gamma\lambda_{\max}(H)]$$

opening downward and having the following two zeros $\gamma_0 = \lambda_{\min}(C)/\lambda_{\max}(H),\ \gamma_1 = 0$. The right-hand side of equality (11) is a parabola in the variable $e^{\frac{1}{2}\gamma\tau}$, where $\gamma \geq 0$

$$h(\gamma) = 4|HA||A|e^{\frac{1}{2}\gamma\tau}\Big(e^{\frac{1}{2}\gamma\tau} - 1\Big),$$

also opening downward. Since $g(0) = h(0) = 0$ and

$$g'(0) = \lambda_{\min}(C) > 2|HA||A|\sqrt{\varphi(H)}\,\tau = h'(0),$$

then a γ^* exists $(0 < \gamma^* < \gamma_0 = \lambda_{\min}(C)/\lambda_{\max}(H))$, such that $g(\gamma^*) = h(\gamma^*)$. The "parabola" $h(\gamma)$ is replaced by the line segment $\overline{h}(\gamma)$ passing through the origin and the point $(\gamma_0, h(\gamma_0))$ and having the form $\overline{h}(\gamma) = h(\gamma_0)\frac{\gamma}{\gamma_0}$. Point $\tilde{\gamma}^*$ is defined as the intersection of the parabola $g(\gamma)$ and the line $\overline{h}(\gamma)$. That is, as the positive solution of the equation

$$\gamma[\lambda_{\min}(C) - \gamma\lambda_{\max}(H)] = h(\gamma_0)\,\frac{\gamma}{\gamma_0}.$$

The latter gives the required value of $\tilde{\gamma}^*$.

Remark 2 Condition (9) is rather approximate but readily calculated one. For example, for the scalar equation

$$\dot{x}(t) = -ax(t-\tau), \quad a > 0$$

the stability condition is $\tau < \pi/2a$ (see [12]). By using the Liapunov function $V(x,t) = e^{\gamma t}x^2$ from inequality (9) we obtain the following stability condition $\tau < 1/a$.

3.2 Nonlinear case

Consider next systems of the form (1) with pure delay in the linear part.

Lemma 4 *Assume there exist constants $\alpha > 0$ and $\gamma > 0$ such that the solution $x(t)$ of system (1) satisfies $(x(T), T) \in \partial V_\alpha^\gamma$ for $t = T$, and $(x(t), t) \in V_\alpha^\gamma$ for $T - 2\tau \leq t < T$. Then the following inequality holds*

$$\begin{aligned} |x(T) - x(T-\tau)| < \frac{2}{\gamma}\,e^{\frac{1}{2}\gamma\tau}\sqrt{\varphi(H)}\,|A|\Big(e^{\frac{1}{2}\gamma\tau} - 1\Big)|x(T)| \\ + \frac{1}{\gamma}\,e^{\frac{1}{2}\gamma\tau}\varphi(H)|B|(e^{\gamma\tau} - 1)|x(T)|^2. \end{aligned} \tag{13}$$

Proof Write system (1) in the integral form

$$x(t) = x(t-\tau) + \int_{t-\tau}^{t} [Ax(s-\tau) + X^{\mathrm{T}}(s)Bx(s-\tau)]\,ds.$$

At the time moment $t = T$ the latter inequality implies

$$|x(T) - x(T-\tau)| \leq \int_{T-\tau}^{T} [|A||x(s-\tau)| + |X(s)||B||x(s-\tau)|]\,ds.$$

From the assumptions of Lemma 4 and estimate (7) it follows that the following inequality holds

$$|x(s-\tau)| < e^{\frac{1}{2}\gamma(T-s+\tau)}\sqrt{\varphi(H)}\,|x(T)|, \quad |x(s)| < e^{\frac{1}{2}\gamma(T-s)}\sqrt{\varphi(H)}\,|x(T)|,$$

for all $T-\tau \le s \le T$. By using the latter in the integral representation we derive

$$\begin{aligned}|x(T)-x(T-\tau)| < &\int_{T-\tau}^{T} |A| e^{\frac{1}{2}\gamma(T-s+\tau)}\sqrt{\varphi(H)}\,|x(T)|\,ds \\ &+ \int_{T-\tau}^{T} e^{\frac{1}{2}(2T-2s+\tau)}\varphi(H)|B||x(T)|^2\,ds,\end{aligned}$$

or

$$|x(T)-x(T-\tau)| < \frac{2}{\gamma}\,e^{\frac{1}{2}\gamma\tau}\sqrt{\varphi(H)}\,|A|\Big(e^{\frac{1}{2}\gamma\tau}-1\Big)|x(T)| + \frac{1}{\gamma}\,e^{\frac{1}{2}\gamma\tau}\varphi(H)|B|(e^{\gamma\tau}-1)|x(T)|^2.$$

Lemma 5 *Every solution $x(t)$ of system (1) satisfies the following inequality*

$$|x(t)| \le (1+|A|\tau)\|x(0)\|_\tau e^{|B\|x(0)\|\|_\tau \tau t} \tag{14}$$

on the interval $0 \le t \le \tau$.

Proof Write system (1) in the integral form

$$x(t) = x(0) + \int_0^t [Ax(s-\tau) + X^{\mathrm{T}}(s)Bx(s-\tau)]\,ds.$$

Then

$$\begin{aligned}|x(t)| &\le |x(0)| + \int_0^t [|A||x(s-\tau| + |X(s)|B||x(s-\tau||]\,ds \\ &\le (|x(0)| + |A|\|x(0)\|_\tau\tau) + |B|\|x(0)\|_\tau \int_0^t |x(s)|\,ds \\ &\le (1+|A|\tau)\|x(0)\|_\tau e^{|B\|x(0)\|\|_\tau\tau t}.\end{aligned}$$

Lemma 6 *Suppose the derivative of the Liapunov function $V(x,t) = e^{\gamma t}x^{\mathrm{T}}Hx$ along solutions of system (1) satisfies the inequality*

$$\frac{d}{dt}V(x(t),t) \le -aV(x(t),t) + be^{-\frac{1}{2}\gamma t}V^{\frac{3}{2}}(x(t),t), \tag{15}$$

for all $t \geq 0$, where $a > 0$, $b > 0$, $\gamma > 0$. Then all the solutions subjected to the initial condition

$$\|x(0)\|_\tau < \frac{a+\gamma}{b\sqrt{\lambda_{\max}(H)}}$$

satisfy the inequality

$$|x(t)| \leq \frac{\sqrt{\varphi(H)}\,\|x(0)\|_\tau e^{-\frac{1}{2}at}}{1-\dfrac{b}{a+\gamma}\Big(1-e^{-\frac{1}{2}(a+\gamma)t}\Big)\sqrt{\lambda_{\max}(H)}\,\|x*(0)\|_\tau}. \tag{16}$$

Proof Inequality (15) is a Bernoulli type inequality. Since $V(x,t) > 0$, divide the inequality by $V^{3/2}(x,t)$. It follows

$$V^{-\frac{3}{2}}(x(t),t)\,\frac{d}{dt}V(x(t),t) \leq -aV^{-\frac{1}{2}}(x(t),t) + be^{-\frac{1}{2}\gamma t}.$$

By using the substitution $V^{-1/2}(x(t),t) = z(t)$, $z(0) > b/a$, we derive

$$\frac{d}{dt}\,z(t) \geq \frac{1}{2}\,az(t) - \frac{1}{2}\,be^{-\frac{1}{2}\gamma t}.$$

By solving the above differential inequality we obtain

$$z(t) \geq \left[z(0) - \frac{b}{a+\gamma}\right]e^{\frac{1}{2}at} + \frac{b}{a+\gamma}e^{-\frac{1}{2}\gamma t}, \quad z(0) \geq \frac{b}{a}.$$

Having returned to the original variables we have

$$\frac{1}{\sqrt{V(x(t),t)}} \geq \left[\frac{1}{\sqrt{V(x(0),0)}} - \frac{b}{a+\gamma}\right]e^{\frac{1}{2}at} + \frac{b}{a+\gamma}\,e^{-\frac{1}{2}\gamma t}$$

or

$$V(x(t),t) \leq \frac{1}{\left\{\left[\dfrac{1}{\sqrt{V(x(0),0)}} - \dfrac{b}{a+\gamma}\right]e^{\frac{1}{2}at} + \dfrac{b}{a+\gamma}e^{-\frac{1}{2}\gamma t}\right\}^2}.$$

Next we see that

$$V(x(t),t) \leq \frac{V(x(0),0)}{\left\{\left[1 - \dfrac{b}{a+\gamma}\sqrt{V(x(0),0)}\right]e^{\frac{1}{2}at} + \dfrac{b}{a+b}e^{-\frac{1}{2}\gamma t}\sqrt{V(x(0),0)}\right\}^2}.$$

Finally by using the standard inequalities for quadratic forms we obtain inequality (16).

Theorem 2 *Assume that matrix A is asymptotically stable. Then for all $\tau < \tau_0$ where τ_0 is defined by (9), the zero solution of the differential system with delay (1) is also asymptotically stable. The stability domain contains the sphere U_δ, where the radius δ is found as the positive solution of the equation*

$$(1 + |A|\tau)\delta e^{|B|\delta\tau} = \frac{a+\gamma}{b\sqrt{\lambda_{\max}(H)}}. \tag{17}$$

Moreover, for the solutions with the initial conditions inside the sphere U_δ the following estimate on the convergence rate holds

$$|x(t)| \le \frac{\sqrt{\varphi(H)}\,\|x(0)\|_\tau e^{-\frac{1}{2}(a+\gamma)t}}{1 - \dfrac{b}{a+\gamma}\Big(1 - e^{-\frac{1}{2}(a+\gamma)t}\Big)\sqrt{\lambda_{\max}(H)}\,\|x(0)\|_\tau}, \tag{18}$$

where

$$a = \frac{1}{\lambda_{\max}(H)}\left\{\lambda_{\min}(C) - \gamma\lambda_{\max}(H) - 4|HA|\,\frac{|A|}{\gamma}\,E^{\frac{1}{2}\gamma\tau}(E^{\frac{1}{2}\gamma\tau} - 1)\sqrt{\varphi(H)}\right\},$$
$$b = \frac{2}{\lambda_{\min}(H)}|B|\sqrt{\varphi(H)}\,E^{\frac{1}{2}\gamma\tau}\left\{|HA|\sqrt{\varphi(H)}\,\frac{1}{\gamma}\,(E^{\gamma\tau} - 1) + \lambda_{\max}(H)\right\}.$$

Proof Suppose the initial condition for the solution $x(t)$ of system (1) satisfies the assumption $\|x(0)\|_\tau < \delta$ where δ is defined by (17). Then inequality (14) of Lemma 5 implies that at the moment $t = \tau$ the following inequality

$$\|x(\tau)\|_\tau \le R, \quad R = (1 + |A|t)\delta e^{|B|\delta t}$$

is true. On the time interval $-\tau \le t \le \tau$ the integral curve satisfies $(x(t), t) \in V_\alpha^\gamma$ where $\gamma > 0$ is a constant and $\alpha = e^{\gamma\tau}\lambda_{\max}(H)R$. We shall show that there exists a constant $\gamma^* > 0$ such that $(x(t), t) \in V_\alpha^{\gamma^*}$ for all $t > \tau$. Assume not. Then there exists $T > \tau$ such that $(x(T), T) \in \partial V_\alpha^\gamma$. We evaluate next the total derivative of the Liapunov function V along the solutions of system (1)

$$\frac{d}{dt}V(x(t)) = e^{\gamma t}\gamma x^{\mathrm{T}}(t)Hx(t) + e^{\gamma t}\{[Ax(t-\tau) + X^{\mathrm{T}}(t)Bx(t-\tau)]Hx(t) + x^{\mathrm{T}}(t)H[Ax(t-\tau) + X^{\mathrm{T}}(t)Bx(t-\tau)]\},$$

or

$$\frac{d}{dt}V(x(t)) = e^{\gamma t}x^{\mathrm{T}}(t)(\gamma H + A^{\mathrm{T}}H + HA)x(t) + 2e^{\gamma t}x^{\mathrm{T}}(t)HA[x(t-\tau) - x(t)] + 2e^{\gamma t}x^{\mathrm{T}}(t)HX^{\mathrm{T}}(t)Bx(t-\tau).$$

If matrix A is asymptotically stable then using the chosen matrix norm and the Liapunov equation (2) we obtain

$$\frac{d}{dt}V(x(t), t) \le -e^{\gamma t}\{\lambda_{\min}(C) - \gamma\lambda_{\max}(H)\}|x(t)|^2 + 2e^{\gamma t}|HA||x(t)||x(t) - x(t-\tau)| + 2e^{\gamma t}\lambda_{\max}(H)|B||x(t)|^2|x(t-\tau)|.$$

Since $(x(T),T) \in \partial V_\alpha^\gamma$ by using inequalities (13) and (14) we obtain the following estimate for the derivative of the Liapunov function

$$\begin{aligned}\frac{d}{dt}V(x(T),T) &\\ &\le -e^{\gamma T}\left\{\lambda_{\min}(C) - \gamma\lambda_{\max}(H) - 4|HA|\,\frac{|A|}{\gamma}\,e^{\frac{1}{2}\gamma\tau}(e^{\frac{1}{2}\gamma\tau}-1)\sqrt{\varphi(H)}\right\}|x(T)|^2\\ &\quad + 2e^{\gamma T}|B|\sqrt{\varphi(H)}e^{\frac{1}{2}\gamma\tau}\left\{|HA|\sqrt{\varphi(H)}\,\frac{1}{\gamma}\,(e^{\gamma\tau}-1) + \lambda_{\max}(H)\right\}|x(T)|^3.\end{aligned}$$

By using the standard inequalities for quadratic forms we obtain

$$\begin{aligned}\frac{d}{dt}V(x(T),T) \le -\frac{1}{\lambda_{\max}(H)}&\left\{\lambda_{\min}(C) - \gamma\lambda_{\max}(H)\right.\\ &- 4|HA|\,\frac{|A|}{\gamma}\,e^{\frac{1}{2}\gamma\tau}\Big(e^{\frac{1}{2}\gamma\tau}-1\Big)\sqrt{\varphi(H)}\Big\}V(x(T),T)\\ &+ \frac{2}{\lambda_{\min}(H)}\,|B|\sqrt{\varphi(H)}\,e^{\frac{1}{2}\gamma\tau}\left\{|HA|\sqrt{\varphi(H)}\,\frac{1}{\gamma}(e^{\gamma\tau}-1)\right.\\ &\left.+\lambda_{\max}(H)\right\}e^{-\frac{1}{2}\gamma T}V^{3/2}(x(T),T).\end{aligned} \tag{19}$$

Let $\tau < \tau_0$, where τ_0 is defined by (8) and let $0 < \gamma < \gamma^*$, where γ^* is the solution of equation (11). Define

$$\begin{aligned}a &= \frac{1}{\lambda_{\max}(H)}\left\{\lambda_{\min}(C) - \gamma\lambda_{\max}(H) - 4|HA|\,\frac{|A|}{\gamma}\,e^{\frac{1}{2}\gamma\tau}\Big(e^{\frac{1}{2}\gamma\tau}-1\Big)\sqrt{\varphi(H)}\right\},\\ b &= \frac{2}{\lambda_{\min}(H)}\,|B|\sqrt{\varphi(H)}\,e^{\frac{1}{2}\gamma\tau}\left\{|HA|\sqrt{\varphi(H)}\,\frac{1}{\gamma}\,(e^{\gamma\tau}-1) + \lambda_{\max}(H)\right\}.\end{aligned}$$

Then $a > 0,\ b > 0$, and inequality (19) has the form (15)

$$\frac{d}{dt}\,V(x(T),T) \le -aV(x(T),T) + bV^{3/2}(x(T),T).$$

By using Lemma 6 we conclude that inequality (16) is true for the solutions $x(t)$ of system (1) satisfying the condition $\|x(\tau)\|_\tau \le R$, where δ is defined by (17). This completes the proof of the theorem.

References

[1] Barbashin, E.A. *Liapunov Functions.* Nauka, Moscow, 1970. [Russian]

[2] Davydov, V.F. Upper Estimates of Solutions of Quadratic Differential Systems with Delay. *Ukrainian Math. J.* **47**(4) (1995) 542–545. [Russian]

[3] Demidovich, B.P. *Lectures on Mathematical Stability Theory.* Nauka, Moscow, 1967. [Russian]

[4] El'sgolts, L.E. and Norkin, S.B. *Introduction to Differential Equations with Deviating Arguments.* Nauka, Moscow, 1971. [Russian]

[5] Galperin E.A. Some generalizations of Lyapunov's approach to stability and control. *Nonlinear Dynamics and Systems Theory* **2**(1) (2002) 1–24.
[6] Gantmaher, F.R. *Theory of Matrices.* Nauka, Moscow, 1966. [Russian]
[7] Khysainov, D.Ya. and Davydov, V.F. Stability of systems of quadratic type. *Dokl. Natz. Akad. Nauk of Ukraine* (7) (1994) 11–13. [Russian]
[8] Khusainov, D.Ya. and Shatyrko, A.V. *The Method of Liapunov Functions in the Study of the Stability of Differential-Functional Systems.* Izd-vo Kiev University , Kiev, 1997. [Russian]
[9] Korenevskiy, D.G. *Stability of Dynamical Systems under Random Perturbations of Parameters. Algebraic Criteria.* Naukova Dumka, Kyiv, 1989. [Russian]
[10] Krasovskii, N.N. *Some Problems of Stability Theory of Motion.* Fizmatgiz, Moscow, 1959. [Russian]
[11] Lakshmikantham, V. and Martynyuk, A.A. Development of Liapunov Direct Method for Systems with Aftereffect. *Prikl. Mekh.* **29**(2) (1993) 3–16. [Russian]
[12] Liapunov, A.M. *General Problem of Stability of Motion.* Gos. Izd-vo Tekh.-Teor. Lit., Moscow–Leningrad, 1950. [Russian]
[13] Martynyuk, A.A. Stability of dynamical systems in metric space. *Nonlinear Dynamics and Systems Theory* **5**(2) (2005) 157–167.
[14] Sivasundaram, S. Stability of dynamic systems on the time scales. *Nonlinear Dynamics and Systems Theory* **2**(2) (2002) 185–202.
[15] Taishan Yi and Lihong Huang. Convergence of solutions to a class of systems of delay differential equations. *Nonlinear Dynamics and Systems Theory* **5**(2) (2005) 189–200.

Nonlinear Dynamics and Systems Theory, **6**(2) (2006) 171–186

A New Approach for Dynamic Analysis of Composite Beam with an Interply Crack

V.Y. Perel*

University of Dayton Research Institute,
300 College Park Avenue, Dayton, Ohio 45469-0168, USA

Received: August 15, 2005; Revised: June 6, 2006

Abstract: In this work, a new approach is developed for dynamic analysis of a composite beam with an interply crack, in which a physically impossible interpenetration of the crack faces is prevented by imposing a special constraint, leading to taking account of a force of contact interaction of the crack faces and to nonlinearity of the formulated boundary value problem. The shear deformation and rotary inertia terms are included into the formulation, to achieve better accuracy. The model is based on the first order shear deformation theory, i.e. the longitudinal displacement is assumed to vary linearly through the beam's thickness. A variational formulation of the problem, nonlinear partial differential equations of motion with boundary conditions and the finite element solution of the partial differential equations with the use of the FEMLAB package are developed. The use of FEMLAB facilitates automatic mesh generation, which is needed if the problem has to be solved many times with different crack lengths. An example problem of a clamped-free beam with a piezoelectric actuator is considered, and its finite element solution is obtained. A noticeable difference of forced vibrations of the delaminated and undelaminated beams due to the contact interaction of the crack faces is predicted by the developed model.

Keywords: *composite delaminated beam; piezoelectric actuator; contact of crack faces; Lagrange multipliers; penalty function method; shear deformation theory; nonlinear partial differential equations; nonlinear finite element analysis.*

Mathematics Subject Classification (2000): 74H45, 74K05, 74M05.

*Corresponding author: vperel@gmail.com

1 Introduction

Several types of models of delaminated beams have been proposed in the literature. In some models, for example [1] and [2], the contact force between the delaminated parts is not taken into account, and the physically impossible mutual penetration of the delaminated parts is allowed. In other models, for example [3], the delaminated parts are constrained to have the same transverse displacement, excluding the possibility of the delamination crack opening during the vibration. In the Reference [4], the interaction between the delaminated parts is modeled with the use of a nonlinear (piecewise-linear) spring between the surfaces of the delaminated parts. Stiffness of the spring depends on the difference of displacements of the lower and upper delaminated parts. If the delamination crack is open, the stiffness of the spring is set equal to zero, making the distributed contact force equal to zero. When the delamination crack is closed, the stiffness of the spring is set either to infinity, or to some finite constant value. The authors set the spring stiffness equal to a constant (either zero, or 0.1, or infinity) before solving the problem, thus assuming that the crack remains either open or closed all the time during the vibration. So, the possibility for the crack to be open in some time intervals and closed in other time intervals during the vibration is not foreseen in this model.

In the paper [5], the contact force between the delaminated sublaminates is introduced as a function of the relative transverse displacement of the sublaminates, in such a way that the contact force automatically turns out to be zero, when the delamination crack is open, and takes on a non-zero value, if the crack is closed. So, this model does not require to specify in advance if the crack is open or closed, and allows for contact and separation of the crack faces during the vibration. However, the physically impossible interpenetration of the crack faces is not always prevented in this model. The interpenetration occurs because a constraint, preventing this phenomenon, is not introduced.

In the model of the delaminated composite beam, presented by the author in the Reference [6], the constraint, preventing the mutual penetration (interpenetration, overlapping) of the delaminated sublaminates (of the crack's faces), was introduced with the use of the Heaviside function and the penalty function method [8], which was the main novelty in solving dynamic problems for beams with cracks. The longitudinal force resultants in the delaminated sublaminates and rotary inertia terms were taken into account also. The use of the constraint, which prevented the interpenetration of the crack faces, and taking account of the longitudinal force resultants led to nonlinear partial differential equations of motion, in which a force of contact interaction of the crack faces was taken into account.

But the model, presented in Reference [6], did not take the shear strain energy into account, and, therefore, produced sufficiently accurate results only for thin beams. To model thicker beams with delamination, one needs to use a beam theory, based on simplifying assumptions, which do not lead to vanishing of the shear strains. The first order shear deformation theory [8], based on assumed linear variation of a longitudinal displacement in the thickness direction, is the simplest approach that satisfies the requirement of a non-zero shear strain. This approach is used in the present paper for modeling a composite delaminated beam with a piezoelectric actuator. In this model, the interpenetration of the crack faces is prevented by a method similar to the one, which was used in Reference [6]: by imposing a constraint, written with the use of the Heaviside function in one of its analytical forms, leading to taking account of a force of contact interaction of the crack faces and to nonlinearity of the formulated boundary value problem.

Besides, in Reference [6], the solution was obtained by the Ritz method in the form of a series in terms of eigenfunctions of an eigenvalue problem, associated with the linearized partial differential equations and linearized natural boundary conditions. This series converged rapidly, providing high accuracy of the solution. But the process of constructing the system of the eigenfunctions for each particular crack length involved solving a nonlinear algebraic eigenvalue problem by an iterative method, which required good initial approximations for each of the frequencies. This caused difficulty in achieving a complete automatization of the process of constructing the eigenfunctions and, therefore, required much time, if the problem had to be solved many times with different crack lengths. This difficulty led to the need of developing a finite element solution of the formulated problem (in conjunction with the first order shear deformation theory, as mentioned above) and the computer program with automatic mesh generation, which became the subject of the present paper. The model is developed to include it, later, into computational procedures for model-aided detection of cracks, with the use of methods presented in Reference [7]. These procedures involve giving small increments to crack lengths at each step of the search algorithm for the crack detection, as a result of which the crack tip does not coincide with the nodes of the initial finite element mesh after each increment of the crack length. This leads to the need of fast and automatic construction of the new finite element mesh after each increment of the crack length, and this task is achieved with the use of the capabilities of the FEMLAB package. In this paper, the FEMLAB is used to solve the partial differential equations derived by the author in Reference [9].

So, the main novelty of the model of the delaminated composite beam, presented in this paper, as compared to the author's model in Reference [6], is that the method of taking account of force of contact interaction of the crack faces, presented in the Reference [6], is combined here with the first order shear deformation theory and the finite element method, with automatic re-meshing after each increment of the crack length. This improvement of the model, as compared to the model in Reference [6], leads to higher accuracy of solutions and allows for full automatization of the solution process.

2 Partial Differential Equations with Boundary Conditions

The partial differential equations, based on the first-order shear deformation theory [8], describing vibration of delaminated clamped-free beam with piezoelectric actuator (Figure 2.1) and with account of contact of the crack faces, are derived by the author in Reference [9] and have the following form.

Partial differential equations:

for Zone 0 (Part 0):

$$KG_0(w_0'' + \phi_0') - B_0\ddot{w}_0 = 0 \quad \text{in} \quad x \in [0,\, a], \tag{1}$$

$$A_0\phi_0'' - KG_0(w_0' + \phi_0) - C_0\ddot{\phi}_0 = I_pV' \quad \text{in} \quad x \in [0,\, a]; \tag{2}$$

for Zone 1 (Part 1):

$$KG_1(w_1'' + \phi_1') - B_1\ddot{w}_1 = 0 \quad \text{in} \quad x \in [a,\ \alpha], \tag{3}$$

$$A_1\phi_1'' - KG_1(w_1' + \phi_1) - C_1\ddot{\phi}_1 = 0 \quad \text{in} \quad x \in [a,\ \alpha]; \tag{4}$$

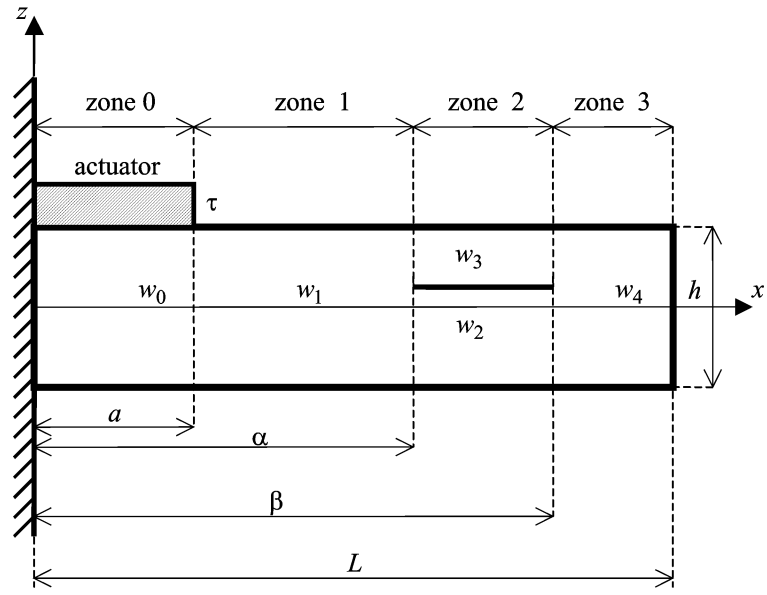

Figure 2.1. Cantilever beam with delamination and piezoelectric actuator.

a is length of the actuator; α is x-coordinate of the left crack tip; β is x-coordinate of the right crack tip; γ is z-coordinate of the crack (distance from x-axis to crack); τ is thickness of the actuator; w_0 is transverse displacement of zone 0; w_1 is transverse displacement of zone 1; w_2 is transverse displacement of lower part of zone 2 (under the crack); w_3 is transverse displacement of upper part of zone 2 (above the crack); w_4 is transverse displacement of zone 3.

for Zone 2 (Part 2 and Part 3):

$$KG_2(w_2'' + \phi_2') - B_2\ddot{w}_2 - \chi(w_3 - w_2)\left(\frac{1}{2} - \frac{1}{\pi}\arctan\frac{w_3 - w_2}{\epsilon}\right) = 0 \quad \text{in} \quad x \in [\alpha,\, \beta], \tag{5}$$

$$A_2\phi_2'' - KG_2(w_2' + \phi_2) - C_2\ddot{\phi}_2 = 0 \quad \text{in} \quad x \in [\alpha,\, \beta]; \tag{6}$$

$$KG_3(w_3'' + \phi_3') - B_3\ddot{w}_3 + \chi(w_3 - w_2)\left(\frac{1}{2} - \frac{1}{\pi}\arctan\frac{w_3 - w_2}{\epsilon}\right) = 0 \quad \text{in} \quad x \in [\alpha,\, \beta], \tag{7}$$

$$A_3\phi_3'' - KG_3(w_3' + \phi_3) - C_3\ddot{\phi}_3 = 0 \quad \text{in} \quad x \in [\alpha,\, \beta]; \tag{8}$$

for Zone 3 (Part 4):

$$KG_4(w_4'' + \phi_4') - B_4\ddot{w}_4 = 0 \quad \text{in} \quad x \in [\beta,\ L], \tag{9}$$

$$A_4\phi_4'' - KG_4(w_4' + \phi_4) - C_4\ddot{\phi}_4 = 0 \quad \text{in} \quad x \in [\beta,\ L]. \tag{10}$$

Essential boundary conditions:

$$R_i(t) = 0, \quad i = 1, 2, \ldots, 12, \tag{11a}$$

where

$$\begin{aligned}
R_1 &\equiv w_0(0,t), & R_2 &\equiv \phi_0(0,t),\\
R_3 &\equiv w_0(a,t) - w_1(a,t), & R_4 &\equiv \phi_0(a,t) - \phi_1(a,t),\\
R_5 &\equiv w_1(\alpha,t) - w_2(\alpha,t), & R_6 &\equiv \phi_1(\alpha,t) - \phi_2(\alpha,t),\\
R_7 &\equiv w_1(\alpha,t) - w_3(\alpha,t), & R_8 &\equiv \phi_1(\alpha,t) - \phi_3(\alpha,t),\\
R_9 &\equiv w_2(\beta,t) - w_4(\beta,t), & R_{10} &\equiv \phi_2(\beta,t) - \phi_4(\beta,t),\\
R_{11} &\equiv w_3(\beta,t) - w_4(\beta,t), & R_{12} &\equiv \phi_3(\beta,t) - \phi_4(\beta,t).
\end{aligned} \tag{11b}$$

Natural boundary conditions:

$$KG_0(\phi_0 + w_0') + \lambda_3 = 0 \quad \text{at} \quad x = a, \tag{12}$$
$$A_0\phi_0' - I_pV(t) + \lambda_4 = 0 \quad \text{at} \quad x = a, \tag{13}$$
$$KG_1(\phi_1 + w_1') + \lambda_3 = 0 \quad \text{at} \quad x = a, \tag{14}$$
$$A_1\phi_1' + \lambda_4 = 0 \quad \text{at} \quad x = a, \tag{15}$$
$$KG_1(\phi_1 + w_1') + \lambda_5 + \lambda_7 = 0 \quad \text{at} \quad x = \alpha, \tag{16}$$
$$A_1\phi_1' + \lambda_6 + \lambda_8 = 0 \quad \text{at} \quad x = \alpha, \tag{17}$$
$$KG_2(\phi_2 + w_2') + \lambda_5 = 0 \quad \text{at} \quad x = \alpha, \tag{18}$$
$$A_2\phi_2' + \lambda_6 = 0 \quad \text{at} \quad x = \alpha, \tag{19}$$
$$KG_3(\phi_3 + w_3') + \lambda_7 = 0 \quad \text{at} \quad x = \alpha, \tag{20}$$
$$A_3\phi_3' + \lambda_8 = 0 \quad \text{at} \quad x = \alpha, \tag{21}$$
$$KG_2(\phi_2 + w_2') + \lambda_9 = 0 \quad \text{at} \quad x = \beta, \tag{22}$$
$$A_2\phi_2' + \lambda_{10} = 0 \quad \text{at} \quad x = \beta, \tag{23}$$
$$KG_3(\phi_3 + w_3') + \lambda_{11} = 0 \quad \text{at} \quad x = \beta, \tag{24}$$
$$A_3\phi_3' + \lambda_{12} = 0 \quad \text{at} \quad x = \beta, \tag{25}$$
$$KG_4(\phi_4 + w_4') + \lambda_9 + \lambda_{11} = 0 \quad \text{at} \quad x = \beta, \tag{26}$$
$$A_4\phi_4' + \lambda_{10} + \lambda_{12} = 0 \quad \text{at} \quad x = \beta, \tag{27}$$
$$KG_4(\phi_4 + w_4') = 0 \quad \text{at} \quad x = L, \tag{28}$$
$$A_4\phi_4' = 0 \quad \text{at} \quad x = L. \tag{29}$$

In the following text it will be assumed that the voltage $V(x,t)$, applied to the piezoelectric actuator, is distributed uniformly over the length of the actuator (over the interval $x \in [0,a]$) and depends on time as $V(x,t) = V(t) = V_0\sin(\Omega t)$. Therefore, the spatial derivative $V' \equiv \dfrac{\partial V(x,t)}{\partial x}$, in the right-hand side of the differential equation (2) will be considered equal to zero in the subsequent text, and the boundary condition (13) will be written as

$$A_0\phi_0' - I_pV_0\sin(\Omega t) + \lambda_4 = 0 \quad \text{at} \quad x = a. \tag{30}$$

3 Formulation in a Form Convenient for FEMLAB Implementation

Unknown functions w_0, w_1, w_2, w_3, w_4, ϕ_0, ϕ_1, ϕ_2, ϕ_3 and ϕ_4 are defined only in the beam's parts, which are indicated by the function's subscripts (Figure 2.1). So, the functions with subscript 0 are defined only in Part 0 (Zone 0); the functions with subscript 1 are defined only in Part 1 (Zone 1); the functions with subscripts 2 and 3 are defined in Part 2 (Zone 2) and Part 3 (Zone 2) respectively; the functions with subscript 4 are defined in Part 4 (Zone 3). But for convenience of using the FEMLAB package, one needs to give some definitions to functions w_1, w_2, w_3, w_4, ϕ_1, ϕ_2, ϕ_3 and ϕ_4 in Zone 0; to functions w_0, w_2, w_3, w_4, ϕ_0, ϕ_2, ϕ_3 and ϕ_4 in Zone 1; to functions w_0, w_1, w_4, ϕ_0, ϕ_1 and ϕ_4 in Zone 2; and to functions w_0, w_1, w_2, w_3, ϕ_0, ϕ_1, ϕ_2 and ϕ_3 in Zone 3. These definitions must not contradict the essential boundary conditions (30). Therefore, the following definitions are introduced:

For Zone 0 (Part 0), i.e. $0 \le x \le a$:

$$\begin{aligned} &w_1 \equiv w_0, \quad w_2 \equiv w_0, \quad w_3 \equiv w_0, \quad w_4 \equiv w_0, \\ &\phi_1 \equiv \phi_0, \quad \phi_2 \equiv \phi_0, \quad \phi_3 \equiv \phi_0, \quad \phi_4 \equiv \phi_0. \end{aligned} \tag{31}$$

For Zone 1 (Part 1), i.e. in $a \le x \le \alpha$:

$$\begin{aligned} &w_0 \equiv w_1, \quad w_2 \equiv w_1, \quad w_3 \equiv w_1, \quad w_4 \equiv w_1, \\ &\phi_0 \equiv \phi_1, \quad \phi_2 \equiv \phi_1, \quad \phi_3 \equiv \phi_1, \quad \phi_4 \equiv \phi_1. \end{aligned} \tag{32}$$

For Zone 2 (Part 2 and Part 3), i.e. in $\alpha \le x \le \beta$:

$$\begin{aligned} &w_0 \equiv w_2, \quad w_1 \equiv w_2, \quad w_4 \equiv w_2, \\ &\phi_0 \equiv \phi_2, \quad \phi_1 \equiv \phi_2, \quad \phi_4 \equiv \phi_2. \end{aligned} \tag{33}$$

For Zone 3 (Part 4), i.e. in $\beta \le x \le L$:

$$\begin{aligned} &w_0 \equiv w_4, \quad w_1 \equiv w_4, \quad w_2 \equiv w_4, \quad w_3 \equiv w_4, \\ &\phi_0 \equiv \phi_4, \quad \phi_1 \equiv \phi_4, \quad \phi_2 \equiv \phi_4, \quad \phi_3 \equiv \phi_4. \end{aligned} \tag{32}$$

In the further presentation, to create a formulation that complies the format, required by the FEMLAB package, the following notations will be introduced for the Lagrange multipliers:

$$\begin{aligned} &\widehat{\lambda}_1 \equiv \lambda_3, \quad \widehat{\lambda}_2 \equiv \lambda_4, \\ &\widetilde{\lambda}_1 \equiv \lambda_5, \quad \widetilde{\lambda}_2 \equiv \lambda_7, \quad \widetilde{\lambda}_3 \equiv \lambda_6, \quad \widetilde{\lambda}_4 \equiv \lambda_8, \\ &\overline{\lambda}_1 \equiv \lambda_9, \quad \overline{\lambda}_2 \equiv \lambda_{11}, \quad \overline{\lambda}_3 \equiv \lambda_{10}, \quad \overline{\lambda}_4 \equiv \lambda_{12}. \end{aligned} \tag{35}$$

In view of definitions (31)–(34), and in view of the notations (35), the partial differential equations and boundary conditions take the form presented below. To comply with the terminology of FEMLAB, the zones will be called subdomains. The Zone 0 will be

called Subdomain 1, the Zone 1 will be called Subdomain 2, the Zone 2 will be called Subdomain 3, the Zone 3 will be called Subdomain 4.

Partial differential equations:
For Zone 0 (Subdomain 1), i.e. in the interval $x \in [0, a]$:

$$-B_0\ddot{w}_0 + KG_0(w_0'' + \phi_0') = 0 \quad \text{in} \quad x \in [0, a], \tag{36}$$
$$-C_0\ddot{\phi}_0 + (A_0\phi_0'' - KG_0w_0') = KG_0\phi_0 \quad \text{in} \quad x \in [0, a], \tag{37}$$
$$0 = w_0 - w_1 \quad \text{in} \quad x \in [0, a], \tag{38}$$
$$0 = w_0 - w_2 \quad \text{in} \quad x \in [0, a], \tag{39}$$
$$0 = w_0 - w_3 \quad \text{in} \quad x \in [0, a], \tag{40}$$
$$0 = w_0 - w_4 \quad \text{in} \quad x \in [0, a], \tag{41}$$
$$0 = \phi_0 - \phi_1 \quad \text{in} \quad x \in [0, a], \tag{42}$$
$$0 = \phi_0 - \phi_2 \quad \text{in} \quad x \in [0, a], \tag{43}$$
$$0 = \phi_0 - \phi_3 \quad \text{in} \quad x \in [0, a], \tag{44}$$
$$0 = \phi_0 - \phi_4 \quad \text{in} \quad x \in [0, a]. \tag{45}$$

For Zone 1 (Subdomain 2), i.e. in the interval $x \in [a, \alpha]$:

$$-B_1\ddot{w}_1 + KG_1(w_1'' + \phi_1') = 0 \quad \text{in} \quad x \in [a, \alpha], \tag{46}$$
$$-C_1\ddot{\phi}_1 + (A_1\phi_1'' - KG_1w_1') = KG_1\phi_1 \quad \text{in} \quad x \in [a, \alpha], \tag{47}$$
$$0 = w_1 - w_0 \quad \text{in} \quad x \in [a, \alpha], \tag{48}$$
$$0 = w_1 - w_2 \quad \text{in} \quad x \in [a, \alpha], \tag{49}$$
$$0 = w_1 - w_3 \quad \text{in} \quad x \in [a, \alpha], \tag{50}$$
$$0 = w_1 - w_4 \quad \text{in} \quad x \in [a, \alpha], \tag{51}$$
$$0 = \phi_1 - \phi_0 \quad \text{in} \quad x \in [a, \alpha], \tag{52}$$
$$0 = \phi_1 - \phi_2 \quad \text{in} \quad x \in [a, \alpha], \tag{53}$$
$$0 = \phi_1 - \phi_3 \quad \text{in} \quad x \in [a, \alpha], \tag{54}$$
$$0 = \phi_1 - \phi_4 \quad \text{in} \quad x \in [a, \alpha]. \tag{55}$$

For Zone 2 (Subdomain 3), i.e. in the interval $x \in [\alpha, \beta]$:

$$-B_2\ddot{w}_2 + KG_2(w_2'' + \phi_2') = \chi(w_3 - w_2)\left(\frac{1}{2} - \frac{1}{\pi}\arctan\frac{w_3 - w_2}{\epsilon}\right) \quad \text{in} \quad x \in [\alpha, \beta], \tag{56}$$
$$-C_2\ddot{\phi}_2 + (A_2\phi_2'' - KG_2w_2') = KG_2\phi_2 \quad \text{in} \quad x \in [\alpha, \beta], \tag{57}$$
$$-B_3\ddot{w}_3 + KG_3(w_3'' + \phi_3') = -\chi(w_3 - w_2)\left(\frac{1}{2} - \frac{1}{\pi}\arctan\frac{w_3 - w_2}{\epsilon}\right) \quad \text{in} \quad x \in [\alpha, \beta], \tag{58}$$
$$-C_3\ddot{\phi}_3 + (A_3\phi_3'' - KG_3w_3\%') = KG_3\phi_3 \quad \text{in} \quad x \in [\alpha, \beta], \tag{59}$$
$$0 = w_2 - w_0 \quad \text{in} \quad x \in [\alpha, \beta], \tag{60}$$

$$0 = w_2 - w_1 \quad \text{in} \quad x \in [\alpha, \beta], \tag{61}$$
$$0 = w_2 - w_4 \quad \text{in} \quad x \in [\alpha, \beta], \tag{62}$$
$$0 = \phi_2 - \phi_0 \quad \text{in} \quad x \in [\alpha, \beta], \tag{63}$$
$$0 = \phi_2 - \phi_1 \quad \text{in} \quad x \in [\alpha, \beta], \tag{64}$$
$$0 = \phi_2 - \phi_4 \quad \text{in} \quad x \in [\alpha, \beta]. \tag{65}$$

For Zone 3 (Subdomain 4) i.e. in the interval $x \in [\beta, L]$:

$$-B_4\ddot{w}_4 + KG_4(w_4'' + \phi_4') = 0 \quad \text{in} \quad x \in [\beta, L], \tag{66}$$
$$-C_4\ddot{\phi}_4 + (A_4\phi_4'' - KG_4w_4') = KG_4\phi_4 \quad \text{in} \quad x \in [\beta, L], \tag{67}$$
$$0 = w_4 - w_0 \quad \text{in} \quad x \in [\beta, L], \tag{68}$$
$$0 = w_4 - w_1 \quad \text{in} \quad x \in [\beta, L], \tag{69}$$
$$0 = w_4 - w_2 \quad \text{in} \quad x \in [\beta, L], \tag{70}$$
$$0 = w_4 - w_3 \quad \text{in} \quad x \in [\beta, L], \tag{71}$$
$$0 = \phi_4 - \phi_0 \quad \text{in} \quad x \in [\beta, L], \tag{72}$$
$$0 = \phi_4 - \phi_1 \quad \text{in} \quad x \in [\beta, L], \tag{73}$$
$$0 = \phi_4 - \phi_2 \quad \text{in} \quad x \in [\beta, L], \tag{74}$$
$$0 = \phi_4 - \phi_3 \quad \text{in} \quad x \in [\beta, L]. \tag{75}$$

Boundary conditions:
Boundary 1, i.e. $x = 0$:

$$w_0 = 0 \quad \text{at} \quad x = 0 \quad \text{(essential BC)}, \tag{76}$$
$$\phi_0 = 0 \quad \text{at} \quad x = 0 \quad \text{(essential BC)}, \tag{77}$$

Boundary 2, i.e. $x = a$:

$$w_0 - w_1 = 0 \quad \text{at} \quad x = a \quad \text{(essential BC)}, \tag{78}$$
$$\phi_0 - \phi_1 = 0 \quad \text{at} \quad x = a \quad \text{(essential BC)}, \tag{79}$$
$$KG_0(w_0' + \phi_0) = -\widehat{\lambda}_1 \quad \text{at} \quad x = a \quad \text{(natural BC)}, \tag{80}$$
$$KG_1(w_1' + \phi_1) = -\widehat{\lambda}_1 \quad \text{at} \quad x = a \quad \text{(natural BC)}, \tag{81}$$
$$A_0\phi_0' - I_pV_0\sin(\Omega t) = -\widehat{\lambda}_2 \quad \text{at} \quad x = a \quad \text{(natural BC)}, \tag{82}$$
$$A_1\phi_1' = -\widehat{\lambda}_2 \quad \text{at} \quad x = a \quad \text{(natural BC)}, \tag{83}$$

Boundary 3, i.e. $x = \alpha$:

$$w_1 - w_2 = 0 \quad \text{at} \quad x = \alpha \quad \text{(essential BC)}, \tag{84}$$
$$w_1 - w_3 = 0 \quad \text{at} \quad x = \alpha \quad \text{(essential BC)}, \tag{85}$$
$$\phi_1 - \phi_2 = 0 \quad \text{at} \quad x = \alpha \quad \text{(essential BC)}, \tag{86}$$
$$\phi_1 - \phi_3 = 0 \quad \text{at} \quad x = \alpha \quad \text{(essential BC)}, \tag{87}$$

$$KG_1(\phi_1 + w_1') = -\widetilde{\lambda}_1 - \widetilde{\lambda}_2 \quad \text{at} \quad x = \alpha \quad \text{(natural BC)}, \tag{88}$$

$$KG_2(\phi_2 + w_2') = -\widetilde{\lambda}_1 \quad \text{at} \quad x = \alpha \quad \text{(natural BC)}, \tag{89}$$

$$KG_3(\phi_3 + w_3') = -\widetilde{\lambda}_2 \quad \text{at} \quad x = \alpha \quad \text{(natural BC)}, \tag{90}$$

$$A_1\phi_1' = -\widetilde{\lambda}_3 - \widetilde{\lambda}_4 \quad \text{at} \quad x = \alpha \quad \text{(natural BC)}, \tag{91}$$

$$A_2\phi_2' = -\widetilde{\lambda}_3 \quad \text{at} \quad x = \alpha \quad \text{(natural BC)}, \tag{92}$$

$$A_3\phi_3' = -\widetilde{\lambda}_4 \quad \text{at} \quad x = \alpha \quad \text{(natural BC)}, \tag{93}$$

Boundary 4, i.e. $x = \beta$:

$$w_2 - w_4 = 0 \quad \text{at} \quad x = \beta \quad \text{(essential BC)}, \tag{94}$$

$$w_3 - w_4 = 0 \quad \text{at} \quad x = \beta \quad \text{(essential BC)}, \tag{95}$$

$$\phi_2 - \phi_4 = 0 \quad \text{at} \quad x = \beta \quad \text{(essential BC)}, \tag{96}$$

$$\phi_3 - \phi_4 = 0 \quad \text{at} \quad x = \beta \quad \text{(essential BC)}, \tag{97}$$

$$KG_4(\phi_4 + w_4') = -\overline{\lambda}_1 - \overline{\lambda}_2 \quad \text{at} \quad x = \beta \quad \text{(natural BC)}, \tag{98}$$

$$KG_2(\phi_2 + w_2') = -\overline{\lambda}_1 \quad \text{at} \quad x = \beta \quad \text{(natural BC)}, \tag{99}$$

$$KG_3(\phi_3 + w_3') = -\overline{\lambda}_2 \quad \text{at} \quad x = \beta \quad \text{(natural BC)}, \tag{100}$$

$$A_4\phi_4' = -\overline{\lambda}_3 - \overline{\lambda}_4 \quad \text{at} \quad x = \beta \quad \text{(natural BC)}, \tag{101}$$

$$A_2\phi_2' = -\overline{\lambda}_3 \quad \text{at} \quad x = \beta \quad \text{(natural BC)}, \tag{102}$$

$$A_3\phi_3' = -\overline{\lambda}_4 \quad \text{at} \quad x = \beta \quad \text{(natural BC)}, \tag{103}$$

Boundary 5, i.e. $x = L$:

$$KG_4(\phi_4 + w_4') = 0 \quad \text{at} \quad x = L \quad \text{(natural BC)}, \tag{104}$$

$$A_4\phi_4' = 0 \quad \text{at} \quad x = L \quad \text{(natural BC)}. \tag{105}$$

In the FEMLAB terminology, natural boundary conditions are called the Neumann boundary conditions, essential boundary conditions are called the Dirichlet boundary conditions, and the mixed boundary conditions (both essential and natural conditions at the same boundary) are called the Dirichlet boundary conditions also. With the use of this terminology, the boundary conditions (76)–(103) at boundaries $x = 0$, $x = a$, $x = \alpha$ and $x = \beta$ are the Dirichlet boundary conditions, and the boundary conditions (104) and (105) at the boundary $x = L$ are the Neumann boundary conditions.

3.1 Standard form of representation of equations in FEMLAB for one-dimensional problems

In FEMLAB, in case of N unknown functions $u_k(x,t)$ $(k = 1, 2, \ldots, N)$ of one special coordinate x and time t, the partial differential equations of the second order and the boundary conditions are written in the following form (summation over repeated indices is implied).

Partial differential equations:

$$M_{mk}\ddot{u}_k + \Gamma_m' = F_m \quad (k,\, m = 1, \ldots, N) \quad \text{in subdomains of } x, \tag{106}$$

Neumann boundary conditions at *external* boundaries:

$$n_x \Gamma_m = -G_m \quad \text{(natural BC)}, \tag{107}$$

Dirichlet boundary conditions at *external* boundaries:

$$R_m = 0 \quad \text{(essential BC)} \ , \tag{108a}$$

and

$$n_x \Gamma_m + \lambda_n \frac{\partial R_n}{\partial u_m} = -G_m \quad \text{(natural BC)}, \tag{108b}$$

where

$$\begin{aligned} \Gamma_m &\equiv -c_{mk} u_k' - \alpha_{mk} u_k + \gamma_m, \\ F_m &\equiv f_m - a_{mk} u_k, \\ G_m &\equiv g_m - q_{mk} u_k, \\ R_m &\equiv h_{mk} u_k - r_m, \end{aligned} \tag{109}$$

and coefficients c_{mk}, α_{mk}, γ_m, f_m, a_{mk}, g_m, q_{mk}, h_{mk}, r_m are, generally, some known functions of the coordinate x and time t. Of course, these coefficients can be functions of coordinates only, time only, or constants. The quantity n_x is an x-component of the subdomain's boundary's outward unit normal vector. In case of one-dimensional problems, as the one considered here, $n_x = 1$ at right edges of subdomains, and $n_x = -1$ at left edges of subdomains, if the x-axis is directed from left to right, as in Figure 2.1.

If boundary conditions are specified at *internal* boundaries, i.e. at the boundaries between two adjacent subdomains (e.g. Subdomain 1 and Subdomain 2), then the Neumann boundary conditions take the form

$$\underbrace{n_x^{(1)}}_{1} \Gamma_m^{(1)} + \underbrace{n_x^{(2)}}_{-1} \Gamma_m^{(2)} = -G_m \quad \text{(natural BC)}, \tag{110}$$

and the Dirichlet boundary conditions take the form

$$R_m = 0 \quad \text{(essential BC)}$$

and

$$\underbrace{n_x^{(1)}}_{1} \Gamma_m^{(1)} + \underbrace{n_x^{(2)}}_{-1} \Gamma_m^{(2)} + \frac{\partial R_k}{\partial u_m} \lambda_k = -G_m \quad \text{(natural BC)}. \tag{111}$$

Either the Neumann or Dirichlet boundary conditions must be chosen at each boundary. If only natural boundary conditions are specified on a boundary of a subdomain, then such boundary conditions have the form of Neumann boundary conditions. If both essential and natural boundary conditions are specified at a boundary, then such boundary conditions have the form of Dirichlet boundary conditions.

Equations (106) – (108) can be written in matrix form as follows.
Partial differential equations:

$$\underset{(N\times N)}{[M]} \frac{\partial^2}{\partial t^2} \underset{(N\times 1)}{\{u\}} + \frac{\partial}{\partial x} \underset{(N\times 1)}{\{\Gamma\}} = \underset{(N\times 1)}{\{F\}} \ , \tag{112}$$

Neumann boundary conditions:

$$n_x \underset{(N\times 1)}{\{\Gamma\}} = - \underset{(N\times 1)}{\{G\}}\,, \tag{113}$$

Dirichlet boundary conditions:

$$\underset{(N\times 1)}{\{R\}} = \underset{(N\times 1)}{\{0\}} \tag{114a}$$

and

$$n_x \begin{Bmatrix} \Gamma_1 \\ \Gamma_2 \\ \vdots \\ \Gamma_N \end{Bmatrix} + \begin{bmatrix} \dfrac{\partial R_1}{\partial u_1} & \dfrac{\partial R_2}{\partial u_1} & \cdots & \dfrac{\partial R_N}{\partial u_1} \\ \dfrac{\partial R_1}{\partial u_2} & \dfrac{\partial R_2}{\partial u_2} & \cdots & \dfrac{\partial R_N}{\partial u_2} \\ \cdots\cdots & \cdots\cdots & \cdots\cdots & \cdots\cdots \\ \dfrac{\partial R_1}{\partial u_{_N}} & \dfrac{\partial R_2}{\partial u_{_N}} & \cdots & \dfrac{\partial R_N}{\partial u_{_N}} \end{bmatrix} \begin{Bmatrix} \lambda_1 \\ \lambda_2 \\ \vdots \\ \lambda_N \end{Bmatrix} = - \begin{Bmatrix} G_1 \\ G_2 \\ \vdots \\ G_N \end{Bmatrix}. \tag{114b}$$

Similarly, the boundary conditions (110) and (111) at an internal boundary, being written in the matrix form, are
Neumann boundary conditions:

$$\underset{(N\times 1)}{\{\Gamma\}}^{(1)} - \underset{(N\times 1)}{\{\Gamma\}}^{(2)} = - \underset{(N\times 1)}{\{G\}}\,, \tag{115}$$

Dirichlet boundary conditions:

$$\underset{(N\times 1)}{\{R\}} = \underset{(N\times 1)}{\{0\}}\,, \tag{116a}$$

and

$$\underset{(N\times 1)}{\{\Gamma\}}^{(1)} - \underset{(N\times 1)}{\{\Gamma\}}^{(2)} + \left[\frac{\partial R_m}{\partial u_k}\right]^{\mathrm{T}} \underset{(N\times 1)}{\{\lambda\}} = - \underset{(N\times 1)}{\{G\}}\,. \tag{116b}$$

3.2 Subdomain and boundary settings of the problem

To comply with the FEMLAB's requirements for notations, the following *alternative notations* are introduced for the unknown functions of the present problem:

$$\underset{(10\times 1)}{\{u\}} \equiv \begin{Bmatrix} u_1 \\ u_2 \\ u_3 \\ u_4 \\ u_5 \\ u_6 \\ u_7 \\ u_8 \\ u_9 \\ u_{10} \end{Bmatrix} \equiv \begin{Bmatrix} w0 \\ p0 \\ w1 \\ p1 \\ w2 \\ p2 \\ w3 \\ p3 \\ w4 \\ p4 \end{Bmatrix} \equiv \begin{Bmatrix} w_0 \\ \phi_0 \\ w_1 \\ \phi_1 \\ w_2 \\ \phi_2 \\ w_3 \\ \phi_3 \\ w_4 \\ \phi_4 \end{Bmatrix}, \tag{117}$$

for the spatial derivatives of the unknown functions:

$$w0x \equiv w_0', \quad p0x \equiv \phi_0', \quad \ldots \tag{118}$$

for the constants and for matrix $[M]$ in equation (112):

$$A0 \equiv A_0, \quad B0 \equiv B_0, \quad \ldots, \quad Omega \equiv \Omega, \quad [d_a] \equiv [M], \tag{119}$$

and all kinds of notations will be used interchangeably in the subsequent text.

Partial differential equations (36)–(45) for Zone 0 (Subdomain 1), i.e. for $x \in [0, a]$ can be written in matrix form as

$$\underset{(10\times10)}{[M]}^{(1)} \frac{\partial^2}{\partial t^2} \underset{(10\times1)}{\{u\}} + \frac{\partial}{\partial x} \underset{(10\times1)}{\{\Gamma\}}^{(1)} = \underset{(10\times1)}{\{F\}}^{(1)}, \tag{120a}$$

where

$$[M]^{(1)} = \begin{bmatrix} -B0 & 0 & 0 & 0 & 0 & 0 & 0 & 0 & 0 & 0 \\ 0 & -C0 & 0 & 0 & 0 & 0 & 0 & 0 & 0 & 0 \\ 0 & 0 & 0 & 0 & 0 & 0 & 0 & 0 & 0 & 0 \\ 0 & 0 & 0 & 0 & 0 & 0 & 0 & 0 & 0 & 0 \\ 0 & 0 & 0 & 0 & 0 & 0 & 0 & 0 & 0 & 0 \\ 0 & 0 & 0 & 0 & 0 & 0 & 0 & 0 & 0 & 0 \\ 0 & 0 & 0 & 0 & 0 & 0 & 0 & 0 & 0 & 0 \\ 0 & 0 & 0 & 0 & 0 & 0 & 0 & 0 & 0 & 0 \\ 0 & 0 & 0 & 0 & 0 & 0 & 0 & 0 & 0 & 0 \\ 0 & 0 & 0 & 0 & 0 & 0 & 0 & 0 & 0 & 0 \end{bmatrix}, \tag{120b}$$

$$\{\Gamma\}^{(1)} = \begin{Bmatrix} K*G0*(w0x+p0) \\ A0*p0x - K*G0*w0 \\ 0 \\ 0 \\ 0 \\ 0 \\ 0 \\ 0 \\ 0 \\ 0 \end{Bmatrix}, \qquad \{F\}^{(1)} = \begin{Bmatrix} 0 \\ K*G0*p0 \\ w0-w1 \\ w0-w2 \\ w0-w3 \\ w0-w4 \\ p0-p1 \\ p0-p2 \\ p0-p3 \\ p0-p4 \end{Bmatrix}. \tag{120c}$$

Similarly, one can write partial differential equations for other zones in the FEMLAB standard form:

Partial differential equations (46) – (55) for Zone 1 (Subdomain 2), i.e. for $x \in [a, \alpha]$:

$$\underset{(10\times10)}{[M]}^{(2)} \frac{\partial^2}{\partial t^2} \underset{(10\times1)}{\{u\}} + \frac{\partial}{\partial x} \underset{(10\times1)}{\{\Gamma\}}^{(2)} = \underset{(10\times1)}{\{F\}}^{(2)}. \tag{121}$$

Partial differential equations (56) – (65) for Zone 2 (Subdomain 3), i.e. for $x \in [\alpha, \beta]$:

$$\underset{(10\times10)}{[M]}^{(3)} \frac{\partial^2}{\partial t^2} \underset{(10\times1)}{\{u\}} + \frac{\partial}{\partial x} \underset{(10\times1)}{\{\Gamma\}}^{(3)} = \underset{(10\times1)}{\{F\}}^{(3)}. \tag{122}$$

Partial differential equations (66) – (75) for Zone 3 (Subdomain 4), i.e. for $x \in [\beta, L]$:

$$\underset{(10\times10)}{[M]}^{(4)} \frac{\partial^2}{\partial t^2} \underset{(10\times1)}{\{u\}} + \frac{\partial}{\partial x} \underset{(10\times1)}{\{\Gamma\}}^{(4)} = \underset{(10\times1)}{\{F\}}^{(4)}. \tag{123}$$

Matrices, which enter into equations (121) – (123) are not written here explicitly for brevity.

The *Dirichlet boundary conditions (76) – (77) at Boundary 1*, i.e. at $x = 0$, written in FEMLAB standard form, are:

$$\underset{(10\times1)}{\{R\}}^{(1)} = \underset{(10\times1)}{\{0\}} \quad \text{and} \quad -\underset{(10\times1)}{\{\Gamma\}}^{(1)} + \underset{(10\times10)}{\left[\frac{\partial R_m^{(1)}}{\partial u_k}\right]^{\mathrm{T}}} \underset{(10\times1)}{\{\underline{\lambda}\}} = -\underset{(10\times1)}{\{G\}}^{(1)}, \tag{124a}$$

where the column-matrix $\{\Gamma\}^{(1)}$ is defined by formula (120c),

$$\underset{(10\times1)}{\{R\}}^{(1)} \equiv \lfloor w0 \quad p0 \quad 0 \quad 0 \quad 0 \quad 0 \quad 0 \quad 0 \quad 0 \quad 0 \rfloor^{\mathrm{T}}, \tag{124b}$$

$$\underset{(10\times1)}{\{G\}}^{(1)} = \underset{(10\times1)}{\{0\}} \tag{124c}$$

and

$$\underset{(10\times10)}{\left[\frac{\partial R_m^{(1)}}{\partial u_k}\right]^{\mathrm{T}}} = \begin{bmatrix} 1 & 0 & 0 & 0 & 0 & 0 & 0 & 0 & 0 & 0 \\ 0 & 1 & 0 & 0 & 0 & 0 & 0 & 0 & 0 & 0 \\ 0 & 0 & 0 & 0 & 0 & 0 & 0 & 0 & 0 & 0 \\ 0 & 0 & 0 & 0 & 0 & 0 & 0 & 0 & 0 & 0 \\ 0 & 0 & 0 & 0 & 0 & 0 & 0 & 0 & 0 & 0 \\ 0 & 0 & 0 & 0 & 0 & 0 & 0 & 0 & 0 & 0 \\ 0 & 0 & 0 & 0 & 0 & 0 & 0 & 0 & 0 & 0 \\ 0 & 0 & 0 & 0 & 0 & 0 & 0 & 0 & 0 & 0 \\ 0 & 0 & 0 & 0 & 0 & 0 & 0 & 0 & 0 & 0 \\ 0 & 0 & 0 & 0 & 0 & 0 & 0 & 0 & 0 & 0 \end{bmatrix}, \tag{124d}$$

but the matrix $\left[\frac{\partial R_m^{(1)}}{\partial u_k}\right]^{\mathrm{T}}$ need not be defined by a user of FEMLAB.

Similarly, one can write boundary conditions for all other external and internal boundaries in the FEMLAB standard form.

The *Dirichlet boundary conditions (78) – (83) at an internal Boundary 2*, i.e. at $x = a$:

$$\underset{(10\times1)}{\{R\}}^{(2)} = \underset{(10\times1)}{\{0\}} \quad \text{and} \quad \underset{(10\times1)}{\{\Gamma\}}^{(1)} - \underset{(10\times1)}{\{\Gamma\}}^{(2)} + \underset{(10\times10)}{\left[\frac{\partial R_m^{(2)}}{\partial u_k}\right]^{\mathrm{T}}} \underset{(10\times1)}{\left\{\widehat{\lambda}\right\}} = -\underset{(10\times1)}{\{G\}}^{(2)}. \tag{125}$$

The *Dirichlet boundary conditions (84) – (93) at an internal Boundary 3*, i.e. at $x = \alpha$:

$$\underset{(10\times1)}{\{R\}}^{(3)} = \underset{(10\times1)}{\{0\}} \quad \text{and} \quad \underset{(10\times1)}{\{\Gamma\}}^{(2)} - \underset{(10\times1)}{\{\Gamma\}}^{(3)} + \underset{(10\times10)}{\left[\frac{\partial R_m^{(3)}}{\partial u_k}\right]^{\mathrm{T}}} \underset{(10\times1)}{\left\{\widehat{\lambda}\right\}} = -\underset{(10\times1)}{\{G\}}^{(3)}. \tag{126}$$

The *Dirichlet boundary conditions (94) – (103) at an internal Boundary 4*, i.e. at $x = \beta$:

$$\underset{(10\times1)}{\{R\}}^{(4)} = \underset{(10\times1)}{\{0\}} \quad \text{and} \quad \underset{(10\times1)}{\{\Gamma\}}^{(3)} - \underset{(10\times1)}{\{\Gamma\}}^{(4)} + \underset{(10\times10)}{\left[\frac{\partial R_m^{(4)}}{\partial u_k}\right]^{\mathrm{T}}} \underset{(10\times1)}{\{\overline{\lambda}\}} = -\underset{(10\times1)}{\{G\}}^{(4)}. \tag{127}$$

The *Neumann boundary conditions (104) and (105) at an external Boundary 5*, i.e. at $x = L$, written in FEMLAB standard form, are

$$\underset{(N\times 1)}{\{\Gamma\}}^{(4)} = -\underset{(N\times 1)}{\{G\}}^{(5)}, \tag{128}$$

Matrices, which enter into equations (125) – (128), are not written here explicitly for brevity.

4 Solution of Example Problems

As an example problem, a clamped-free wooden beam with the following characteristics (Figure 2.1) is considered: length $L = 20 \times 10^{-2} m$, width $b = 2.76 \times 10^{-2} m$, thickness $h = 0.99 \times 10^{-2} m$, wood density $\rho^{(0)} = 418.02 \frac{kg}{m^3}$, Young's modulus of the wood in the direction of fibbers $E_1^{(0)} = 1.0897 \times 10^{10} \frac{N}{m^2}$. The piezoelectric actuator is QP10W (Active Control Experts). Thickness of the actuator is $\tau = 3.81 \times 10^{-4} m$, its length is $a = 5.08 \times 10^{-2} m$, the piezoelectric constant in the range of applied voltage (from 0 to $200V$) is $\overline{d}_{31} \approx -1.05 \times 10^{-9} \frac{m}{V}$, the Young's modulus of the actuator with its packaging is $E_1^{(p)} = 2.57 \times 10^{10} \frac{N}{m^2}$, mass density of the actuator with its packaging is $\rho^{(p)} = 6151.1 \frac{kg}{m^3}$. The voltage $V(t)$, applied to the piezoelectric actuator, is distributed uniformly along the length of the actuator and varies with time as

$$V(t) = V_a \sin(\Omega t),$$

where $V_a = 200\ V$, $\Omega = 600 \frac{1}{s}$. The wooden beam is cut along its fibbers, so that the angle θ in the formula (6) is equal to zero, and, therefore, the elastic compliance coefficient $\overline{S}_{11}$ for the wood is equal to $\overline{S}_{11}^{(0)} = \frac{1}{E_1^{(0)}} = 9.1768 \times 10^{-11} \frac{m^2}{N}$. For the piezoelectric actuator, the material coordinate system coincides with the problem coordinate system, so that the elastic compliance coefficient $\overline{S}_{11}$ for the material of the piezo-actuator is $\overline{S}_{11}^{(p)} = \frac{1}{E_1^{(p)}} = 3.8911 \times 10^{-11} \frac{m^2}{N}$. Coordinates of the crack tips are: $\alpha = 10 \times 10^{-2} m$, $\beta = 15 \times 10^{-2} m$, $\gamma = 0.66 \times 10^{-2} - \frac{h}{2} = 1.65 \times 10^{-3} m$. Then the constants, entering into the variational formulation and the differential equations of the problem, have the following values in SI units [9]: $A_0 = 31.463$, $B_0 = 0.178\,9$, $C_0 = 2.642\,9 \times 10^{-6}$, $G_0 = 1.299\,10 \times 10^6$, $A_1 = 24.319$, $B_1 = 0.114\,22$, $C_1 = 9.328\,9 \times 10^{-7}$, $G_1 = 1.190999 \times 10^6$, $A_2 = 12.61$, $B_2 = 7.614\,7 \times 10^{-2}$, $C_2 = 4.837\,2 \times 10^{-7}$, $G_2 = 7.93999 \times 10^5$, $A_3 = 11.709$, $B_3 = 3.807\,3 \times 10^{-2}$, $C_3 = 4.491\,7 \times 10^{-7}$, $G_3 = 3.969995 \times 10^5$, $A_4 = 24.319$, $B_4 = 0.114\,22$, $C_4 = 9.328\,9 \times 10^{-7}$, $G_4 = 1.190999 \times 10^6$, $I_p = -3.828\,5 \times 10^{-3}$, $a = 5.08 \times 10^{-2}$, $V_a = 200$, $\Omega = 600$, $\alpha = 10 \times 10^{-2}$, $\beta = 15 \times 10^{-2}$, $\gamma = 1.65 \times 10^{-3}$, $b = 2.76 \times 10^{-2}$, $h = 0.99 \times 10^{-2}$. The small constant ϵ and the large constant χ in equations (5) and (6) are chosen to be $\epsilon = 1 \times 10^{-3}$ and $\chi = 1 \times 10^6$. The shear correction factor K in expressions for strain energy is set to $K = \frac{5}{6}$.

4.1 Time-domain response to dynamic excitation

A system of ordinary differential equations of a global (assembled) semi-discrete finite element model has the form

$$[M]\{\ddot{\Theta}\} + [K]\{\Theta\} + \{R\}_{\text{nonlin}} = \{F\}. \tag{129}$$

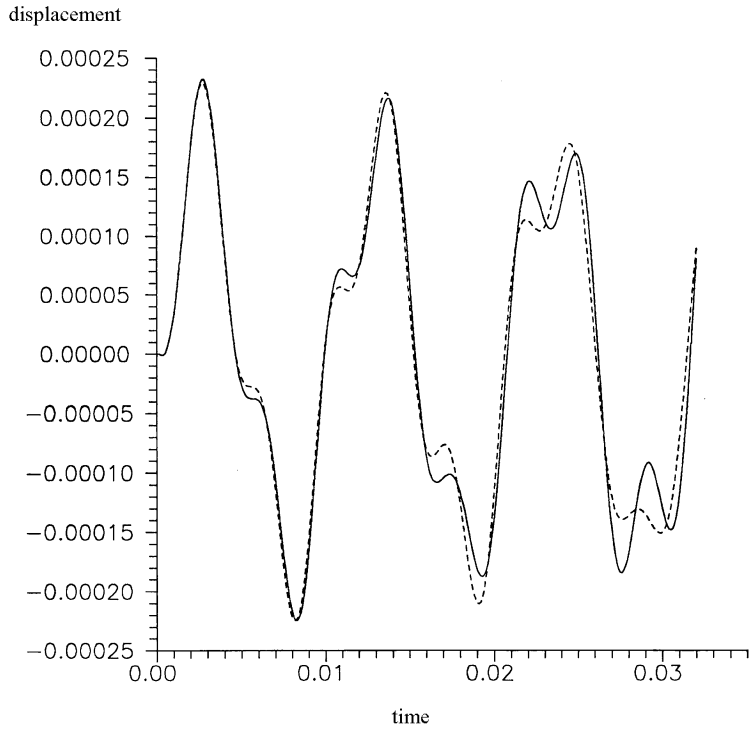

Figure 4.1. Transverse displacement of free end of delaminated beam (solid line) and undelaminated beam (dashed line). Coordinates of the crack tips of the delaminated beam are $\alpha = 0,1m$, $\beta = 0,15m$, $\gamma = 1,65 \times 10^{-3}m$.

In the last equation, $\{R\}_{\text{nonlin}}$ is a column-matrix, which contains components that depend nonlinearly on the unknown nodal parameters Θ_i. Transverse displacements as functions of time at free ends of delaminated and undelaminated beams, obtained by solving equations (129), are shown in graphs of Figure 4.1 These graphs are noticeably different. Numerical experiments show that this difference is mainly due to the mutual impact of the crack faces during the vibration.

So, taking account of nonlinearity of the forced response of the delaminated beam due to the contact interaction of the crack faces can be important for model-aided detection of cracks in composite beams.

References

[1] Ramkumar, R.L., Kulkarni, S.V. and Pipes, R.B. Free vibration frequencies of a delaminated beam. In: *34th Annual Technical Conference, 1979. Reinforced Plastics/Composites Institute.* The Society of the Plastics Industry Inc., 1979, 22-E: P.1–5.

[2] Wang, J.T.S., Liu, Y.Y. and Gibby, J.A. Vibrations of split beams. *J. Sound and Vibrations* **84** (1982) 491–502.

[3] Mujumdar, P.M. and Suryanarayan, S. Flexural vibrations of beams with delaminations. *J. Sound and Vibrations* **125** (1988) 441–461.

[4] Luo, H. and Hanagud, S. Dynamics of delaminated beams. *Int. J. Solids and Structures* **37** (2000) 1501–1519.

[5] Wang, J. and Tong, L. A study of the vibration of delaminated beams using a nonlinear anti-interpenetration constraint model. *Composite Structures* **57** (2002) 483–488.
[6] Perel, V.Y. A numerical-analytical solution for dynamics of composite delaminated beam with piezoelectric actuator, with account of nonpenetration constraint for the delamination crack faces. *J. Composite Materials* **39**(1) (2005) 67–103.
[7] Liu, G.R. and Han, X. *Computational Inverse Techniques in Nondestructive Evaluation*. CRC Press, Boca Raton 2003.
[8] Reddy, J.N. *Energy and Variational Methods in Applied Mechanics*. John Wiley & Sons, New York, 1984.
[9] Perel, V.Y. A nonlinear model for dynamics of delaminated composite beam with account of contact of the delamination crack faces, based on the first order shear deformation theory. *Nonlinear Dynamics and Systems Theory* **5**(1) (2005) 61–90.

Nonlinear Dynamics and Systems Theory, **6**(2) (2006) 187–190

A Periodic Version of Lie Series for Normal Mode Dynamics

V.N. Pilipchuk*

General Motors Technical Center, Warren, USA

Received: January 23, 2006; Revised: June 2, 2006

Abstract: Lie series solutions of smooth dynamical systems are adapted for the classof periodic motions by invoking the temporal mode shapes of the classicimpact oscillator.

Keywords: *Periodic solutions; dynamical systems; Lie series.*

Mathematics Subject Classification (2000): 34C25, 37C27, 22E70.

Despite the fact that perfectly periodic motions never indeed happen, the class of periodic solutions of the differential equations of motion appears to be very important even when dealing with the chaotic dynamics [1]. Typical problem formulations and practical reasons for considering the periodic solutions can be also found in reference [2].

Let us consider a multiple degrees of freedom dynamical system described by the differential equations of motion with respect to the coordinate and velocity vectors

$$\begin{aligned} \dot{x} &= v, \\ \dot{v} &= -f(x, v, t), \\ \dot{t} &= 1, \end{aligned} \tag{1}$$

where the vector-function f is assumed to have as many derivatives as needed in a physically reasonable domain of the variables. Then, the dynamics of system (1) can be locally described by the Lie series [3]

$$x = \exp[(t - t_0)G]x_0 \equiv \left[1 + (t - t_0)G + \frac{1}{2!}(t - t_0)^2 G^2 + \dots\right] x_0, \tag{2}$$

$$G = v_0 \cdot \frac{\partial}{\partial x_0} - f(x_0, v_0, t_0) \cdot \frac{\partial}{\partial v_0} + \frac{\partial}{\partial t_0} \tag{3}$$

*Corresponding author: valery.pylypchuk@gm.com

where G is Lie operator associated with system (1), and $\{x_0, v_0, t_0\}$ is some initial point in the system' phase space.

Series (2) is simply Taylor series whose coefficients are calculated by enforcing equations (1). Unfortunately, this general idea is still of little use for oscillatory processes probably due to locality of expansion (2). In other words, even entire expansion (2) does not explicitly reveal such global characteristics of oscillations as their amplitude and period. Moreover, the corresponding truncated series produce increasingly growing errors as the time t runs away from the selected initial point t_0. In order to overcome these disadvantages, it is suggested to adapt the Lie series solution for the class of periodic motions as follows.

Theorem 1 *Assume that system (1) admits a periodic solution $x(t)$ of the period $T = 4a$ so that $x(t + 4a) = x(t)$ for any t, and some point $\{x_0, v_0, t_0\}$ belongs to this solution. Then such a solution can be expressed in the form*

$$x = \exp(aG)\{\cosh[a(\tau - 1)G] + e \sinh[a(\tau - 1)G]\}x_0, \tag{4}$$

where τ and e are triangular sine and rectangular cosine, whose periods are normalized to four and amplitudes are normalized to unity as

$$\tau(\varphi) = (2/\pi) \arcsin \sin(\pi\varphi/2) \tag{5}$$

and,

$$e(\varphi) = \operatorname{sgn} \cos(\pi\varphi/2) \tag{6}$$

respectively, and $\varphi = (t - t_0)/a$ is a re-scaled time. If, in addition, the solution is odd with respect to one half of the period, $x(t + 2a) = -x(t)$, then expression (4) simplifies to

$$\begin{aligned} x &= [\sinh(a\tau G) + e \cosh(a\tau G)]x_0 \\ &\equiv \left[a\tau G + \frac{1}{3!}(a\tau G)^3 + \cdots\right] x_0 + e\left[1 + \frac{1}{2!}(a\tau G)^2 + \cdots\right] x_0 \end{aligned} \tag{7}$$

Proof of expression (4) is obtained by substituting the identity [4]

$$\varphi = 1 + [\tau(\varphi) - 1]e(\varphi) \quad (-1 < \varphi < 3) \tag{8}$$

in (2) and taking into account that

$$e^2 = 1 \tag{9}$$

at almost every time instance[1]. In order to prove the particular case (7), one should keep in mind that $\exp(2aG)x_0 = x(t_0 + 2a) = -x_0$, as it follows from (2), and the oddness condition assumed.

Note that τ and e are indeed quite simple piece-wise linear functions; the above analytical expressions (5) and (6) just define them in the unit-form which enables one to avoid conditioning of computation in the original temporal scale, $t_0 \le t < \infty$. This possibility becomes essential when the dynamics includes some evolutionary component.

Physical meaning of relationship (8) is that, during the whole period, the time variable φ is expressed through the coordinate τ and velocity e of a classic particle freely oscillating

[1]The set of isolated points $\{\varphi\colon \tau(\varphi) = \pm 1\}$ appears to have no effect on the results [4].

between the two absolutely stiff barriers with no energy loss. Due to (9), this relationship possesses the algebraic structure of "hyperbolic complex numbers" as revealed by (4).

Let us outline possible applications of expressions (4) and (7). For the sake of simplicity, consider the particular case (7). Of course, formal expression (7) does not guarantee the existence of periodic solutions. In case some periodic solution does exist, one should be able to find the corresponding vectors x_0 and v_0 from appropriate conditions. In autonomous case, the scalar parameter, a, is also unknown and must be determined.

The related conditions are formulated as a requirement of smoothness of expression (7), which is generally non-smooth or even discontinuous due to the presence of non-smooth and discontinuous functions τ and e, respectively. The "smoothing" relations are obtained by eliminating the step-wise discontinuities of the coordinate and velocity vectors imposing the constraints

$$\begin{aligned} \cosh(aG)x_0 &= 0, \\ \cosh(aG)v_0 &= 0. \end{aligned} \tag{10}$$

In autonomous case, algebraic equations (10) represent a nonlinear eigenvalue problem, where a is an eigenvalue, and $\{x_0, v_0\}$ is a combined (state) eigenvector.

By narrowing the class of periodic motions to those on which the system passes its trajectory twice in the configurations space during the same period, one obtains a subclass of normal mode motions. For more physically meaningful definitions and discussions, see reference [5]. Let us formulate the corresponding problem based on the periodic Lie series solutions.

Consider the vibrating system

$$\ddot{x} + f(x) = 0, \quad x \in R^n, \tag{11}$$

where $f(-x) = -f(x)$, and the initial conditions are $x|_{t=0} = x_0 = 0$ and $\dot{x}|_{t=0} = v_0$.

The normal mode solutions of system (11) are obtained as a particular case of (7) and (10)

$$x = \sinh(a\tau G)x_0|_{x_0=0}, \tag{12}$$

$$\cosh(aG)v_0|_{x_0=0}, \tag{13}$$

where the initial vector $x_0 = 0$ is substituted into the expressions only after all degrees of the differential operator

$$G = v_0 \cdot \frac{\partial}{\partial x_0} - f(x_0) \cdot \frac{\partial}{\partial v_0}$$

have been applied.

Relationship (12) can be interpreted as a parametric equation of normal mode trajectories of the system with the parameter interval $-1 \le \tau \le 1$.

Let us illustrate relationships (12) and (13) based on the linear system so that the result could be compared with the well known conventional solution.

Example 1 Suppose that $f(x) = Kx$, where K is positively defined symmetric $n \times n$-matrix with eigen-system $\{v_0, \omega^2\}$ so that $Kv_0 = \omega^2 v_0$. In this case, by applying the operator G twice, one obtains that v_0 is also an eigenvector of the operator G^2, namely,

$G^2 v_0 = -\omega^2 v_0$. Then, keeping in mind the power series form of expressions (12) and (13) as those in (7) and sequentially applying the operator G^2, gives $x = (v_0/\omega)\sin(a\omega\tau)$ and $\cos(a\omega\tau) = 0$, respectively. Notably, the last equation shows that there exist an infinite number of roots $\{a\}$ related to the same eigenfrequency ω! However, it is easily to find that all the roots produce the same solution in terms of the original time t. The minimal quarter of the period is $a = \pi/(2\omega)$, therefore $x = (v_0/\omega)\sin(\pi\tau/2)$, and $\tau = (2/\pi)\arcsin\sin\omega t$.

Nonlinear cases and the related problems dealing with truncated expansions of (13) will be further discussed in a full-length paper.

References

[1] Ott, E., Grebogi, C. and Yorke, J.A. Controlling chaos. *Phys. Rev. Lett.* **64**(11) (1990) 1196–1199.

[2] Mitropolsky, Yu.A. and Martynyuk, A.A. About some results and actual problems in the theory of periodic motions in nonlinear mechanics. *Prikl. Mekh.* **24**(3) (1988) 3–14.

[3] Ince, E.L. *Ordinary Differential Equations.* Dover, New York, 1956.

[4] Pilipchuk, V.N. Temporal transformations and visualization diagrams for nonsmooth periodic motions. *Int. J. of Bifurcation and Chaos* **15**(6) (2005) 1879–1899.

[5] Vakakis, A.F., Manevitch, L.I., Mikhlin, Yu.V., Pilipchuk, V.N. and Zevin, A.A. *Normal modes and localization in nonlinear systems.* John Wiley & Sons Inc., New York, 1996.

Nonlinear Dynamics and Systems Theory, **6**(2) (2006) 191–203

Stability Conditions and Stability Boundaries of a SHARON Bioreactor Model with Multiple Equilibrium Points

M. Sbarciog[1*], E.I.P. Volcke[2], M. Loccufier[1] and E. Noldus[1]

[1] *Department of Electrical Energy, Systems and Automation, Ghent University, Technologiepark 913, B-9052 Zwijnaarde, Belgium*
[2] *BIOMATH, Department of Applied Mathematics, Biometrics and Process Control, Ghent University, Coupure Links 653, B-9000 Ghent, Belgium*

Received: December 10, 2005; Revised: May 25, 2006

Abstract: This paper addresses the dynamics of a SHARON bioreactor for ammonium removal from concentrated wastewater streams. It is shown that multiple equilibrium points occur for a simplified reactor model. Conditions are determined for which the system possesses multiple equilibrium points and the corresponding phase portraits are analysed. In case the reactor model possesses two locally asymptotically stable equilibrium points, the stability boundary, that separates their attraction regions, is visualized. Subsequently, it is examined how small parameter changes affect the number of equilibrium points and the corresponding phase portraits. The analytically obtained results are illustrated by means of simulations.

Keywords: *biochemical reactors; nonlinear systems; stability analysis.*

Mathematics Subject Classification (2000): 34A34, 34A50, 34D20.

1 Introduction

Throughout the years, biological nitrogen removal from wastewater has proven its effectiveness and has been adopted widely in favour of the more expensive physicochemical processes. Typically, biological nitrogen removal is performed through nitrification of ammonium (i.e. the main form in which nitrogen is present in wastewater) via nitrite to nitrate, followed by denitrification of nitrate to nitrogen gas.

Several novel nitrogen removal processes have been developed, among which the SHARON process (single reactor system for high activity ammonia removal over nitrite),

*Corresponding author: mihaela@autoctrl.UGent.be

that is ideally suited to remove nitrogen from wastewater streams with high ammonium concentration [5].

The SHARON reactor is operated as a continuously stirred tank reactor (CSTR) without biomass retention. At the prevailing pH (about 7) and high temperature (30-40°C), ammonium oxidizers grow faster than nitrite oxidizers. For this reason, it is possible to establish ammonium oxidation to nitrite only and prevent further oxidation of nitrite to nitrate by setting an appropriate dilution rate. In this way, substantial savings in aeration costs are realized, in comparison with oxidation of ammonium to nitrate. Additional savings can be made when the SHARON reactor is coupled with an Anammox process, in which an almost equimolar mixture of ammonium and nitrite is converted to nitrogen gas [9].

In this paper, the dynamics of the SHARON reactor model with inhibition kinetics is analysed. Starting from a simplified model, conditions under which the reactor exhibits multiple equilibrium points are identified and their importance is discussed from a technological point of view. The global convergence properties of the set of the equilibrium points is discussed and phase trajectories are drawn for the different cases distinguished. In case multiple stable equilibrium points occur at the same time, their stability boundary is visualized by means of a trajectory reversing technique. In order to examine the effect of varying parameter values on the number of equilibrium points, an extended model is considered, that is obtained by small modifications of the simplified model. The equilibrium points are calculated analytically and phase trajectories are drawn to verify the results.

2 The SHARON Reactor Model

For a wide class of biotechnological reaction systems in which n components are involved in m reactions $(n > m)$, the state equations can be written in the general form [1]

$$\dot{\xi} = C\rho(\xi) - D\xi + F. \tag{1}$$

The state ξ, of dimension n, is the vector of reactor concentrations of the various components participating in the process. $F = \mathrm{col}\,(F_i),\ i = 1, \ldots, n$, represents the supply rates, while D is the dilution rate. F and D are assumed to remain constant and satisfy

$$F_i \geq 0, \quad i = 1, \ldots, n, \quad D > 0. \tag{2}$$

For a CSTR with constant reactor volume, the supply rate can be written as $F = D\xi_{in}$, with ξ_{in} representing the vector of influent concentrations of the various process components.

$\rho(\xi) = \mathrm{col}\,(\rho_j(\xi)),\ j = 1, \ldots, m$, is the reaction rate function. Let $\rho(\xi) \in \mathcal{C}^1$ (continuous with continuous partial derivatives w.r.t. the components of ξ). This condition ensures the existence and the uniqueness of the solutions of (1) for given initial conditions. For all values of the composition vector $\xi,\ \rho_j(\xi) \geq 0,\ j = 1, \ldots, m$.

$C \in R^{n \times m}$, with $\mathrm{rank}\, C = m$, is the matrix of yield coefficients. Without loss of generality C can be written as

$$C = \begin{bmatrix} C_b \\ C_a \end{bmatrix} \tag{3}$$

where $C_a \in R^{m \times m}$ is nonsingular.

It has been proven [2, 7] that under some fairly general assumptions, including the principle of mass conservation, the state variables of the system (1) cannot become negative and remain upper bounded for increasing time. Moreover the system (1) can be brought in a canonical form by the state transformation

$$x_b \triangleq A_0\xi_a + \xi_b \in R^{n-m}, \quad x_a \triangleq \xi_a \in R^{+^m} \tag{4}$$

with $A_0 = -C_bC_a^{-1}$. The canonical model consists of a linear part of dimension $(n-m)$ dynamically coupled with a nonlinear part of dimension m.

The SHARON reactor model considers two nitrification reactions $(m = 2)$: oxidation of ammonium to nitrite and consecutive oxidation of nitrite to nitrate. Four components $(n = 4)$ are involved in the biochemical reactions: ammonium, nitrite, ammonium oxidizers and nitrite oxidizers. Ammonium and nitrite oxidations are described by their respective reaction rates

$$\rho_1(\xi) = a_1 \cdot \frac{\xi_1}{b_1 + \xi_1} \cdot \frac{c_1}{c_1 + \xi_2} \cdot \xi_3 \tag{5}$$

and

$$\rho_2(\xi) = a_2 \cdot \frac{\xi_2}{b_2 + \xi_2} \cdot \frac{\xi_1}{c_2 + \xi_1} \cdot \frac{d_2}{d_2 + \xi_2} \cdot \frac{e_2}{e_2 + \xi_1} \cdot \xi_4 \tag{6}$$

in which a_1, b_1, c_1, a_2, b_2 c_2, d_2 and e_2 are constant, at least for a SHARON reactor in which temperature and pH are controlled at a fixed level, as is assumed further. The model considers inhibition of ammonium oxidation by nitrite (with inhibition constant c_1), as well as inhibition of nitrite oxidation by ammonium and by nitrite (with inhibition constants e_2 and d_2 respectively). The matrix of yield coefficients has the form:

$$C = \begin{bmatrix} -a & -b \\ c & -d \\ 1 & 0 \\ 0 & 1 \end{bmatrix} \tag{7}$$

Assuming a constant reactor volume, under the state transformation (4), the canonical model of the SHARON reactor becomes:

$$\dot{x}_b = D(w_b - x_b), \tag{8}$$

$$\dot{x}_a = D(w_a - x_a) + C_a\rho(x), \tag{9}$$

where

$$x_a \triangleq \begin{bmatrix} x_3 \\ x_4 \end{bmatrix} \in R^{+^2}, \quad x_b \triangleq \begin{bmatrix} x_1 \\ x_2 \end{bmatrix} \in R^2, \quad C_a = I_2,$$

$$\rho(x) \triangleq \begin{bmatrix} \rho_1(x) \\ \rho_2(x) \end{bmatrix} \in R^{+^2}; \quad w_a = \begin{bmatrix} w_3 \\ w_4 \end{bmatrix} \triangleq \begin{bmatrix} \xi_{in_3} \\ \xi_{in_4} \end{bmatrix} \in R^{+^2};$$

$$w_b = \begin{bmatrix} w_1 \\ w_2 \end{bmatrix} \triangleq \begin{bmatrix} \xi_{in_1} + a\xi_{in_3} + b\xi_{in_4} \\ \xi_{in_2} - c\xi_{in_3} + d\xi_{in_4} \end{bmatrix} \in R^2,$$

$$\rho_i(x) = \rho_i(\xi)|_{\xi_a = x_a;\ \xi_b = x_b + C_bC_a^{-1}x_a}, \quad i = 1, 2.$$

Biochemical reactors are positive systems, which means their state variables ξ_i, $i = 1, \ldots, n$, cannot become negative. Hence the states of the canonical model (8), (9) must fulfill the following physical boundary conditions:

$$w_1 - ax_3 - bx_4 \geq 0, \tag{10}$$

$$w_2 + cx_3 - dx_4 \geq 0, \tag{11}$$

$$x_3 \geq 0, \tag{12}$$

$$x_4 \geq 0. \tag{13}$$

Table 2.1 gives the numerical values/ranges for the SHARON model parameters and input variables, applied in this study. These values are the same as applied in [10], except for the values of a_1 and b_2, that were slightly changed in this study to avoid numerical instabilities, without qualitatively affecting the results.

Table 2.1. Numerical values/ranges SHARON model parameters and input variables.

a_1	1.35×10^{-5}	day^{-1}	a	16	mole mole^{-1}
b_1	4.73	mole m^{-3}	b	0.2	mole mole^{-1}
c_1	837	mole m^{-3}	c	58.6	mole mole^{-1}
a_2	1.22×10^{-5}	day^{-1}	d	15.8	mole mole^{-1}
b_2	60	mole m^{-3}	D	$[0 \quad 3 \times 10^{-5}]$	day^{-1}
c_2	0.01	mole m^{-3}	ξ_{in_1}	$[0 \quad 2000]$	mole m^{-3}
d_2	1000	mole m^{-3}	ξ_{in_2}	0	mole m^{-3}
e_2	1000	mole m^{-3}	$\xi_{in_3} = \xi_{in_4}$	0.01	mole m^{-3}

Since all solutions of the SHARON reactor remain bounded for increasing time, it can easily be established [4], using basic Lyapunov theory, that all trajectories of the canonical model converge to the quarter hyperplane

$$\Delta = \{x_3 \geq 0, \quad x_4 \geq 0, \quad x_b = w_b\}. \tag{14}$$

On the hyperplane Δ the dynamics are described by the autonomous second order system (9) in which $x_b \equiv w_b$, whose the solutions remain bounded for $t \to +\infty$. Hence by Poincaré–Bendixson's theorem (see e.g. [6], P. 321) every solution either converges to an equilibrium point or to a closed trajectory (limit cycle). If there are no closed trajectories in the state space of this system then the set of the equilibrium points is globally convergent. More detailed considerations on the convergence of biochemical reactors of rank two can be found in [8]. Here it was concluded that for processes such as the SHARON reactor, working under operating conditions which violate analytical criteria such as Bendixson's negative criterion [6], the absence of limit cycles must be verified by simulation.

3 Analysis of a Simplified SHARON Reactor Model

In this section, the existence, uniqueness and stability of the equilibrium points is studied for the SHARON reactor model, that is further simplified. The simplified model is obtained by assuming that the inflow does not contain any nitrite, ammonium oxidizers or nitrite oxidizers. Furthermore, nitrite limitation of ammonium oxidizers as well as ammonium inhibition of nitrite oxidizers are not considered. These simplifications are expressed mathematically as

$$\xi_{in_i} = 0, \quad i = 2, \ldots, 4, \tag{15}$$

$$c_1 = +\infty, \quad c_2 = 0, \quad e_2 = +\infty. \tag{16}$$

The equilibrium points of the corresponding canonical model satisfy

$$x_1 = w_1 = \xi_{in_1}, \tag{17}$$

$$x_2 = w_2 = 0, \tag{18}$$

$$[-D + \rho_1(x)]\, x_3 = 0, \tag{19}$$

$$[-D + \rho_2(x)]\, x_4 = 0, \tag{20}$$

where

$$\rho_1(x) = a_1 \cdot \frac{\xi_1}{b_1 + \xi_1}, \tag{21}$$

$$\rho_2(x) = a_2 \cdot \frac{\xi_2}{b_2 + \xi_2} \cdot \frac{d_2}{d_2 + \xi_2}, \tag{22}$$

$$\xi_1 = w_1 - ax_3 - bx_4, \tag{23}$$

$$\xi_2 = cx_3 - dx_4. \tag{24}$$

There are three valid possibilities resulting from (19), (20).

Case 1. $x_3 = 0, \;\; x_4 = 0.$

This gives the equilibrium point:

$$\hat{x}_A = \mathrm{col}\,(\xi_{in_1}, 0, 0, 0). \tag{25}$$

This equilibrium point occurs independently of the choice of dilution rate D and of ammonium concentration in the inflow ξ_{in_1}. It is the wash-out state of the system, in which no biomass remains in the reactor and, consequently, no conversion is realized.

It is worth noting that, if in an equilibrium point there are no ammonium oxidizers present $(x_3 = 0)$, then the concentration of nitrite oxidizers (x_4) must also be zero, otherwise the physical boundary $\xi_2 \geq 0$ is violated. This is logical regarding the fact that, in a SHARON reactor, ammonium oxidizers grow faster than nitrite oxidizers.

Case 2. $x_4 = 0, \;\; \rho_1(x) = D.$

Denoting by $\hat{\xi}_{B_1}$ the solution of $\rho_1(x) = D$,

$$\hat{\xi}_{B_1} = \frac{Db_1}{a_1 - D} \tag{26}$$

the second equilibrium point of the system is found as

$$\hat{x}_B = \mathrm{col}\left(\xi_{in_1},\, 0,\, \frac{\xi_{in_1} - \hat{\xi}_{B_1}}{a},\, 0\right), \tag{27}$$

$\hat{x}_B$ is a physical state of the system only if $D < \dfrac{a_1 \xi_{in_1}}{b_1 + \xi_{in_1}}$. This second equilibrium point corresponds with a situation in which only ammonium oxidizers are present in the reactor, so only nitrite is formed. Nitrate formation is successfully suppressed by keeping out nitrite oxidizers, as is the aim of a SHARON reactor.

Case 3. $\rho_1(x) = D,\ \ \rho_2(x) = D.$

As before, the first equality results in

$$\hat{\xi}_{C_1} = \frac{D b_1}{a_1 - D} \tag{28}$$

under the condition $D < a_1,$ while the second equality will have two solutions $\hat{\xi}_{C_2}$ and $\hat{\xi}_{D_2}$ if $D < a_2 \cdot \dfrac{d_2}{(\sqrt{b_2} + \sqrt{d_2})^2}$. Let $\hat{\xi}_{D_2} > \hat{\xi}_{C_2}$. Then a third physical equilibrium point

$$\hat{x}_C = \begin{bmatrix} \xi_{in_1} \\ 0 \\ \dfrac{d(\xi_{in_1} - \hat{\xi}_{C_1}) + b\hat{\xi}_{C_2}}{ad + bc} \\ \dfrac{c(\xi_{in_1} - \hat{\xi}_{C_1}) - a\hat{\xi}_{C_2}}{ad + bc} \end{bmatrix} \tag{29}$$

will occur if in addition $\hat{\xi}_{C_2} < \dfrac{c}{a}(\xi_{in_1} - \hat{\xi}_{C_1})$. Moreover, if also $\hat{\xi}_{D_2} < \dfrac{c}{a}(\xi_{in_1} - \hat{\xi}_{D_1})$, where $\hat{\xi}_{D_1} = \hat{\xi}_{C_1}$ then the fourth equilibrium point

$$\hat{x}_D = \begin{bmatrix} \xi_{in_1} \\ 0 \\ \dfrac{d(\xi_{in_1} - \hat{\xi}_{D_1}) + b\hat{\xi}_{D_2}}{ad + bc} \\ \dfrac{c(\xi_{in_1} - \hat{\xi}_{D_1}) - a\hat{\xi}_{D_2}}{ad + bc} \end{bmatrix} \tag{30}$$

is also a physical equilibrium point of the system. The equilibrium points $\hat{x}_C$ and $\hat{x}_D$ correspond with situations in which nitrite oxidizers are present, so in which at least part of the nitrite is further oxidized to nitrate. This is mostly not desirable in a SHARON reactor, as more oxygen is consumed. Also for coupling with an Anammox process, nitrate formation should be avoided. Note that, as $\hat{\xi}_{D_2} > \hat{\xi}_{C_2}$, more ammonium oxidizers and less nitrite oxidizers are present, which means that less nitrate is produced in $\hat{x}_D$ than in $\hat{x}_C$.

Summarizing, depending on the values of the dilution rate D and the ammonium concentration in the influent ξ_{in_1}, the simplified model of the SHARON reactor may possess one, two, three or four equilibrium points. The boundaries delimiting the regions with various numbers of equilibrium points are illustrated in Figure 3.1. For high dilution rates

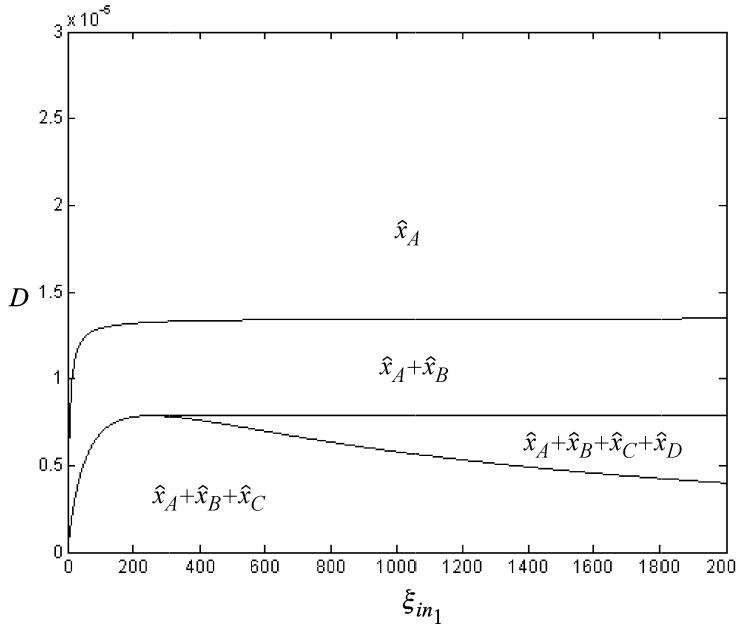

Figure 3.1. Boundaries of regions with various numbers of equilibrium points.

D, the wash-out equilibrium point $\hat{x}_A$, in which both ammonium and nitrite oxidizers are washed out of the reactor, is the only equilibrium point. In case the dilution rate is set lower so that ammonium oxidizers can maintain themselves in the reactor, but still high enough so that nitrite oxidizers are washed out, the equilibrium point $\hat{x}_B$, corresponding with only nitrite formation, occurs besides the wash-out equilibrium point $\hat{x}_A$. If the dilution rate becomes so low that also nitrite oxidizers can grow in the reactor, a third equilibrium point $\hat{x}_C$ appears, and even a fourth equilibrium point $\hat{x}_D$, depending on the influent ammonium concentration ξ_{in_1}. Note, however, that the influent ammonium concentration often cannot be set by the user but should rather be seen as a process disturbance.

The analytically obtained results for the simplified reactor model have been checked by simulations. Figure 3.2 shows the obtained phase portraits of the system on the hyperplane Δ for different combinations of dilution rate and influent ammonium concentration. One combination was selected in each one of the four regions in the $\xi_{in_1} - D$ plane:

1. $D = 2 \times 10^{-5}\,\mathrm{day}^{-1},\ \xi_{in_1} = 1000$ mole m^{-3}.
   In this case the system has only one equilibrium point, $\hat{x}_A$, which is globally asymptotically stable (Figure 3.2a). All trajectories of the system converge to $\hat{x}_A$, where all ammonium and nitrite oxidizers are washed out of the bioreactor.
2. $D = 1.33 \times 10^{-5}\,\mathrm{day}^{-1},\ \xi_{in_1} = 1000$ mole m^{-3}.
   For this choice of inputs the simplified reactor model possesses two equilibrium points (Figure 3.2b): the wash-out state $\hat{x}_A$ which is unstable and a desired operating point $\hat{x}_B$ which is asymptotically stable. All trajectories, except for the wash-out state, converge to the operating point $\hat{x}_B$.
3. $D = 0.786 \times 10^{-5}\,\mathrm{day}^{-1},\ \xi_{in_1} = 275$ mole m^{-3}.
   Three equilibrium points occur in this situation (Figure 3.2c): two unstable ones

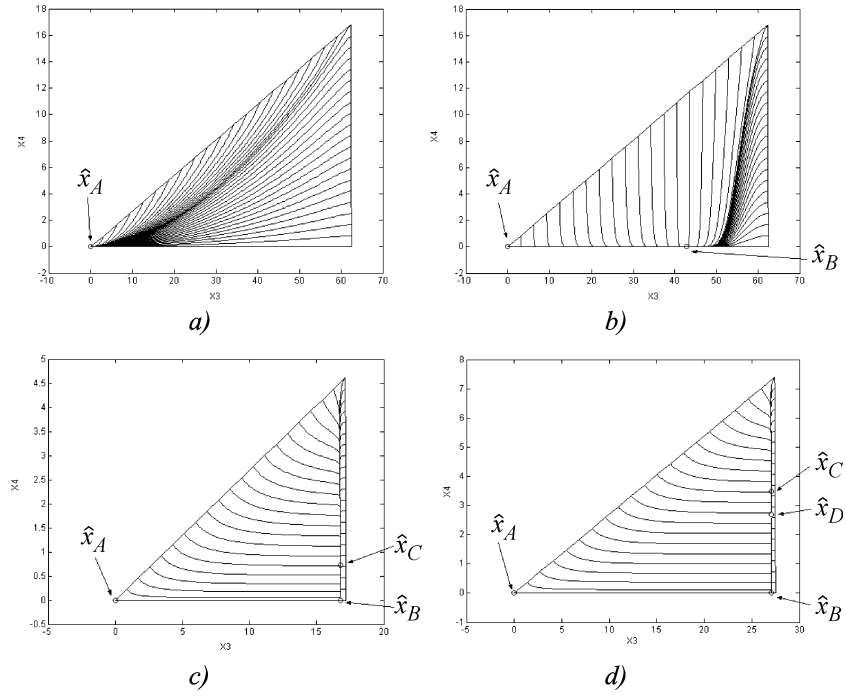

Figure 3.2. Phase portraits in the $x_3 - x_4$ plane.

$(\hat{x}_A, \hat{x}_B)$ and an asymptotically stable operating point $\hat{x}_C$. All trajectories, except those starting with $x_4(0) = 0$, converge to $\hat{x}_C$.

4. $D = 0.786 \times 10^{-5}\,\text{day}^{-1}$, $\xi_{in_1} = 440$ mole m^{-3}.
   This situation corresponds to the occurrence of four equilibrium points (Figure 3.2d). There are two unstable equilibrium points ($\hat{x}_A$ and $\hat{x}_D$) and two locally asymptotically stable equilibrium points ($\hat{x}_B$ and $\hat{x}_C$). Because $\hat{\xi}_{B_2} > \hat{\xi}_{C_2}$ and $\hat{\xi}_{B_1} = \hat{\xi}_{C_1}$, in practice $\hat{x}_B$ is a better operating point than $\hat{x}_C$.

4 Estimation of a Stability Boundary

For the practical situation, in which two stable equilibrium points occur at the same time, as in Case 4 of the previous section, it is essential to forecast from which initial states the process will converge to the desired operating point $\hat{x}_B$, corresponding with only nitrite formation, and which initial conditions will lead the system to the operating point $\hat{x}_C$, in which nitrate is formed. This corresponds to estimating the stability boundary

$$\partial\Omega(\hat{x}_B) = \partial\Omega(\hat{x}_C) \tag{31}$$

separating the regions of attraction $\Omega(\hat{x}_B)$ and $\Omega(\hat{x}_C)$ of the stable equilibria. For systems such as the SHARON reactor, algorithms to find an estimate of the stability boundary $\partial\Omega_{est}(\hat{x}_B)$ that approaches the true stability boundary $\partial\Omega(\hat{x}_B)$ as some algorithmic parameter $\varepsilon \to 0$, have been described in [8]. In the present case

$$\partial\Omega(\hat{x}_B) = W^s(\hat{x}_D) \tag{32}$$

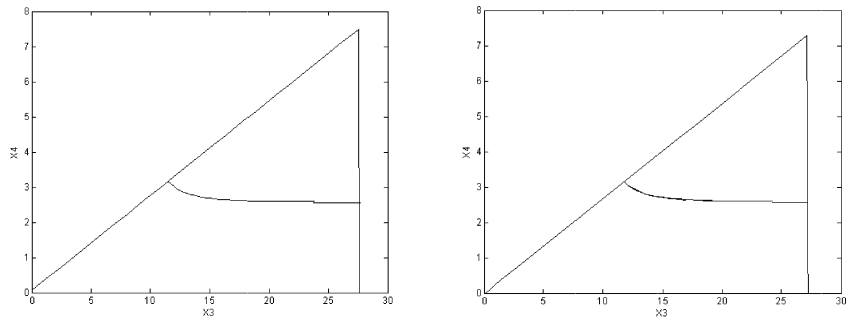

Figure 4.1. Intersections of the stability boundary with the planes H_1, H_2.

where the right hand side of (32) denotes the stable manifold of $\hat{x}_D$. An estimate $W^s_{est}(\hat{x}_D)$ can be found by a trajectory reversing technique such as described e.g. in [3].

The extent of the stability boundary in the four-dimensional state space of the system can be visualized by computing intersections of $\partial\Omega_{est}(\hat{x}_B)$ with the set $H = \{x_b = \eta\}$ for constant vectors $\eta = [\eta_1, \eta_2]^{\mathrm{T}}$. For a numerical technique to accomplish such visualizations see [8].

Figure 4.1 presents the intersection of the estimated stability boundary with the planes H_1 and H_2 corresponding respectively to $\eta_1 = \hat{x}_{D_1} + 2$, $\eta_2 = \hat{x}_{D_2} + 4$ and $\eta_1 = \hat{x}_{D_1} - 4$, $\eta_2 = \hat{x}_{D_2} - 2$. The obtained intersections practically coincide with the curve $W^s(\hat{x}_D)$ on the Δ hyperplane (Figure 3.2d). If the initial conditions of the process are chosen in such a way that the states x_3 and x_4 are below this intersection line (e.g. by ensuring that the initial amount of nitrite oxidizers, $x_4(t = 0)$ is small) and inside the physical boundaries, then the SHARON reactor will converge to the desired operating point $\hat{x}_B$, in which only nitrite is formed.

Summarizing, even for high dilution rates, stable nitrite formation is possible, as long as the influent ammonium concentration is sufficiently high to have four equilibrium points (see Figure 3.1) and if the initial concentration of nitrite oxidizers is sufficiently low.

5 Effect of Changing Parameter and Input Values

For biological systems, it is often difficult to determine exact parameter values. Also, parameter values may change in time e.g. because of biomass adaptation. Besides, also the input values may be uncertain. For this reason, the effect of changing parameter and input values is assessed by the analysis of an extended model of the SHARON reactor. Let

$$c_3 \triangleq \frac{1}{c_1}, \quad e_3 \triangleq \frac{1}{e_2} \tag{33}$$

and suppose that ξ_{in_i}, $i = 2, \ldots, 4$, c_2, c_3 and e_3 have small positive values. We investigate the effect of these values on the position of equilibrium points. Note that the index, hence the local asymptotic stability or instability, of the equilibrium points are not affected by these small parameters because all the equilibrium points of the reactor

are hyperbolic. The equilibrium points of the extended model are the solutions of:

$$x_1 = w_1, \tag{34}$$

$$x_2 = w_2, \tag{35}$$

$$[-D + \rho_1(x)]\, x_3 + D\xi_{in_3} = 0, \tag{36}$$

$$[-D + \rho_2(x)]\, x_4 + D\xi_{in_4} = 0, \tag{37}$$

where

$$\rho_1(x) = a_1 \cdot \frac{\xi_1}{b_1 + \xi_1} \cdot \frac{1}{1 + c_3\xi_2}\,, \tag{38}$$

$$\rho_2(x) = a_2 \cdot \frac{\xi_2}{b_2 + \xi_2} \cdot \frac{d_2}{d_2 + \xi_2} \cdot \frac{\xi_1}{c_2 + \xi_1} \cdot \frac{1}{1 + e_3\xi_1}\,. \tag{39}$$

We calculate the equilibrium points of the extended model as variations of the solutions of the simplified model, neglecting higher order terms in the small parameter values.

Case 1. $\tilde{x}_A = \hat{x}_A + \Delta\hat{x}_A$. This equilibrium point is given by

$$\tilde{x}_A = \begin{bmatrix} \xi_{in_1} + a\xi_{in_3} + b\xi_{in_4} \\ \xi_{in_2} - c\xi_{in_3} + d\xi_{in_4} \\ \dfrac{D\xi_{in_3}}{D - a_1 \frac{\xi_{in_1}}{b_1 + \xi_{in_1}}} \\ \xi_{in_4} \end{bmatrix}. \tag{40}$$

It is a physical equilibrium point if $D > a_1 \dfrac{\xi_{in_1}}{b_1 + \xi_{in_1}}$. This corresponds to the case in which $\hat{x}_B$ is not a physical equilibrium point of the simplified model.

Case 2. $\tilde{x}_B = \hat{x}_B + \Delta\hat{x}_B$,

$$\tilde{x}_B = \begin{bmatrix} \xi_{in_1} + a\xi_{in_3} + b\xi_{in_4} \\ \xi_{in_2} - c\xi_{in_3} + d\xi_{in_4} \\ \hat{x}_{B_3} + \Delta\hat{x}_{B_3} \\ \Delta\hat{x}_{B_4} \end{bmatrix} \tag{41}$$

where

$$\Delta\hat{x}_{B_3} = \frac{1}{a\hat{x}_{B_3} \frac{b_1}{b_1 + \hat{\xi}_{B_1}} + c_3\hat{\xi}_{B_2}\hat{\xi}_{B_1}}\, \hat{x}_{B_3} \left[-c_3\hat{\xi}_{B_2}\hat{\xi}_{B_1} + \frac{b_1}{b_1 + \hat{\xi}_{B_1}} \left(a\xi_{in_3} + b\xi_{in_4} - b\Delta\hat{x}_{B_4}\right)\right],$$

$$\Delta\hat{x}_{B_4} = \frac{D\xi_{in_4}}{D - a_2 \frac{\hat{\xi}_{B_2}}{b_2 + \hat{\xi}_{B_2}} \cdot \frac{d_2}{d_2 + \hat{\xi}_{B_2}}}. \tag{42}$$

It can be shown that $\tilde{x}_B$ is a physical equilibrium point of the extended model in the region where the simplified model has two equilibrium points $(\hat{x}_A, \hat{x}_B)$ and also in the region where the simplified model possesses four equilibrium points $(\hat{x}_A, \hat{x}_B, \hat{x}_C, \hat{x}_D)$.

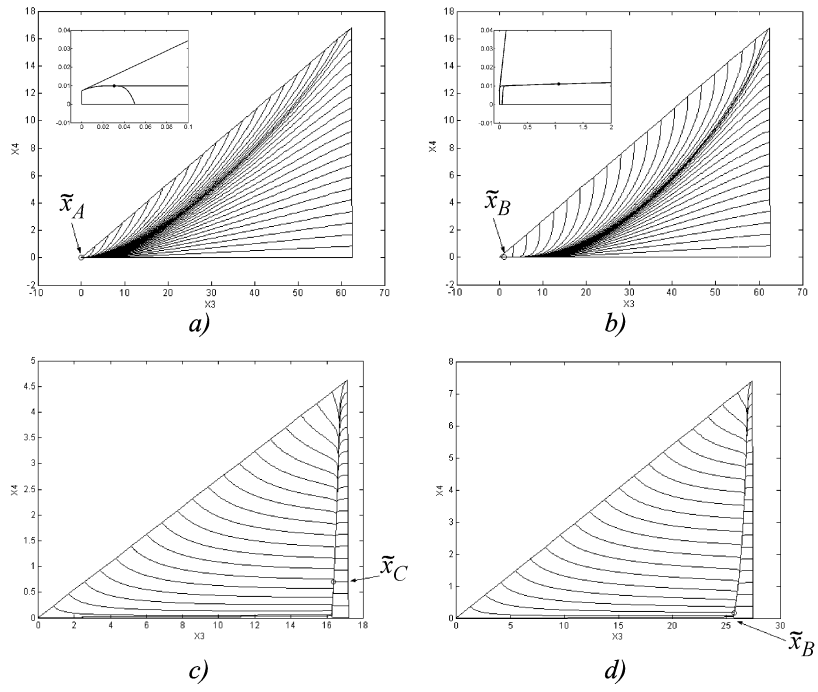

Figure 5.1. Phase portraits in the $x_3 - x_4$ plane for the extended model. a) $\tilde{x}_A = [0.03 \quad 0.01]^T$; b) $\tilde{x}_B = [1.06 \quad 0.01]^T$; c) $\tilde{x}_C = [16.37 \quad 0.7]^T$; d) $\tilde{x}_B = [25.71 \quad 0.16]^T$.

Case 3. $\tilde{x}_C = \hat{x}_C + \Delta\hat{x}_C$ and $\tilde{x}_D = \hat{x}_D + \Delta\hat{x}_D$,

$$\tilde{x}_C = \begin{bmatrix} \xi_{in_1} + a\xi_{in_3} + b\xi_{in_4} \\ \xi_{in_2} - c\xi_{in_3} + d\xi_{in_4} \\ \hat{x}_{C_3} + \Delta\hat{x}_{C_3} \\ \hat{x}_{C_4} + \Delta\hat{x}_{C_4} \end{bmatrix}, \quad \tilde{x}_D = \begin{bmatrix} \xi_{in_1} + a\xi_{in_3} + b\xi_{in_4} \\ \xi_{in_2} - c\xi_{in_3} + d\xi_{in_4} \\ \hat{x}_{D_3} + \Delta\hat{x}_{D_3} \\ \hat{x}_{D_4} + \Delta\hat{x}_{D_4} \end{bmatrix}. \tag{43}$$

These equilibrium points can be determined in a similar way as $\tilde{x}_A$ and $\tilde{x}_B$. They are lying in the neighborhood of $\hat{x}_C$ and $\hat{x}_D$ and therefore they are physical equilibrium points.

The equilibrium points of the extended model can also be determined using a numerical search algorithm. Figure 5.1 displays the phase portraits in the $x_3 - x_4$ plane of the extended model for the same combinations of dilution rate and ammonium concentration in the inflow as considered for the simplified model. For the selected parameter values and inputs the analytical calculation of the equilibrium points proved to be reasonably accurate. Similar values for the equilibria were obtained from the simulation of the phase portraits. While in the cases 1, 3 and 4 the phase portrait of the extended model is very similar to the phase portrait of the simplified model, this is not true however in case 2. Here small variations of the component concentration in the inflow and a more detailed reaction rate function have a great impact on the technological relevance of the equilibrium point: $\hat{x}_B$ changes from a desirable operating point in the case of the simplified model to a non-desirable equilibrium point in the case of the extended model.

More specifically, in the first situation (Figure 5.1a), the globally asymptotically stable wash-out state $\tilde{x}_A$ moves into the interior of the physical state space, however the change is not sufficiently significant to make $\tilde{x}_A$ a desirable operating point. For the second choice of inputs (Figure 5.1b), $\tilde{x}_A$ moves out of the physical state space. Only one physical equilibrium point occurs, namely $\tilde{x}_B$, which changes from a desired operating point to an almost wash-out state, that is undesirable. Apparently, the assumed parameter and input variations affect the model behavior significantly.

In the third situation (Figure 5.1c) both $\tilde{x}_A$ and $\tilde{x}_B$ move out of the physical state space. Now the extended reactor model possesses only one physical equilibrium point $\tilde{x}_C$, where the rate of conversion to nitrite is smaller than in the case of Figure 3.2. The last situation presents a particularity of the SHARON reactor: although the calculations indicate the occurrence of three physical equilibrium points ($\tilde{x}_B$, $\tilde{x}_C$, $\tilde{x}_D$), while $\tilde{x}_A$ has moved out of the physical state space, the phase portrait (Figure 5.1d) shows $\tilde{x}_B$ as a globally asymptotically stable equilibrium point, while it was expected to be only locally asymptotically stable. Due to numerical limitations, the equilibrium points $\tilde{x}_C$ and $\tilde{x}_D$ could not be detected. This is due to the fact that for the extended reactor model the equilibrium points $\tilde{x}_C$ (locally asymptotically stable) and $\tilde{x}_D$ (unstable) move so close to each other that they practically cancel each other and do not noticeable affect the phase portrait. The remaining equilibrium point $\tilde{x}_D$ corresponds with good reactor operation, as only nitrite is formed.

6 Conclusion

In this paper, the dynamic behavior of a SHARON reactor with constant volume, considering two consecutive nitrification reactions, is assessed. The reactor models that have been studied, are valid for constant temperature and pH.

First, the behavior of a simplified reactor model is analysed. The only inhibition effect considered in this model, is nitrite inhibition of nitrite oxidation. It is further assumed that the reactor influent does not contain biomass. It was shown that multiple equilibrium points occur, depending on the dilution rate and the influent ammonium concentration. For the case in which two stable equilibrium points occur at the same time, the stability boundary has been estimated, to determine the initial states which will lead the reactor to the most desirable operating point. Four situations are identified, corresponding to the occurrence of one, two, three or four equilibrium points respectively. From a technological point of view, the SHARON reactor should be operated in such a way that only nitrite is produced and nitrate formation is suppressed. Good operation of the SHARON reactor is ensured in case the dilution rate is sufficiently low to make sure the ammonium oxidizers can maintain themselves in the reactor, while nitrite oxidizers are washed out (case 2), but also for lower dilution rates and at the same time sufficiently high ammonium influent concentrations, provided a rather low concentration of nitrite oxidizers initially present in the reactor (case 4).

Subsequently, an extended reactor model has been studied to determine the effect of changing parameter and input values. Small influent biomass concentrations were considered, as well as additional inhibition effects in in the reaction rate functions. However, even the slight modifications applied, significantly affect the reactor performance. The moderate dilution rate and influent ammonium concentration corresponding with case 2, that allow good performance of the simplified reactor model, now corresponds with almost wash-out of biomass. On the other hand, the relatively high dilution rate,

high influent ammonium concentration and low initial concentration of nitrite oxidizers, corresponding with case 4, still allow good operation of the SHARON reactor.

References

[1] Bastin, G. and Van Impe, J.F. Nonlinear and adaptive control in biotechnology: a tutorial. *European J. of Control* **1** (1995) 37–53.

[2] Bastin, G. and Dochain, D. *On-line Estimation and Adaptive Control of Bioreactors*. Elsevier, Amsterdam, 1990.

[3] Chiang, H., Hirsch, M. and Wu, F. Stability regions of nonlinear autonomous dynamical systems. *IEEE Trans. A. C.* **33** (1988) 16–27.

[4] Khalil, H.K. *Nonlinear Systems*. 2nd ed., Prentice-Hall, New Jersey, 1996.

[5] Khin, T. and Annachhatre, A.P. Novel microbial nitrogen removal processes. *Biotechnology Advances* **22** (2004) 519–532.

[6] Jordan, D.W. and Smith, P. *Nonlinear Ordinary Differential Equations*. Clarendon Press, Oxford, 1977.

[7] Sbarciog, M., Loccufier, M. and Noldus, E. Global convergence and stability properties of a class of biochemical reactor systems. *Proc. VIII triennial Int. SAUM Conf. on Systems, Automatic Control and Measurements*. Belgrade, 2004, 34–41.

[8] Sbarciog, M., Loccufier, M. and Noldus, E. Anticipating operational and wash-out conditions in biotechnological reactors. Accepted to be published in: *American Institute of Physics Conference Proceedings*.

[9] van Dongen, U., Jetten, M.S.M. and van Loosdrecht, M.C.M. The SHARON-Anammox process for treatment of ammonium rich wastewater. *Water Science and Technology* **44**(1) (2001) 153–160.

[10] Volcke, E.I.P. Modelling, analysis and control of partial nitritation in a SHARON reactor. *PhD thesis, Ghent University, Belgium*, 2006.

Nonlinear Dynamics and Systems Theory, **6**(2) (2006) 205–210

Existence of Nonoscillatory Solution of High-Order Nonlinear Difference Equation

Xiaozhu Zhong[1], Jingcui Liang[1], Yan Shi[2*], Donghua Wang[1] and Lixia Ge[1]

[1] *School of Science, Yanshan University, Qinghuangdao 066004, China*
[2] *School of Information Science, Kyushu Tokai University, Kumamoto 862-8652, Japan*

Received: March 25, 2005; Revised: May 25, 2006

Abstract: In this paper, the existence of the nonoscillatory solution to the equation of a class of high-order nonlinear neutral delay difference is investigated. By using fixed point theorem, a sufficient condition is proposed for the existence of eventually positive solution.

Keywords: *Difference equation; oscillation; positive solution.*

Mathematics Subject Classification (2000): 35D05, 35E05.

1 Introduction

In the computer designing and the ecomodeling, a class of neutral difference equation is proposed. In recent years, the oscillatory behavior of neutral difference equations was intensively studied, and some good results were obtained [1–4]. Now we consider the nonlinear high-order difference equation

$$\Delta^m(x_n - px_{n-\tau}) + q_n f(x_{n-\sigma}) = 0, \tag{1}$$

where m is a positive odd number; $n \in N = \{0, 1, 2, \dots\}$, $p \in R$; for $n \in N$, $q_n \in R^+$, $\sigma \in N$, $\tau \in N\backslash\{0\}$, $\mu = \max\{\tau, \sigma\}$, $f \in C(R, R)$ satisfying that $xf(x) > 0$ for $x \neq 0$ and for $\forall\, x, y \in R$,

$$|f(x) - f(y)| \leq L|x - y| \tag{2}$$

where L is a positive constant. The case of $p = 1$ was studied in [5], the case of the equation (1) of even order was studied in [6]. In this paper, by using fixed point theorem, the case of the equation (1) of odd order is studied under the condition of $p \neq \pm 1$, and

*Corresponding author: shi@ktmail.ktokai-u.ac.jp

a sufficient condition for the existence of the positive solution to the equation (1) is obtained.

The real sequence $\{y_n\}_{n=-\mu}^{\infty}$ is called a solution to the equation (1) if each item y_n satisfies the equation (1) for $n \geq 0$. It is called an eventually positive solution if $y_n > 0$ for sufficiently large n.

2 Main Results and Proofs

Theorem 2.1 *Suppose $p \neq \pm 1$, $f(x)$ satisfy the condition (2) and*

$$\sum_{n=0}^{+\infty} n^{m-1} q_n < +\infty. \tag{3}$$

Then there is a bounded eventually positive solution to the equation (1).

Proof Let L_∞ denote a Banach space of all the bounded real sequences $x = \{x_n\}_{n=N-\mu}^{\infty}$ and define the norm $\|x\| = \sup\limits_{n \geq N-\mu} |x_n|$. We introduce the following notation

$$u^{(l)} = \prod_{i=0}^{l-1} (u-i), \quad u \geq l, \tag{4}$$

and let $u^{(0)} = 1$. There are four situations to be discussed:

Case 1: $0 \leq p < 1$.

Let $M = \max\{f(t)\colon\ 1 \leq t \leq 2\}$, $A = \max\{M, L\}$. (3)implies that there exists a positive integer N which is large enough, such that

$$\frac{A}{(m-1)!} \sum_{k=N}^{+\infty} k^{m-1} q_k \leq \frac{1-p}{2}. \tag{5}$$

Define a subset $\Omega = \{x \in L_\infty : 1 \leq x_n \leq 2,\ n \geq N-\mu\}$ on L_∞. Then Ω is a bounded closed convex subset on L_∞. Define a mapping $T\colon\ \Omega \to L_\infty$ as following:

$$(Tx)_n = \begin{cases} 1 - p + p x_{n-\tau} + \sum\limits_{k=n}^{+\infty} \frac{(k-n+1)^{(m-1)}}{(m-1)!}\, q_k f(x_{k-\sigma}), & n \geq N, \\ (Tx)_N, & N-\mu \leq n < N. \end{cases} \tag{6}$$

Next, we show that T is a continuous operator. Let $x^i \in \Omega$, $i = 1, 2 \ldots$, such that $\lim\limits_{i \to +\infty} \|x^i - x\| = 0$. As Ω is a closed subset, so $x \in \Omega$. For $n \geq N$, from (6) one obtains

$$\begin{aligned} |(Tx^i)_n - (Tx)_n| &\leq p|x^i_{n-\tau} - x_{n-\tau}| + \sum_{k=n}^{+\infty} \frac{(k-n+1)^{(m-1)}}{(m-1)!}\, q_k |f(x^i_{k-\sigma}) - f(x_{k-\sigma})| \\ &\leq p\|x^i - x\| + \sum_{k=n}^{+\infty} \frac{(k-n+1)^{(m-1)}}{(m-1)!}\, q_k |f(x^i_{k-\sigma}) - f(x_{k-\sigma})|. \end{aligned}$$

As $f(x)$ is continuous, based on the Lebesgue dominated convergence theorem, one can obtain

$$\lim_{i\to+\infty}\sup_{n\geq N}\|(Tx^i)_n-(Tx)_n\|=0.$$

Obviously, the above formula is also hold for $N-\mu\leq n<N$. So it is easy to deduce

$$\lim_{i\to+\infty}\|Tx^i-Tx\|=0.$$

Namely T is a continuous operator.

For $\forall\, x\in\Omega,$ when $n\geq N,$ we can get from (6)

$$(Tx)_n=1-p+px_{n-\tau}+\sum_{k=n}^{+\infty}\frac{(k-n+1)^{(m-1)}}{(m-1)!}\,q_kf(x_{k-\sigma})\leq 1-p+2p+A\sum_{k=n}^{+\infty}\frac{k^{m-1}}{(m-1)!}\,q_k.$$

Thus from (5) we can immediately obtain

$$(Tx)_n\leq 1-p+2p+\frac{1-p}{2}=\frac{3+p}{2}<2.$$

Similarly, from (6) we also have

$$(Tx)_n=1-p+px_{n-\tau}+\sum_{k=n}^{+\infty}\frac{(k-n+1)^{(m-1)}}{(m-1)!}\,q_kf(x_{k-\sigma})>1-p+p=1.$$

Obviously, when $N-\mu\leq n<N,\ 1<(Tx)_n<2$ also holds. Hence $T\Omega\in\Omega,$ namely T is a self-mapping on Ω.

In what follows, we will prove that T is a contraction mapping on Ω.

For $\forall\, x,y\in\Omega,$ when $n\geq N,$ from the definition of T one obtains

$$\begin{aligned}|(Tx)_n-(Ty)_n|&\leq|x_{n-\tau}-x_{n-\tau}|+L\sum_{k=n}^{+\infty}\frac{(k-n+1)^{(m-1)}}{(m-1)!}\,q_k|x_{k-\sigma}-y_{k-\sigma}|\\&\leq\|x-y\|\left(p+A\sum_{k=N}^{+\infty}\frac{(k-n+1)^{(m-1)}}{(m-1)!}\,q_k\right).\end{aligned}$$

Then it follows from (5) that

$$|(Tx)_n-(Ty)_n|\leq\|x-y\|\left(p+\frac{1-p}{2}\right)=\frac{1+p}{2}\,\|x-y\|.$$

Obviously, when $N-\mu\leq n<N,\ |(Tx)_n-(Ty)_n|\leq\frac{1+p}{2}\|x-y\|$ also holds. Hence, we have

$$\|Tx-Ty\|=\sup_{n\geq N-\mu}|(Tx)_n-(Ty)_n|\leq\frac{1+p}{2}\,\|x-y\|$$

when $0\leq p<1,\ 0<\frac{1+p}{2}<1,$ so T is a contraction mapping on Ω.

We can conclude from the Banach contraction mapping principle that there exists a fixed point $x\in\Omega,$ such that $Tx=x$. In what follows, we will prove that the fixed point x is a bounded positive solution to the equation (1).

As a matter of fact, when $n \geq N - \mu,\ x_n \geq 1 > 0,$ each item of the fixed point satisfies

$$x_n = \begin{cases} 1 - p + px_{n-\tau} + \sum\limits_{k=n}^{+\infty} \dfrac{(k-n+1)^{(m-1)}}{(m-1)!} q_k f(x_{k-\sigma}), & n \geq N, \\ x_N, & N - \mu \leq n < N, \end{cases}$$

so

$$x_n - px_{n-\tau} = 1 - p + \sum_{k=n}^{+\infty} \frac{(k-n+1)^{(m-1)}}{(m-1)!} q_k f(x_{k-\sigma}), \quad n \geq N.$$

From (4), we can deduce that

$$(k-n)^{(m-1)} - (k-n+1)^{(m-1)} = (1-m)(k-n)^{(m-2)}.$$

Hence

$$\Delta(x_n - px_{n-\tau}) = -\sum_{k=n}^{+\infty} \frac{(k-n)^{(m-2)}}{(m-2)!} q_k f(x_{k-\sigma}), \quad n \geq N.$$

From (4), we can also deduce that

$$(k-n-1)^{(m-2)} - (k-n)^{(m-2)} = (2-m)(k-n-1)^{(m-3)}.$$

Then

$$\Delta^2(x_n - px_{n-\tau}) = \sum_{k=n}^{+\infty} \frac{(k-n-1)^{(m-3)}}{(m-3)!} q_k f(x_{k-\sigma}), \quad n \geq N.$$

In general, we can have

$$\Delta^i(x_n - px_{n-\tau}) = (-1)^i \sum_{k=n}^{+\infty} \frac{(k-n-i+1)^{(m-i-1)}}{(m-i-1)!} q_k f(x_{k-\sigma}), \quad n \geq N,$$

where $u^{(0)} = 1,\ i = 1, 2, \ldots, m-1.$ Because m is an odd number, we get

$$\Delta^m(x_n - px_{n-\tau}) = -q_n f(x_{n-\sigma}).$$

So the fixed point x is a bounded positive solution to the equation (1). Thus the proof of the situation (1) is completed.

Case 2: $p > 1$.

Let $M = \max\{f(t)\colon \frac{p-1}{2} \leq t \leq p\},\ A = \max\{M, L\}$. (3) implies that there exists a positive integer N which is large enough, such that

$$\frac{A}{(m-1)!} \sum_{k=N}^{+\infty} k^{m-1} q_k \leq \frac{p-1}{2}.$$

Define a subset $\Omega = \{x \in L_\infty\colon \frac{p-1}{2} \leq x_n \leq p,\ n \geq N - \mu\}$ on L_∞. Then Ω is a bounded closed convex subset on L_∞. Define a mapping $T\colon \Omega \to L_\infty$ as following:

$$(Tx)_n = \begin{cases} p - 1 + \frac{1}{p} x_{n+\tau} - \frac{1}{p} \sum\limits_{k=n+\tau}^{+\infty} \frac{(k-n-\tau+1)^{(m-1)}}{(m-1)!} q_k f(x_{k-\sigma}), & n \geq N, \\ (Tx)_N, & N - \mu \leq n < N. \end{cases}$$

Case 3: $-1 < p < 0$.

Let $M = \max\{f(t)\colon\ 1+p \le t \le 2\},\ A = \max\{M, L\}$. (3) implies that there exists a positive integer N which is large enough, such that

$$\frac{A}{(m-1)!}\sum_{k=N}^{+\infty} k^{m-1} q_k \le \frac{1+p}{2}.$$

Define a subset $\Omega = \{x \in L_\infty\colon\ p+1 \le x_n \le 2,\ n \ge N-\mu\}$ on L_∞. Then Ω is a bounded closed convex subset on L_∞. Define a mapping $T\colon\ \Omega \to L_\infty$ as following:

$$(Tx)_n = \begin{cases} 1-p+px_{n-\tau} + \sum\limits_{k=n}^{+\infty} \dfrac{(k-n+1)^{(m-1)}}{(m-1)!}\, q_k f(x_{k-\sigma}), & n \ge N, \\ (Tx)_N, & N-\mu \le n < N. \end{cases}$$

Case 4: $p < -1$.

Let $M = \max\{f(t)\colon\ \frac{(p+1)^2}{p(p-1)} \le t \le \frac{2(p+1}{p-1}\},\ A = \max\{M, L\}$. (3) implies that there exists a positive integer N which is large enough, such that

$$\frac{A}{(m-1)!}\sum_{k=N}^{+\infty} k^{m-1} q_k \le \frac{(p+1)^2}{p}.$$

Define a subset $\Omega = \{x \in L_\infty\colon\ \frac{(p+1)^2}{p(p-1)} \le x_n \le \frac{2(p+1}{p-1},\ n \ge N-\mu\}$ on L_∞. Then Ω is a bounded closed convex subset on L_∞. Define a mapping $T\colon\ \Omega \to L_\infty$ as following:

$$(Tx)_n = \begin{cases} 1+\frac{1}{p}+\frac{1}{p}x_{n+\tau} - \frac{1}{p}\sum\limits_{k=n+\tau}^{+\infty} \frac{(k-n-\tau+1)^{(m-1)}}{(m-1)!}\, q_k f(x_{k-\sigma}), & n \ge N, \\ (Tx)_N, & N-\mu \le n < N. \end{cases}$$

The proofs of case 2, 3, 4 are similar to that of case 1, so they are omitted.

3 Conclusions

For the high-order equation (1), the case of $p = 1$ was studied in [5], the case of even order equation was studied in [6]. The result obtained here is an extension of works in [5] and [6], that is to say, the case of odd order equation is studied under the condition of $p \ne \pm 1$. By using fixed point theorem, a sufficient condition for the existence of the positive solution to the odd order equation (1) is obtained. Thus all the cases of equation (1), say of both the odd order and the even order, have been studied. So the result in this paper is not only simpler than that in [6] but also more general than it.

Acknowledgment

The authors gratefully acknowledge the helpful comments and suggestions of the reviewers.

References

[1] Lalli, B.S. Oscillation theorems for neutral difference equations. *Computers Math. Applic* **28**(1-3) (1994) 191–202.
[2] Zhang, B.G. and Cheng, S.S. Oscillation criteria and comparison theorems for delay difference equations. *Fasciculi Mathematici* **25** (1995) 13–32.
[3] Zhang, B.G. and Yang, B. Oscillation of nonlinear high order difference equation. *Chinese Annals of Mathematics* **20A**(1) (1999) 71–80.
[4] Yang, F.J. and Liu, J.C. Positive solution of even order nonlinear neutral difference equations with variable delay. *System Science and Mathematics Science* **22**(1) (2002) 85–89.
[5] Zhou, Z.H. and Yu, J.S. The linearized oscillation theorem for odd order neutral difference equations. *Mathematica Applicata* **12**(4) (1999) 65–68.
[6] Zhang, Q.Q. Linearized oscillations for odd-order neutral differential equations. *Mathematics in Economics* **16**(1) (1999) 64–71.
[7] Wang, Y., Shi, Y. and Sasaki, H. A criterion for stability of nonlinear time-varying dynamic system. *Nonlinear Dynamics and Systems Theory* **4** (2004) 217–230.
[8] Lakshmikantham, V. and Vatsala, A.S. Set differential equations and monotone flows. *Nonlinear Dynamics and Systems Theory* **4** (2004) 241–242.